TRACE FISSION PRODUCT RATIOS FOR NUCLEAR FORENSICS ATTRIBUTION OF WEAPONS-GRADE PLUTONIUM FROM FAST BREEDER REACTOR BLANKETS

A Thesis

by

JEREMY MICHAEL OSBORN

Submitted to the Office of Graduate and Professional Studies of
Texas A&M University
in partial fulfilment of the requirements for the degree of

MASTER OF SCIENCE

Chair of Committee,	Sunil S. Chirayath
Committee Members,	William S. Charlton
	Wolfgang Bangerth
Head of Department,	Yassin A. Hassan

August 2014

Major Subject: Nuclear Engineering

ABSTRACT

A nuclear terrorist attack is one of the most serious threats to the national security of the United States, and in the wake of an attack, attribution of responsibility will be of the utmost importance. Plutonium, a by-product in spent nuclear reactor fuel, can be used in a nuclear weapon when obtained from reactor fuel discharged at a low burnup (1 MWd/kg). Characteristics of plutonium reprocessed from reactor fuel depend on factors such as the reactor type (thermal or fast reactor), fuel burnup, production history and the plutonium separation process used. Detailed understanding of the plutonium isotopic composition and fission product contaminant concentrations in separated plutonium would aid nuclear forensics activities aimed at source attribution in the case of interdicted smuggled plutonium, bolstering nuclear deterrence. The study presented here shows that trace fission product to plutonium ratios are amenable for nuclear forensics attribution. Through computational reactor core physics simulations, results are obtained for weapons-grade plutonium produced in a Fast Breeder Reactor (FBR). These fission product to plutonium ratios for the FBR are further compared with results reported elsewhere for a thermal Pressurized Heavy Water Reactor. This comparison of isotopic ratios results in substantial differences between fast and thermal neutron reactor systems, leading to the determination that a suite of selected isotopic ratios can attribute separated weapons-grade plutonium to a fast or thermal neutron source reactor system.

ACKNOWLEDGEMENTS

I would like to thank my advisor and friend, Dr. Sunil Chirayath for all his guidance, support, and assistance throughout the course of this research. Very special thanks go to Dr. William Charlton for his helping hand in the weekly research group meetings. I would also like to thank my committee member, Dr. Wolfgang Bangerth.

I must thank my parents, Sean and Amy Osborn, for all of their endless support.

Finally, I would like to acknowledge the funding support from NSF and DHS joint ARI program (NSF Grant No. ECCS-1140018 and DNDO-2012-DN-077-ARI1057-02) which was utilized to carry out this research work. The views and conclusions expressed in this thesis are not an official position of the funding agencies.

NOMENCLATURE

CANDU	–	Canada Deuterium Uranium reactor
CSR	–	Control Safety Rod
DF	–	Decontamination Factor
DSR	–	Diverse Safety Rod
FBR	–	Fast Breeder Reactor
HFIR	–	High Flux Isotope Reactor
IAEA	–	International Atomic Energy Agency
ITWG	–	International Technical Working Group
LANL	–	Los Alamos National Laboratory
MCNP	–	Monte Carlo N-Particle
MOX	–	Mixed Oxide
MWd/kg	–	Megawatt-day per kilogram of heavy metal
MWe	–	Megawatt electric
NPT	–	Treaty on the Non-Proliferation of Nuclear Weapons
ORNL	–	Oak Ridge National Laboratory
PFBR	–	Prototype Fast Breeder Reactor
PHWR	–	Pressurized Heavy Water Reactor
PuO_2	–	Plutonium Dioxide
PUREX	–	Plutonium Uranium Recovery by Extraction

PWR	–	Pressurized Water Reactor
RB	–	Radial Blanket
RDD	–	Radiological Dispersal Device
UO_2	–	Uranium Dioxide

TABLE OF CONTENTS

LIST OF FIGURES

LIST OF TABLES

I. INTRODUCTION

The Nuclear Forensics and Attribution Act, signed into law by President Barack Obama in 2010, states that a nuclear terrorist attack is one of the most serious threats to the national security of the United States, and that in the wake of an attack, attribution of responsibility would be of the utmost importance.[1] Attribution begins with technical nuclear forensics, the process by which intercepted, illicit nuclear material is analyzed in order to identify the origin and source of the material.[2] Recognizing a threat illustrates the value of a robust forensics and attribution capability that results in establishing a credible nuclear deterrent.

There are two basic techniques for attributing reactor characteristics from results of analyzed material. These consist of a database method and an inverse analysis method. With the database method the measured results from material analyses are compared to a database of isotopic results to find the closest solution. In an inverse analysis method the data obtained from the measured material is used to develop model parameters for the forward model.[3] The forward model being a reactor physics code. Both methods have their disadvantages. For example, a downside of the database method is that the database is never certain to be complete. Therefore, forensic analysis for attribution using a database method requires that data concerning foreign-origin materials be available and studied.[4] However, it is possible that well validated computational models may be able to substitute data for cases where known material samples are not available.

I.A. Background and Motivation

Plutonium, a byproduct in spent nuclear fuel, is bred in nuclear reactor fuel by the conversion of uranium. The production of ^{239}Pu is through the neutron capture of ^{238}U:

$$^{238}_{92}\mathrm{U} + {}^{1}_{0}\mathrm{n} \xrightarrow{(\mathrm{n},\gamma)} {}^{239}_{92}\mathrm{U} \xrightarrow{\beta^-} {}^{239}_{93}\mathrm{Np} \xrightarrow{\beta^-} {}^{239}_{94}\mathrm{Pu}\ , \quad (1)$$

where the half-lives for the beta decays of ^{239}U and ^{239}Np are 23.47 minutes and 2.355 days, respectively.[5] As the fuel burnup increases, neutron capture reactions in ^{239}Pu and successive isotopes of plutonium lead to the production of higher mass number plutonium isotopes. Eventually a full composition of plutonium isotopes (^{238}Pu, ^{239}Pu, ^{240}Pu, ^{241}Pu, and ^{242}Pu) exist in the irradiated fuel. Fuel burnup is defined as the thermal energy produced per unit mass of fuel, expressed in Megawatt-day per kilogram of heavy metal (MWd/kg). The isotopic composition of the plutonium is dependent upon the fuel enrichment, the amount of fuel burnup, the nature of the reactor neutron energy spectrum to which the fuel is exposed, and the cooling time after the irradiation has occurred. Thus, the resulting composition of the discharged fuel may be able to provide information on the reactor system which produced the plutonium.

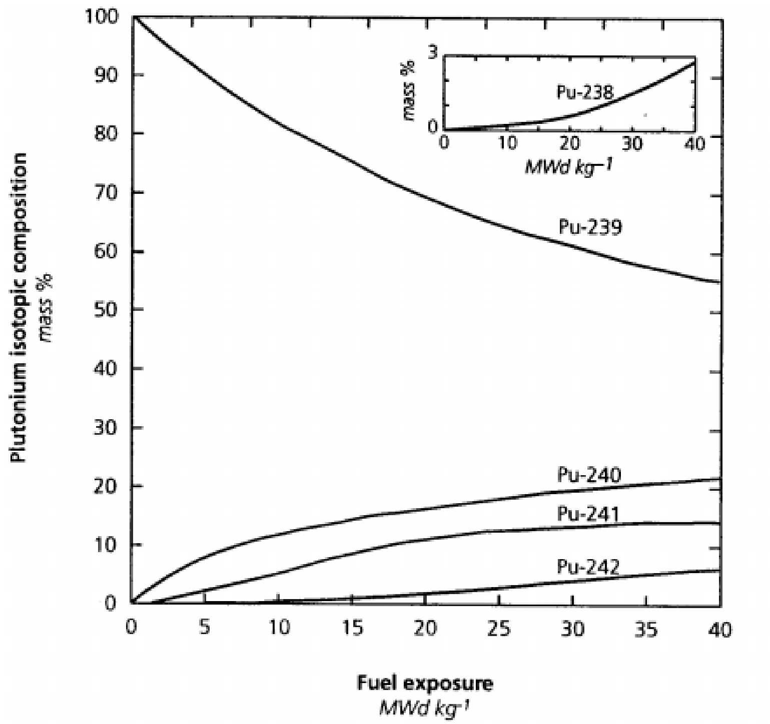

Figure 1. Plutonium isotopic composition as a function of fuel burnup in a PWR.

Fuel burnup is the major contributing factor to the plutonium isotopic composition. Figure 1, taken from reference 6, illustrates the change in plutonium composition as a function of fuel burnup in the case of a typical pressurized water reactor (PWR).[6] It can be seen from Figure 1 that as the fuel burnup increases, the concentration of ^{239}Pu, and thus the quality of the plutonium with respect to weapons usability, decreases. For levels of fuel burnup (7 to 45 MWd/kg) commonly achieved in power reactors, the resulting plutonium is reactor-grade rather than weapons-grade.[6] However, a reactor could, in theory, be designed or misused to discharge fuel at a low burnup (1 to 2 MWd/kg) for the purpose of obtaining weapons-grade plutonium. If a reactor is to discharge uranium fuel subject to a low burnup of around 1 MWd/kg, the plutonium produced will be weapons-grade, irrespective of the reactor type in which the uranium is irradiated. The characteristics of the plutonium composition defining plutonium grade as per reference 6 are listed in Table I.[6]

Table I

Approximate isotopic composition of various grades of plutonium.

Grade	**Isotope (%)**				
	^{238}Pu	^{239}Pu	^{240}Pu	^{241}Pu	^{242}Pu
Super-grade	-	98	2	-	-
Weapons-grade	0.12	93.8	5.8	0.25	0.022
Reactor-grade	1.3	60.3	24.3	9.1	5
MOX-grade	1.9	40.4	32.1	17.8	7.8
FBR blanket	-	96	4	-	-

From Table I, FBR (fast breeder reactor) blanket plutonium is estimated to be weapons-grade. This is because during the standard burn cycle of an FBR the blanket material situated at the periphery of the reactor core is exposed to a burnup around 1 MWd/kg, whereas it is unusual for a power reactor to discharge regular uranium fuel at that low of a burnup. Therefore, any country operating an FBR will be generating significant quantities of weapons-grade plutonium in the fuel blankets. Countries including India and China currently have FBR programs where they are actively developing and operating FBRs for research and power production purposes.[7]

India's 500 MWe Prototype Fast Breeder Reactor (PFBR)[8] is in the advanced stages of its construction, at the time of this writing, and will produce significant quantities of weapons-grade plutonium during normal operation. Previous work has estimated that about 140 kg of weapons-grade plutonium will be produced in the blankets of the PFBR each year.[9] This capability is significant as India is a non-signatory of the Treaty on the Non-Proliferation of Nuclear Weapons (NPT). If India uses the PFBR and other reactors, only to meet civilian energy needs, international safeguards would provide confidence that plutonium is not being diverted from their power reactors. In 2010, the United States and India enacted a nuclear deal based on India's civilian and military nuclear separation plan which would allow access for international safeguards on Indian power reactors in exchange for India's ability to receive full civil nuclear energy cooperation, including fuel supplies for safeguarded nuclear power reactors.[10] In accordance with the Indo-US 123 agreement, civilian power reactors will be placed under permanent International Atomic Energy Agency (IAEA) safeguards. However, India retains the sole right to determine whether nuclear facilities are civilian or military. Thus per the agreement, the PFBR as well as eight of their twenty-two, CANDU derived, Indian Pressurized Heavy Water Reactors (PHWRs) are exempt from IAEA safeguards.[10] Both of these reactor types have the ability to produce weapons-grade plutonium, which can be used for the purpose of weapons production.

Operating in a non-safeguarded manner, the PHWRs are of particular interest because of their unique online refueling capabilities. Light water reactors undergo batch refueling which require a reactor shutdown to be performed, whereas heavy water reactors are frequently refueled while online and in operation. Their use of natural uranium fuel (0.72% ^{235}U), having a low reactivity, leads to typically refueling one fuel channel (eight fuel bundles ~100 kg U) per day. The PHWRs usually reach an average fuel burnup of about 6.7 MWd/kg.[11] However, the online refueling makes the reactors more susceptible to the diversion of material from the core, and this allows the potential for the fuel to be intentionally exposed to a low burnup and then removed from the core for purposes outside civilian energy production.

Due to the prevalent risk of misuse of these two types of reactors and the ability to produce weapons-grade plutonium from both, it is of interest to have detailed characterizations of weapons-grade plutonium produced by FBR and PHWR types. This research develops a suite of fission product to plutonium ratios for separated plutonium produced in the PFBR radial blanket, followed by a comparison of those ratios to material from a PHWR source reported elsewhere.[12] Detailed understanding of the characteristics, such as plutonium composition and fission product contaminant concentrations in separated plutonium would aid nuclear forensics activities which are aimed at source attribution in the case of interdicted smuggled plutonium in a pre-detonation state as well as to some extent for post-detonation analyses, bolstering nuclear deterrence.

I.B. Previous Work

Multiple studies on technical nuclear forensics research have been published which demonstrate the ability of isotopic data to retain information about the source of the produced special nuclear material. An environmental monitoring system was developed at Los Alamos National Laboratory (LANL) using fissiogenic noble gases, namely xenon and krypton, as a verification technique for reprocessing facilities.[13] The relative concentrations of stable xenon and krypton isotopes depend on several reactor operating parameters. Measurements of isotopic ratios of these noble fission gases could thus be used to verify operator declarations or determine fuel parameters such as fuel type, burnup, and reactor type. The technique developed uses a high-precision mass spectrometer to measure stable noble gas isotope compositions in samples taken from a reprocessing plant exhaust stack. Selected isotopic ratios were determined and using sophisticated data analysis the ratios were compared to a database of isotopic ratios to infer the fuel parameters. The calculated database of xenon and krypton isotopic ratios was created using a series of reactor analysis codes to model essentially all types of reactors. The isotopic ratios were calculated as a function of burnup for pressurized water reactors, boiling water reactors, CANDUs, graphite moderated reactors, and FBRs. To verify the accuracy of the calculated database, the reactor models were benchmarked to a dozen measurements from literature. Computer modeling showed the ability of the isotopic ratios to distinguish between light-water reactors, heavy-water reactors, and breeder reactors. This system utilizes the fact that noble gases are not chemically bound to the fuel and are thus released during reprocessing.[13] However, the isotopic ratios and database developed by this technique are not useful when it comes to analyzing post-processed materials; which is the focus of this thesis study.

A thesis study was performed by M.R. Scott[14] to create a forensics methodology for attributing spent fuel used in a radiological dispersal device (RDD) to a source reactor. The attributes which were determined included the spent fuel burnup, age from discharge, reactor type, and initial fuel enrichment. The attribution process was theorized to begin by accurately measuring the isotopic composition of the RDD debris with mass spectrometry. The method for finding the correct reactor type is a forward model, in which several reactor types are modeled with coupled MCNP (core physics analysis code) and ORIGEN (fuel burnup simulation code). The isotope measurements will be compared to the library of computationally calculated isotopes for different reactor types. An error will exist between the measured isotopes and computationally calculated isotopes. The reactor types will be ranked based on the lowest error as to which type is most likely to be the source reactor. To find a distinction between reactor types, isotopes with cross sections and yields that change significantly between reactor types were needed. Ratios of the chosen isotopes were plotted versus burnup for each reactor. The results showed that these isotopes could easily differentiate between a fast reactor and thermal reactor.[14] The work, however, was focused on higher burnup levels which are more commonly achieved in power reactors, rather than low burnup weapons-grade plutonium. Isotopes coming from more complex production chains do not have sufficient time to be produced in low burnup material. As a result, the monitors identified in Scott's study were not suitable for the nuclear forensics analysis of low-burnup fuel reported in the current study.

A previous study was completed by Wallenius et al. in which plutonium isotopics were analyzed and used for the purposes of origin determination of plutonium seized in the illicit trafficking of nuclear material.[15] This study used the reactor fuel burnup simulation code, ORIGEN2, to calculate the plutonium composition for multiple reactors, as well as a thermal ionization mass spectrometer to measure plutonium isotope ratios of five plutonium samples. The sources of the plutonium samples included two from the National Bureau of Standards, two from the former Soviet Union, and one sample from an (ITWG) International Technical Working Group round-robin test. Following the measurements, a source reactor for each sample was then inferred by comparing the measured and computationally calculated isotopic compositions. Their study raises a number of concerns, though, with regards to the isotopics and computer modeling. The isotopic analyses consisted of plutonium and actinides only, with no investigation of contaminant fission products. The isotope generation and depletion code, ORIGEN2, uses a zero-dimensional fuel model giving the composition averaged over the whole reactor core. This could be problematic with an FBR, whose core consists of very different fuel and blanket regions. Additionally, irradiation times were considered to be continuous and no cooling time corrections were made to the material. Burnup levels obtained for the computational models were equivalent to typical burnup for each reactor with the exception of the FBR. Here, the FBR blanket material has a burnup of 20 MWd/kg, which is relatively high. This burnup level is likely due to the averaging of core and blanket fuel, as a result of ORIGEN2 modeling.

A paper was published by A. Glaser[16] over the isotopic signatures of weapons-grade plutonium produced in reactor types which have been historically used for plutonium production. The computer code system, MCODE, which links MCNP and ORIGEN2 was used to model three types of reactors: the Hanford-type, NRX-type, and Calder Hall-type reactors. For each of these reactor types, the plutonium composition was obtained and ratios of plutonium isotopes were analyzed. In addition, sample data, from previous publications, of the same plutonium isotopic ratios from more reactor types were included in Glaser's analysis. It was determined that predictive signatures derived from the plutonium isotopic ratios can distinguish weapons-grade plutonium from basic reactor types including fast breeder reactors, light water reactors using low-enriched fuel, and reactors fueled with natural uranium.[16] Analyses of fission products are absent in the study done by Glaser. While a forensics methodology consisting purely of plutonium isotope ratios could be beneficial due to independence from the separation technique, the plutonium isotopics may be assisted by the inclusion of fission product compositions.

From the literature review, it was evident that previous studies have developed plutonium or fission product isotope analysis techniques which attribute nuclear material to a source reactor. Most of the research completed however, has been focused on reactor spent fuel, irradiated typically to an average burnup level, where the composition of plutonium produced is not of weapons-grade. Lacking are the investigations into isotopic characteristics of fission product contaminants in weapons-grade material as a result of low burnup fuel from reactor misuse or a breeder reactor blanket. Using ratios of fission products to plutonium in separated weapons-grade plutonium, attempted in the present study, for nuclear forensics isotope analysis, is a novel approach for source reactor attribution.

II. THEORY

Technical nuclear forensics capabilities for the attribution of nuclear material to a source reactor are vital to establishing a credible nuclear deterrent. Previous nuclear forensics research has demonstrated the ability for isotopics within the material to retain information on the system which produced the material. With fast breeder reactors becoming more prevalent there is a need to continue research with a focus on FBR systems and weapons-grade plutonium from low burnup fuel. The theory involved with the creation and remaining presence of isotope characteristics in a material which possess information from the source system is discussed throughout this chapter.

A detailed characterization of weapons-grade plutonium will include fission product contaminants in addition to plutonium isotopics. The potential for trace amounts of fission products in separated plutonium is due to the non-ideal chemical process used to separate plutonium from irradiated nuclear fuel. The degree of purification achieved by a separation process can be quantified by decontamination factors (DF), which are the ratios of a stated impurity to desired component in the feed divided by the equivalent ratio in the product.[17]

$$DF = \frac{\left[\frac{Impurity}{Desired\ Component}\right]_{Feed}}{\left[\frac{Impurity}{Desired\ Component}\right]_{Product}} \tag{2}$$

The most commonly employed technique for plutonium separation is the Plutonium Uranium Recovery by EXtraction (PUREX) process.[18] Using the PUREX process, decontamination factors of 10^6 - 10^8 have been achieved[17] for the reduction of fission products in separated plutonium, however a measurable contaminant concentration will remain. The DF is largely insensitive to mass-dependent fractionation. Thus, different mass isotopes of the same element will be separated together and equally during chemical separation.

II.A. Neutron Energy Spectrum

Similar to the plutonium composition, fission product inventories have a large dependency on parameters such as fuel burnup, the type of fuel, enrichment, the neutron energy spectrum of the reactor, and the fuel cooling time after irradiation. The objective of this research is to analyze plutonium and fission products from an FBR blanket fuel with a burnup of 1 MWd/kg, followed by a comparison to PHWR fuel also with 1 MWd/kg burnup. The fast neutron energy spectrum of a sodium cooled FBR is drastically different from the heavy-water moderated PHWR thermal neutron energy spectrum. For these reactor fuels exposed to equal levels of burnup, the neutron energy spectrum will be the source of variations in fission product inventories. The fuel used in PHWR is natural uranium (0.72 atom percent ^{235}U), whereas that used in an FBR blanket fuel is depleted uranium (0.25 atom percent ^{235}U). The energy production in the FBR core is from the seed fuel subassemblies containing mixed oxides (MOX) of PuO_2 and UO_2. A plot of fast and thermal neutron energy spectra can be seen in Figure 2 which was obtained from reference 19.[19]

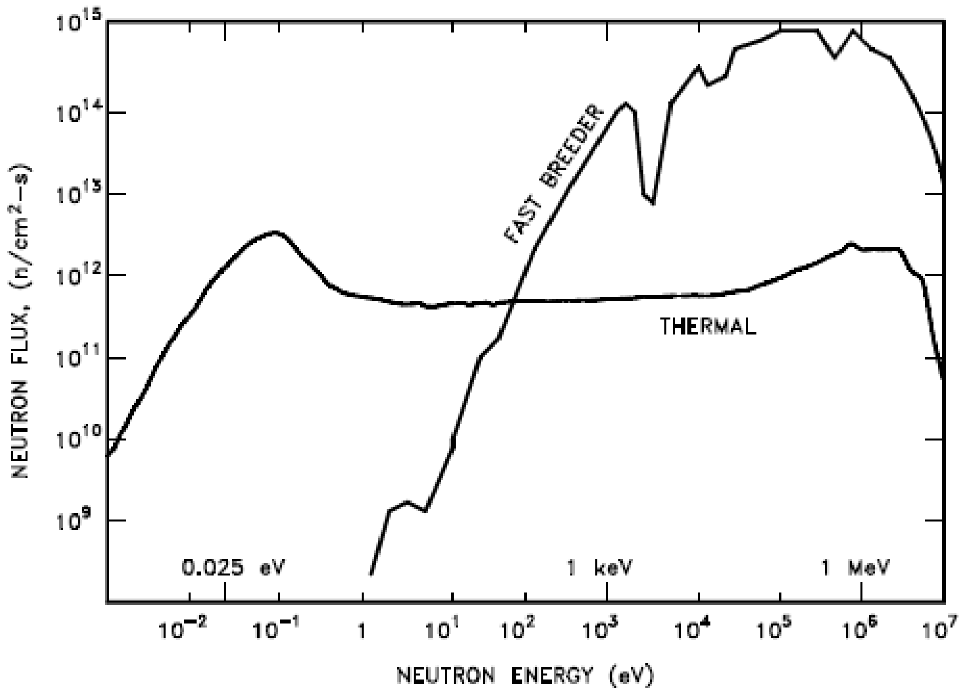

Figure 2. Neutron energy spectra for that of a fast reactor and thermal reactor.

The dissimilarity of the neutron spectra can lead to changes in characteristics of plutonium and fission product concentrations in the fuel. Variations in the fission yield for several fission products, variations in neutron interaction probabilities (cross-sections) for fission product isotopes, and variations in the neutron interaction probabilities for the plutonium isotopes can all lead to characteristic differences in fission product to plutonium ratios, which is the focus of this study. Figure 3 displays the fission product yield curves for the thermal fission of ^{235}U to represent a PHWR, and for the fast fission of ^{238}U and ^{239}Pu which represents an FBR.[20] It can be seen from Figure 3 that the fission product yields are, in fact, different between the neutron energy and uranium and plutonium isotopes and thus analysis of fission product inventories, a small portion of which will be contaminant in the separated plutonium, can assist in attributing plutonium to a source reactor. It should be noted that energy for the fast fission yield in Figure 3 is at a neutron energy of 500 keV. This is a slightly higher energy than the energy of the dominant neutrons in a MOX-fueled FBR, which varies between 100 keV to 400 keV.

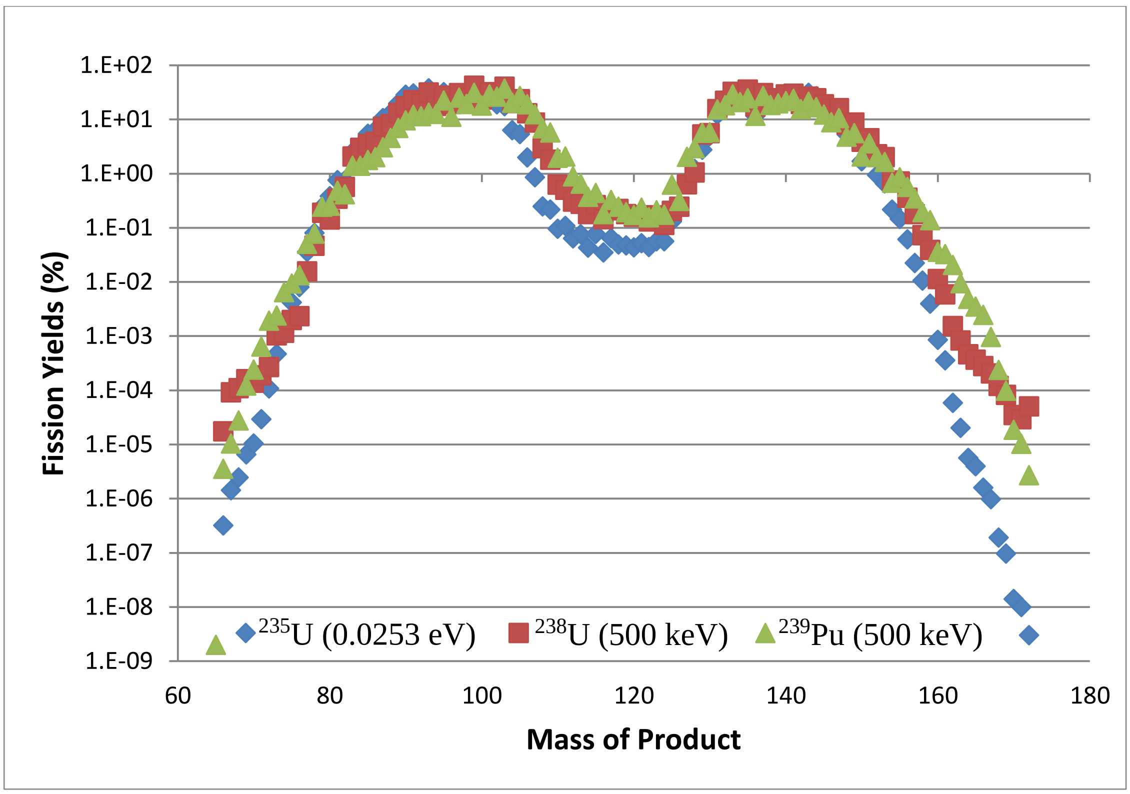

Figure 3. Cumulative fission yield curves for various isotopes and neutron energies.

II.B. India's Three Stage Nuclear Program

Dr. Homi J. Bhabha is regarded as the "father" of India's nuclear program. Dr. Bhabha conceived the idea of a three stage nuclear program as a way for India to work around the country's limited amount of uranium while utilizing its vast thorium reserves. The strategy is to develop a Th – U fuel cycle, breeding fissile ^{233}U from the fertile ^{232}Th. Stage one consists of natural-uranium fueled thermal reactors (PHWRs) used to generate power. The second stage of the program involves a fleet of fast breeder reactors. The stage two fast breeder reactors, beginning with the PFBR, will be fueled with reactor-grade plutonium and depleted uranium from the reprocessed spent fuel of stage one reactors and will breed more plutonium than it consumes. With enough plutonium fuel stockpiled, the FBRs can then switch to a plutonium – thorium breeder cycle capable of producing ^{233}U. The third stage will then be a ^{233}U – Th breeder cycle, which best utilizes India's resources.[21] Figure 4 gives a visual representation of India's three stage nuclear power program.

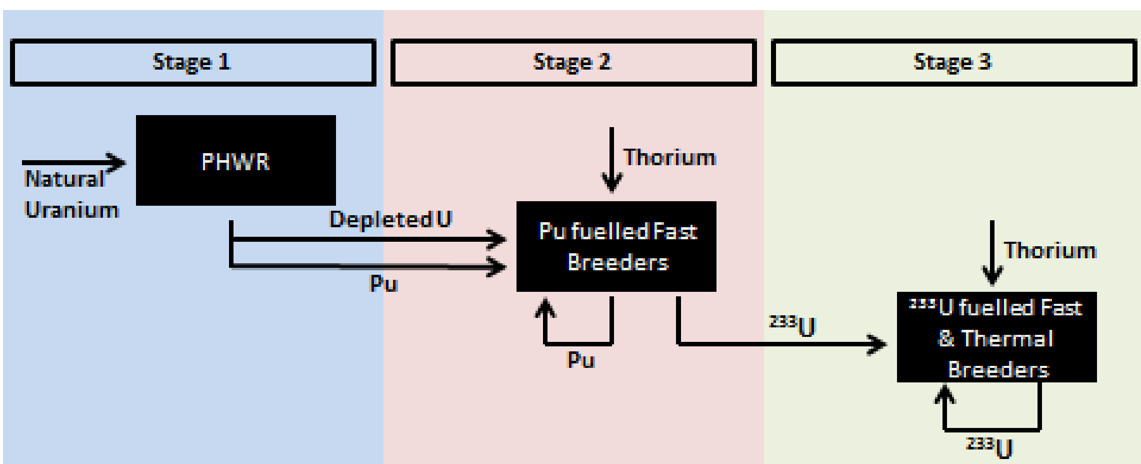

Figure 4. India's three stage nuclear power program.

II.C. The Indian PFBR

The Indian PFBR is the specific fast breeder reactor modeled in this study due to core characteristics being available in open literature.[22] However, the objective of this thesis study is to analyze a fast breeder reactor system and the results obtained are applicable to general FBR systems. Design information for the 500-MWe Indian PFBR was obtained from Chirayath et al.[22] and essential parameters are listed in Table II. There is an active core, one meter in height, which consists of an inner core and outer core of MOX "driver" fuel. The MOX fuel of the active core has PuO_2 enrichments of 20.7% for the inner core and 27.7% for the outer core. This increases the amount of fissile material around the radial periphery of the active core, thus desirably flattening the neutron flux profile across the reactor. Axial blankets of length 0.3 m each sit above and below the active core, all of which are surrounded by 1.6 m tall radial blankets. Both core blankets are comprised of depleted UO_2 "target" fuel, capturing the neutrons leaking from the core. This large amount of ^{238}U is where the weapons-grade plutonium breeding will take place, due to the low fuel burnup experienced in the blanket regions. The plutonium bred in the axial and radial blankets are likely to have similar characteristics; however, this project is focused on the plutonium produced in the radial blankets only. A core map of the PFBR, in Figure 5, highlights the inner core, control safety rods (CSR), diverse safety rods (DSR), outer core, and radial blanket.

Table II

PFBR core design parameters.

Core parameter	Value
Reactor power (MWe)	500
Thermal Efficiency (%)	40
Maximum linear heat rating (W/cm)	450
Fuel pin clad O.D./I.D. (cm)	0.66/0.57
Fuel pellet diameter (cm)	0.555
Fuel pins per sub-assembly	217
Fuel pin triangular pitch (cm)	0.825
Assembly pitch (cm)	13.5
Radial blanket pin clad O.D./I.D. (cm)	1.433/1.323
Radial blanket pellet diameter (cm)	1.29
Pins per radial blanket sub-assembly	61
Radial blanket pin triangular pitch (cm)	1.553
Fuel assembly sheath thickness and sub-assembly size (cm)	0.32/13.13
Active core height	100
Axial blanket height top + bottom (cm)	30 + 30
Radial blanket height (cm)	160
Fuel – Density of fuel (g/cm^3)	PuO_2 – UO_2 [a] (11.0)
Axial/Radial blanket fuel	Depleted UO_2 [a]
Fuel clad material	20% CW D9 steel
Core Pu enrichments in MOX, inner core and outer core (%)	20.7/27.7 [PuO_2 / (PuO_2 + UO_2)]
Plutonium isotope ratios in fuel: $^{239}Pu/^{240}Pu/^{241}Pu/^{242}Pu$ (%)	68.8/24.6/5.3/1.3
Plutonium inventory (t)	1.99
Primary coolant	Liquid sodium
Primary inlet/outlet temperature (°C)	397/547
Fuel average temperature (°C)	1289
Fuel cycle (effective full power days)	180

[a] Depleted uranium: ^{235}U (0.25 at.%) and ^{238}U (99.75 at.%)

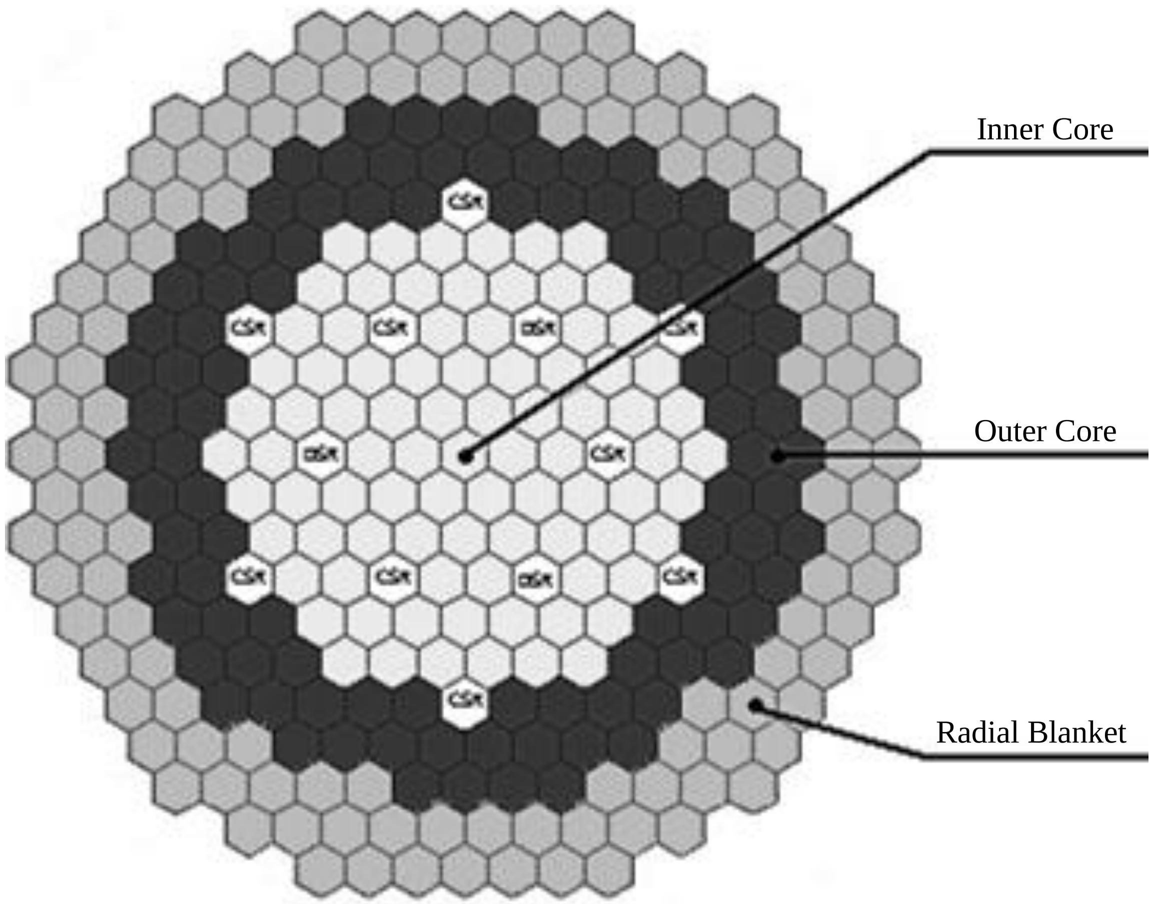

Figure 5. Core map of the PFBR.

II.D. Monte Carlo N-Particle (MCNP) Transport Code

MCNPX Version 2.7, a general-purpose Monte Carlo radiation transport code designed to track particle interactions, was utilized for modeling the PFBR core.[23] A user created input deck contains information regarding geometry specifications, material descriptions, selection of neutron interaction cross-section evaluations, location and characteristics of the radiation particle source, type of output information desired, and any variance reduction techniques if applicable.[24] The geometry of MCNPX treats an arbitrary three-dimensional configuration in geometric cells bounded by first-, second-, and fourth-degree surfaces. The cells are defined by the intersections, unions, and complements of the regions bounded by the surface. The variety of flux estimators available, including flux averaged over a volume, flux averaged over a surface, and flux at a point, make MCNPX a versatile and powerful code for radiation transport calculations.[23] MCNP will read variables of the user input file and perform appropriate particle simulations.

The Monte Carlo method is a numerical analysis technique, which uses random sampling procedures to construct the solution of a physical or mathematical problem. A stochastic model is set up, and by sampling from appropriate probability distributions, estimates the required numerical answers to the problem by statistical means.[25] Monte Carlo thus duplicates the process of nuclear particle interactions with matter by sampling, via random numbers, probability distributions calculated from transport data.[24]

A Monte Carlo code must have a supply of truly random numbers, which are uniformly distributed between 0 and 1. Each particle is followed from its birth to its death or escape from the system, with random sampling of probability distributions contained in radiation transport equations to determine the outcome at each step of its life.[24] In the life of a particle, events may include distance traveled to the next collision, collision nuclide selection, and nuclear reaction selection for a nuclide. Probabilities representing the physical process, at each event, are calculated based on physics, transport data and the materials involved. A random number is selected at an event and applied to the probability distribution to determine the events outcome. This process is repeated along the particle's history, or path from birth until death, with a particle's death coming from absorption or leakage from the system. As a large number of histories are tracked, the average particle behavior more accurately simulates the physical process.[24]

The Monte Carlo method indirectly solves the Boltzmann Transport Equation by simulating individual particles and averaging the behavior of a large number of particles. Monte Carlo is well suited for solving complicated three-dimensional, time-dependent problems[24] and thus is ideal for use in this thesis work.

II.E. CINDER90 Depletion

During the operation of a nuclear reactor the material compositions undergo changes, mainly, due to nuclear reactions caused by neutron interactions. The neutron interaction probabilities of the nuclides, along with the neutron flux, dictate the rate of change of the isotopic composition. As the isotopic compositions of the materials change, the nuclear reaction rates of the system are further altered. It is therefore essential to calculate the isotopic changes of the materials in the reactor in order to accurately simulate the reactor's operation.[26]

MCNPX comes equipped with the depletion/burnup code, CINDER90, built-in to the code package.[23] An advantage of this integration is that only a single input is needed to run both the transport calculations as well as the isotope generation and depletion calculations. MCNPX runs a steady-state calculation to determine 63-group neutron fluxes, which are then energy-integrated with nuclide transport cross-sections resulting in reaction rates. CINDER90 takes the MCNPX-generated data, including reaction rates, collapses the 63-group cross-sections into a one-group cross-section and performs the depletion calculation to obtain new isotopic compositions for the next time step. This process is repeated for each burnup time step, specified by the user, until the entire core burnup simulation is completed.[27]

Solving for the time-dependent change in an isotope composition requires accounting for nuclear reactions which causes a production or loss of the nuclide, and may be described by the Bateman equations.[26] A simplified form of the Bateman equations for a specified isotope is[26,27]

$$\frac{dN_i}{dt} = -N_i(t)\beta_i + \overline{Y}_i + \sum N_k(t)\gamma_{k\rightarrow i} \tag{3}$$

where:

$\frac{dN_i}{dt}$ = time-dependent change in isotope i,

$N_i(t)$ = the time-dependent atom density of isotope i,

β_i = the total transmutation probability of isotope i,

$\overline{Y}_i$ = production of isotope i via an external source, and

$\gamma_{k\rightarrow i}$ = the probability of an isotope k transmuting, by decay or absorption, into isotope i.

Equation 3 is nonlinear because the transmutation probabilities rely on the time-integrated flux, which is also reliant upon the time-dependent isotope compositions.[27] To make the equation linear, the assumption must be made that the transmutation probabilities remain constant over the time step. This assumption thus requires attention when selecting the number and duration of time steps. A larger number of steps means more computational run time, however a time step of a long duration may not be sufficiently accurate in accounting for composition transmutations. In CINDER90, the set of coupled differential equations is reduced to a set of linear differential equations using the Markov Linear Chain method.[26] Linear chains are created for each isotope transmutation path, starting from the initial concentrations:

$$\frac{dN_i}{dt} = -N_i(t)\beta_i + \overline{Y}_i + N_{i-1}(t)\gamma_{i-1} \tag{4}$$

where γ_{i-1} is the transmutation probability of forming isotope N_i.[27] The solution to each linear chain determines a partial isotope composition, which is then summed to obtain the total isotope inventory. Because of the use of these linear chains, the isotopic inventory is only coupled to preceding elements in the sequence, where the parameters are assumed known.[26] The general solution to such a linear sequence is as follows:[26,27]

$$N_n(t) = \prod_{k=1}^{n-1} \gamma_k \left\{ \overline{Y}_m \left[\frac{1}{\prod_{l=1}^{n} \beta_l} - \sum_{j=1}^{n} \frac{e^{-\beta_j t}}{\prod_{i=1,\neq j}^{n} (\beta_i - \beta_j)} \right] + N_1^0 \sum_{j=1}^{n} \frac{e^{-\beta_j t}}{\prod_{i=1,\neq j}^{n} (\beta_i - \beta_j)} \right\} \tag{5}$$

II.F. ORIGEN & Matrix Exponential Method

Multiple depletion codes exist with a commonly used system being ORIGEN2.2.[28] The point-depletion and radioactive-decay code can simulate nuclear fuel cycles and calculate nuclide compositions and characteristics of materials contained in the nuclear fuel.[28] Both ORIGEN2.2 and CINDER90 are zero dimensional depletion codes that can be linked to MCNP flux generation, but the two codes solve the depletion equation differently. CINDER90 utilizes the Markov Linear Chain Method whereas ORIGEN2.2 is based on the Matrix Exponential Method. The basic equation ORIGEN solves is the first order differential equation for nuclide decay. The solution method will be a matrix of first order differential equations of size N x N, with N being the number of nuclides. The large sparse matrix requires a large amount of memory in order to store all the necessary computations.[26] Thus, to accelerate calculations the number of nuclides followed in the set of equations is limited. ORIGEN2.2 has the ability to track 1700 isotopes, while the CINDER90 library contains 3456 isotopes. Due to the current research work's interest in predicting and analyzing quantities for a vast number of fission product isotopes, CINDER90 was chosen as the ideal isotope generation and depletion code for use.

III. PFBR CORE MODELING AND FUEL BURNUP SIMULATIONS

III.A. PFBR Model & Simulation

In simulating the operation of the PFBR, a detailed pin-by-pin 3D model of the PFBR core was created with MCNPX-2.7. An input deck is attached in Appendix A. As stated previously, the PFBR core is comprised of inner core sub-assemblies, outer core sub-assemblies, and radial blanket (RB) sub-assemblies. The inner and outer core sub-assemblies are geometrically identical with varying fuel enrichments. Cross-sectional views of the fuel pin arrangements for a core sub-assembly and a radial blanket sub-assembly, as generated by MCNP, can be seen in Figure 6.

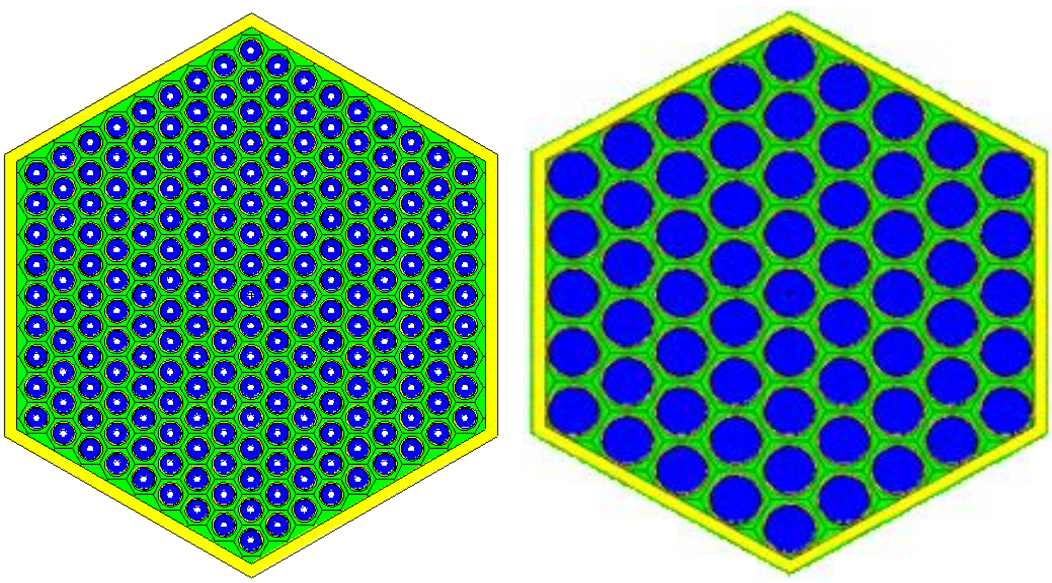

(Core fuel sub-assembly) (Radial Blanket sub-assembly)

Figure 6. Fuel pin arrangement for core and radial blanket sub-assemblies.

To realistically simulate reactor operations a separate input deck had to be developed for every refueling cycle, which consisted of 180 days full-power operation followed by 60 days of refueling shutdown and decay. The first input deck was built for the fresh PFBR core and two input decks were built, each having material comprised of the predecessor's output, to accurately simulate the refueling and altering of the core as it reached an equilibrium core configuration in the third fuel cycle. When the equilibrium core configuration is reached, the subsequent cycles will continue to have the same core configuration as the equilibrium core. The MCNPX simulations are computer intensive. The run time for each simulation was just above 30 days while running in parallel on a 32 core, 2.7 GHz, 64 GB RAM machine. These computer simulations provided an estimate of the plutonium composition and fission product composition within the discharged PFBR blanket fuel.

MCNPX output data was analyzed to perform checks on the accuracy of the model simulations. The global parameter, neutron multiplication factor (k_{eff}), was obtained for each step and plotted versus time. The values of k_{eff} as a function of time for the first three cycles of operation, shown in Figure 7, were compared with expected values[22] and were seen to behave as anticipated. The value for k_{eff} is larger than 1.0 because the lack of control rods in the model. As can be seen in Figure 5 the reactor control rods are not in close proximity to the radial blanket, and therefore the lack of control rods in the model simulations will not have an impact on the radial blanket results. The neutron energy spectrum calculated by MCNPX was used as another check to the model. Figure 8 displays the neutron spectra in the inner core, outer core, and radial blanket regions. The shape of the neutron spectra are as expected and matched the values for the average neutron flux throughout the PFBR found in Chirayath et al.[22] The dominant neutron energy in the inner and outer core can be seen from Figure 8 as between 100 keV to 400 keV. The radial blanket spectrum is slightly softer than the active core, indicative of the small thermalization from the oxygen of the MOX fuel as the neutrons' travel length increases.

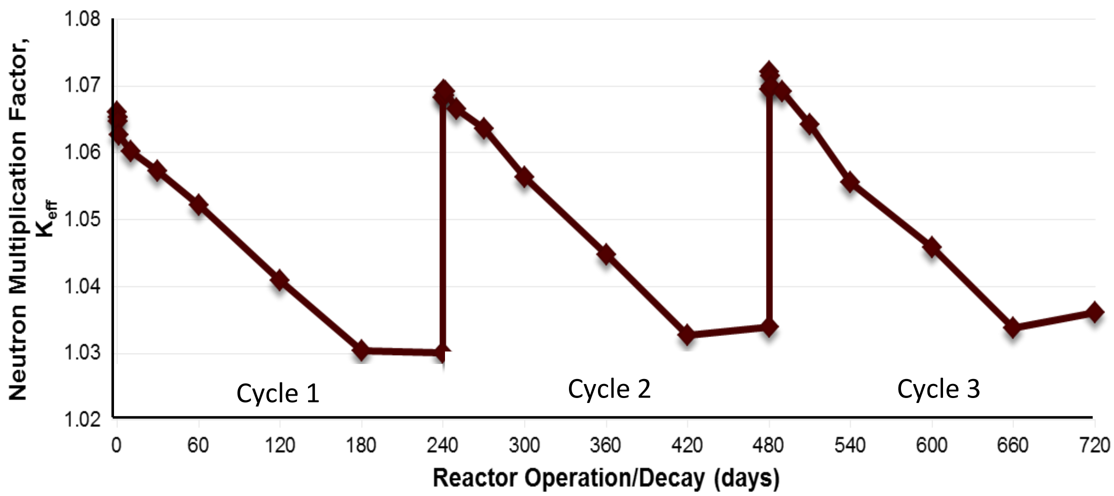

Figure 7. Variation of k_{eff} as a function of reactor operation.

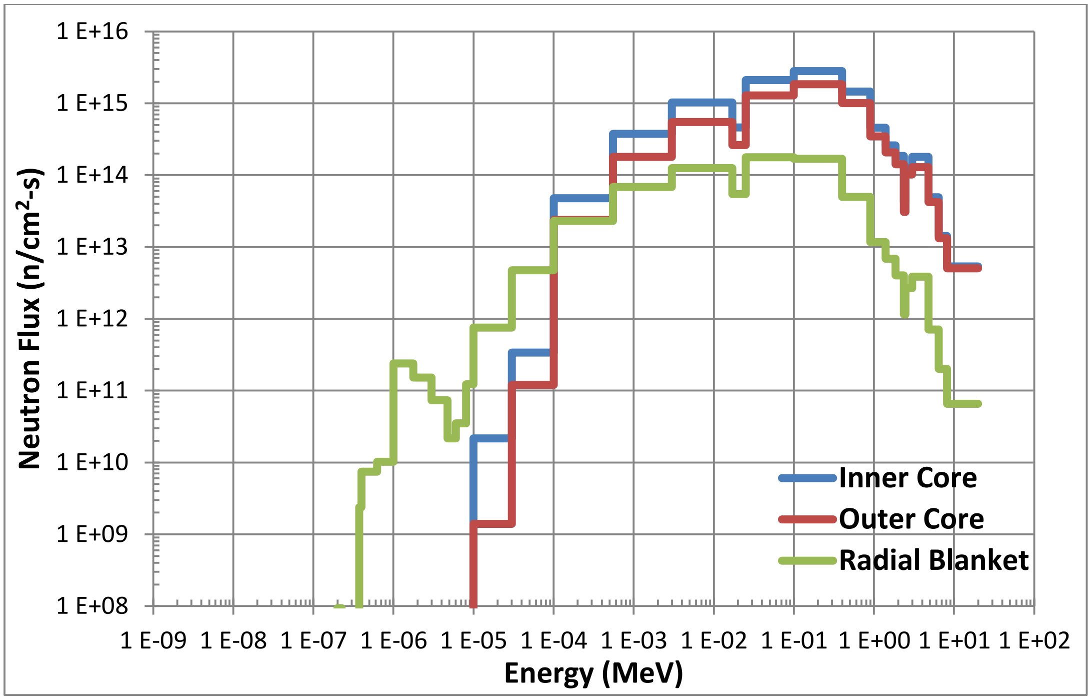

Figure 8. MCNPX-generated neutron energy spectra for the Indian PFBR core.

The standard operating scheme of the PFBR will be cycles of 180 days full-power operation followed by 60 days shutdown and refueling, with one-third of the active core being refueled at the end of each cycle.[22] Conversely, the radial blanket sub-assemblies are refueled with a slightly different pattern, yet still on the basis of fuel burnup. Typical operation of the PFBR will be to discharge the radial blanket sub-assemblies during the refueling stage in which the burnup is nearest to 1 MWd/kg. Thus the radial blanket is split into three sections. Forty-two blanket sub-assemblies, which are in close proximity to the core, and therefore exposed to a large neutron flux, are replaced after every cycle of 180 days. Six radial blanket sub-assemblies are refueled after every two cycles, and seventy-two blanket sub-assemblies that are located farther from the core are irradiated for three cycles before being refueled. Figure 9 displays a core map of the PFBR, highlighting the three radial blanket groups. The radial blanket sub-assemblies which are replaced after a single cycle are shown in red, two cycles in yellow, and the sub-assemblies which are irradiated for three cycles before being replaced are shown in blue. Table III gives the fuel burnup estimated through MCNPX simulations for each radial blanket group at the end of life. It can be seen that the group which is exposed to three irradiation cycles reaches a burnup closest to the target of 1 MWd/kg. Therefore the "three cycles" group of radial blanket sub-assemblies is the material of reference for the analyses and isotope selection described later.

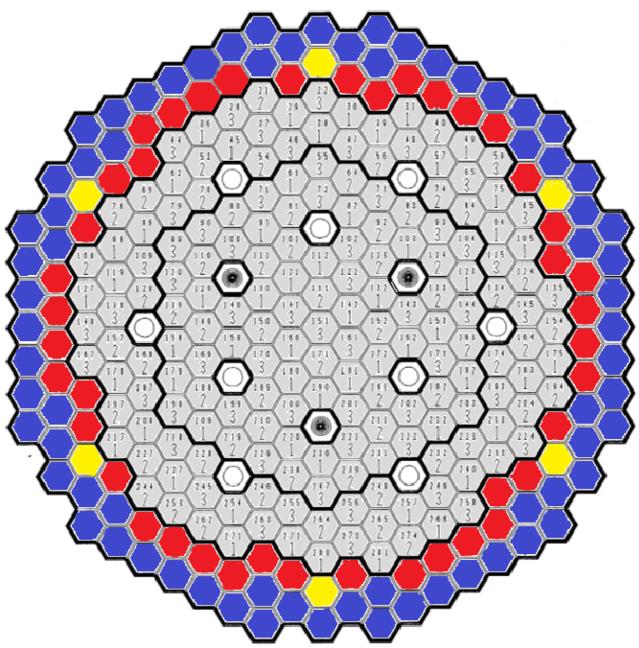

Figure 9. Core map highlighting the three radial blanket refueling groups.

Table III

End of life burnup level for radial blanket groups.

Irradiation Time & No. of RB Assemblies Discharged	Burnup (MWd/kg)
One Cycle (42 RBs)	0.710
Two Cycles (6 RBs)	1.302
Three Cycles (72 RBs)	1.016

III.B. Radial Splitting

As mentioned in the previous chapter, CINDER90 is a zero-dimensional depletion code and therefore has no knowledge of the spatial dependence of the transmutation rates.[26] CINDER90 assumes the flux in each burned material is not spatially dependent throughout that material. This averaging of the flux over each material region may affect the isotope concentrations if the spatial dependence of the flux would result in overall transmutation rates significantly different from the average. If necessary, splitting the material region can reduce the magnitude and the effects of the average flux.

The cylindrical fuel pins of the PFBR radial blanket can be split both radially and axially. Radially, transmutation rates may change with the flux and neutron properties as the neutron travels through the fuel. However, the fast neutrons of the PFBR are at high energies. Analytic calculations showed that the mean free path of neutrons at energies common in the PFBR are more than five times larger than the diameter of the radial blanket fuel pins. Thus, there is no need to radially split the fuel pins due to the fast neutron spectrum.

III.C. Axial Splitting & Super Cell

Figure 10 shows the neutron flux profile as a function of core height for the outer core and the radial blanket groups obtained by running 20E+6 histories (or 20 Megahistories). It is clear that the neutron flux is not constant along the height of the fuel pin, which may affect the final isotopic concentrations from inaccurate burn and production as a result of the difference between the local flux and average flux. To test if, and how many, axial regions are needed, a case should be modeled with increasing axial regions until the resultant data converges. A full-core cycle simulation is too computer intensive, though, to run multiple times. Consequently, a super cell was modeled to accurately represent the full core, while at the same time being small and simple. An MCNPX-generated image of the super cell can be seen in Figure 11.

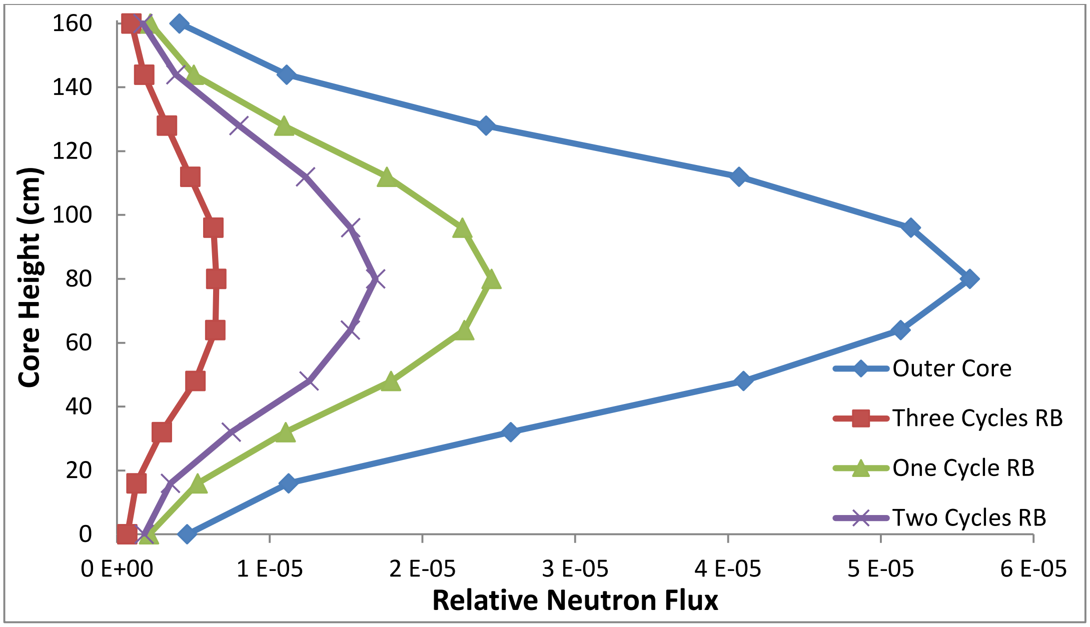

Figure 10. Flux profile as a function of pin height.

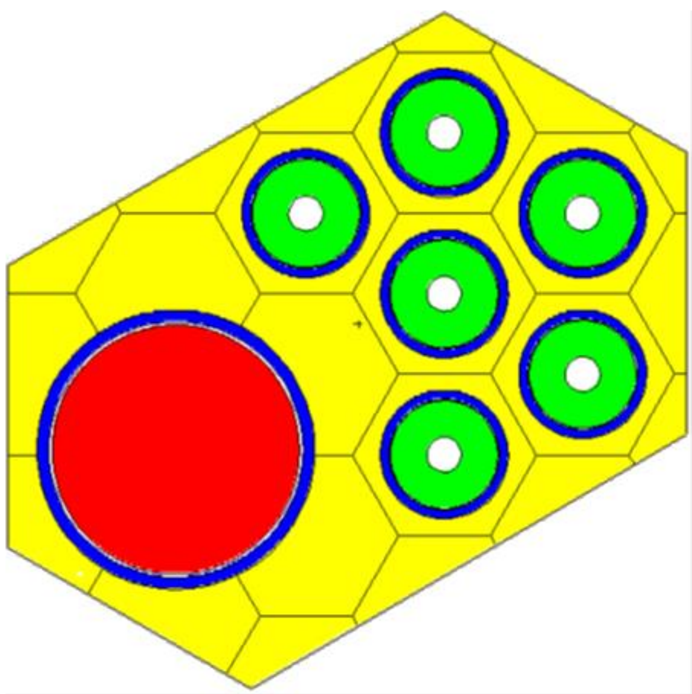

Figure 11. MCNP-generated image of the super cell model.

A super cell was used to determine the appropriate number of axial regions to split the radial blanket pins into. The small and simple super cell model has a short run time and is therefore conducive to several replications. The super cell consists of six outer core fuel pins at the same pitch found in the full core, and a radial blanket fuel pin appropriately placed from the outer core fuel pins and the boundary. The six faces comprising the elongated hexagon have a reflecting boundary condition. This design resulted in a neutron multiplication factor, k_{eff}, for the system of about one. The power of the super cell was set to achieve the same neutron flux as in the full core, and the radial blanket material was burned to the target, 1 MWd/kg.

Simulation of the super cell was repeated four times with 1, 3, 5, and 7 axial regions. For each simulation, the amounts of ^{137}Cs and total plutonium were summed up for the entire radial blanket pin. The results from the super cell simulations are shown in Table IV. For the mass of plutonium the relative error was less than 0.1%, and for the masses of ^{134}Cs, ^{137}Cs, ^{148}Nd, and ^{150}Sm the relative errors were all around 2%. This error was deemed insignificant, and a single axial region was used in the subsequent full core simulations. Thus, for simplicity of the model and shorter computational run time, the blanket fuel pins were not split axially.

Table IV

Super cell simulation results for axial splitting.

Number of Axial Regions	^{134}Cs mass (g)	^{137}Cs mass (g)	^{148}Nd mass (g)	^{150}Sm mass (g)	Plutonium mass (g)
1	1.294 E-4	3.827 E-2	1.374 E-2	2.033 E-4	6.726
3	1.336 E-4	3.843 E-2	1.367 E-2	1.906 E-4	6.716
5	1.356 E-4	3.842 E-2	1.366 E-2	1.921 E-4	6.719
7	1.372 E-4	3.848 E-2	1.368 E-2	1.943 E-4	6.716

III.D. MODEL VERIFICATION

After verifying the neutron energy spectrum and time-dependent multiplication factor (k_{eff}) discussed in section III.A, further model verifications were made. To verify the reactor simulation, the production behaviors of a few select isotopes of interest were analyzed. The isotope mass within each radial blanket (RB) region was plotted as a function of fuel burnup and compared to expected behavior. Mass buildup of ^{137}Cs, ^{148}Nd, ^{134}Cs, and ^{239}Pu are displayed in Figures 12, 13, 14, and 15, respectively.

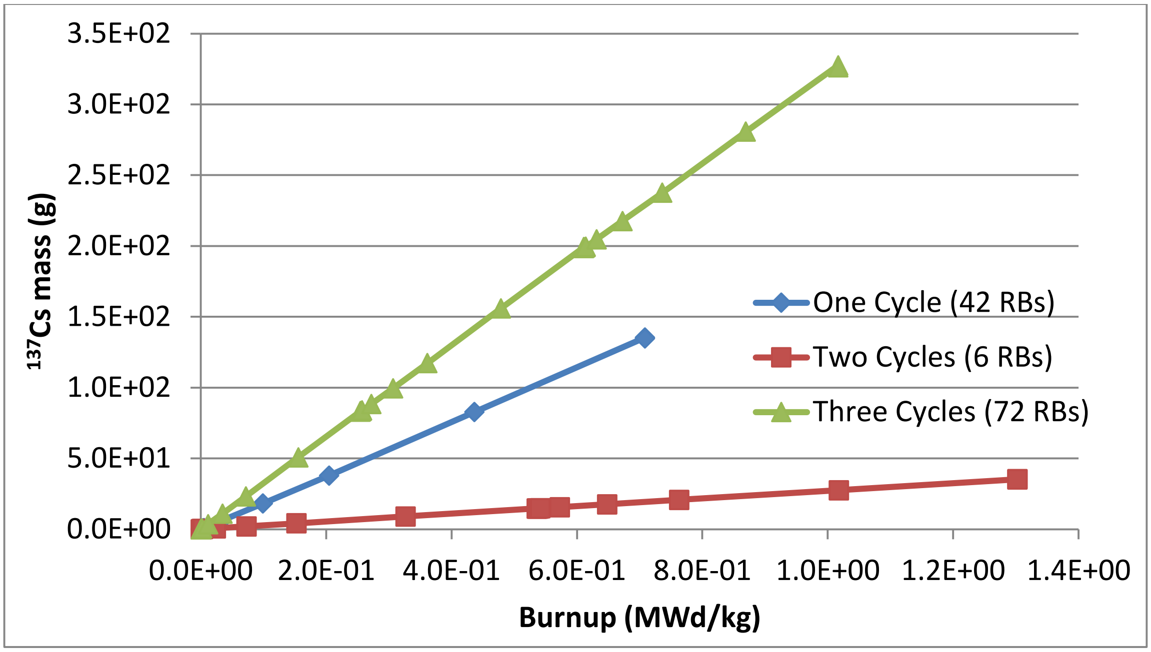

Figure 12. Production of ^{137}Cs as a function of burnup in radial blanket regions.

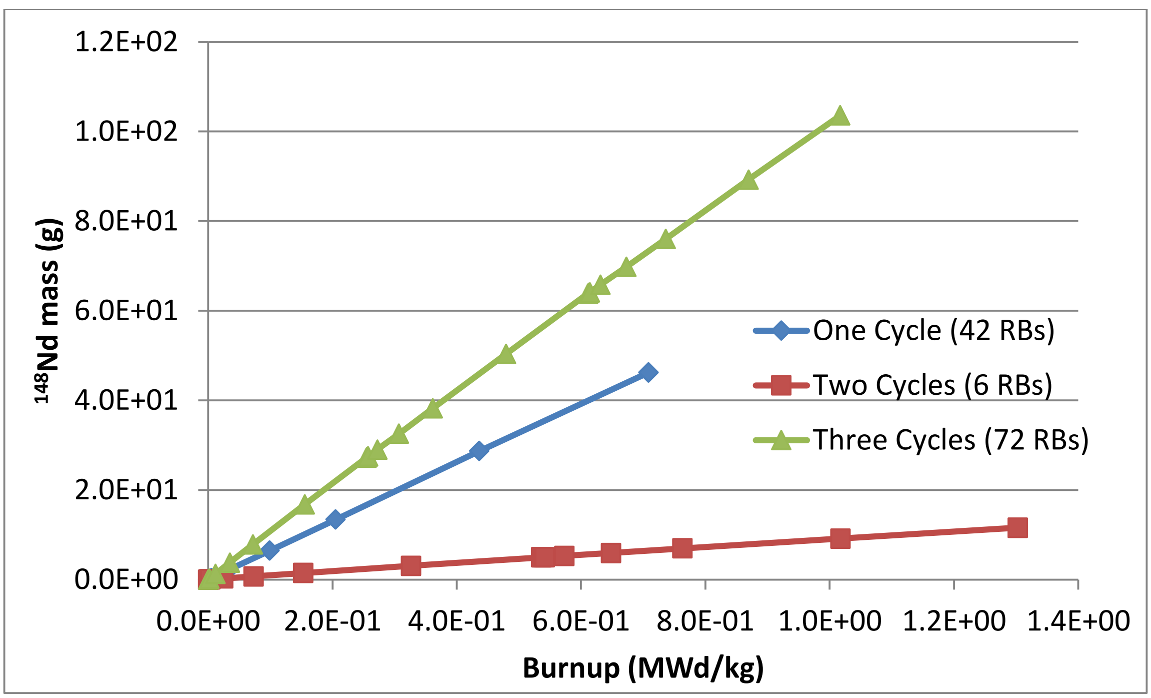

Figure 13. Production of ^{148}Nd as a function of burnup in radial blanket regions.

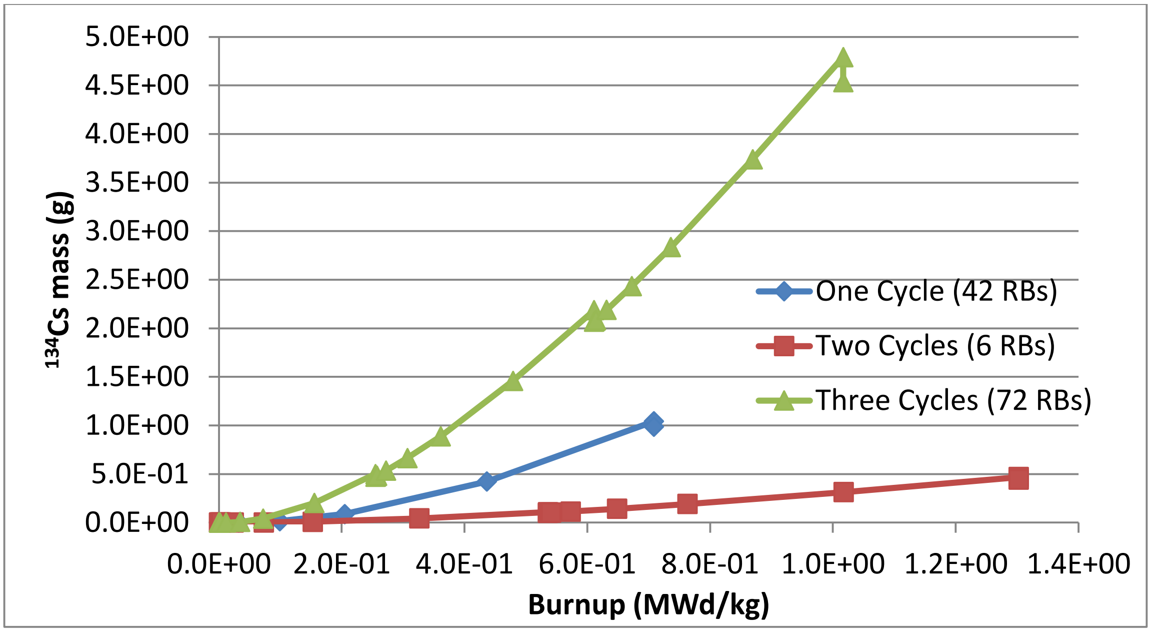

Figure 14. Production of ^{134}Cs as a function of burnup in radial blanket regions.

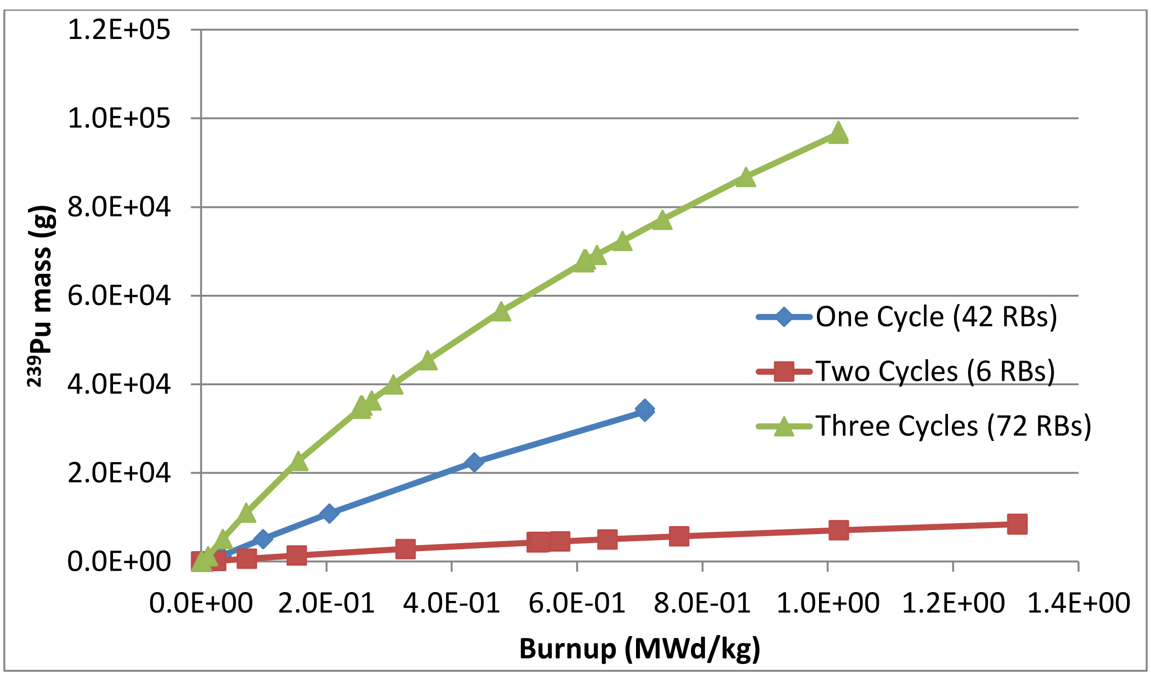

Figure 15. Production of ^{239}Pu as a function of burnup in radial blanket regions.

For each isotope, the isotope production versus material burnup is plotted for the three radial blanket regions. The difference in the rates of production for the three radial blanket regions is due to the mass of fuel, or number of radial blanket sub-assemblies. Forty-two, six and seventy-two radial blanket sub-assemblies are refueled in one cycle, two cycles and three cycles respectively. For all four isotopes, when normalized by fuel mass in each region, the lines for isotope mass as a function of burnup all fall on top of one another, irrespective of the radial blanket region refueled. Both ^{137}Cs and ^{148}Nd are expected to increase linearly with burnup and are common burnup monitors.[29] Both isotopes are direct fission products, and have negligible neutron cross-sections for loss mechanisms.[30] During the 60-day shutdown periods no significant decay will occur as the half-life of ^{137}Cs is about 30.1 years and ^{148}Nd is stable. Two production methods exist for ^{134}Cs, as a direct fission product and from the neutron capture of the fission product ^{133}Cs. The neutron cross-sections for loss mechanisms of ^{134}Cs are insignificant.[30] The production of ^{134}Cs is, therefore, proportional to the square of the neutron flux.[29] With a short half-life of around 2.06 years, an observable amount of ^{134}Cs decays away during the 60-day shutdowns. The production of ^{239}Pu, as seen in equation 1, is nearly linear at low levels of fuel burnup. However, due to the cross-sections for radiative capture and fission the amount of ^{239}Pu approaches an asymptotic composition.[30] Figures 12 through 15 match the expected production behavior of the four selected isotopes, indicating the model is correctly simulating reality.

IV. RESULTS AND DISCUSSIONS

IV.A. Plutonium Production

The significant quantity (SQ), defined as the approximate amount of nuclear material for which the possibility of manufacturing a nuclear explosive device cannot be excluded, is 8 kg for plutonium.[31] Estimations for the amount of plutonium produced, as well as isotopic composition, in the PFBR radial blanket were obtained using MCNPX-2.7 burnup simulations. Results from the simulations for the three radial blanket regions are shown in Table V. Model simulations show that the PFBR does, in fact, produce high quality plutonium on a large scale. Based on the concentrations of ^{239}Pu , ^{240}Pu, and the grade definitions found in Table I, the resulting plutonium is categorized as super-grade. With three radial blanket regions and their various refueling frequencies, a refueling pattern is repeated every six cycles. Table VI shows the pattern and the mass of plutonium discharged at the end of each refueling cycle. Six full refueling cycles equals 1440 days, or almost four years. In this period, 432.9 kg of plutonium will be discharged from the radial blanket regions. On average, standard operation of PFBR will yield over 100 kg per year of super-grade, weapons-usable plutonium, from the radial blankets alone.

Table V

Plutonium produced in the PFBR radial blanket regions at the end of the regions' life.

Irradiation Time (Number of Cycles)	No. of Assem-blies	Burnup (MWd/kg)	Total Mass of Plutonium (kg)	Plutonium Isotopes (%)				
				^{238}Pu	^{239}Pu	^{240}Pu	^{241}Pu	^{242}Pu
3	72	1.0157	99.06	0.0052	98.05	1.907	0.0382	0.00028
2	6	1.3023	8.664	0.0074	98.24	1.729	0.0236	0.00016
1	42	0.7096	34.85	0.0047	99.01	0.975	0.0073	0.00003

Table VI

Plutonium yield from the PFBR radial blanket regions.

Cycle Number	Days	Mass of Plutonium Discharged From One Cycle RB Group	Mass of Plutonium Discharged From Two Cycles RB Group	Mass of Plutonium Discharged From Three Cycles RB Group
1	240	34.8 kg	-	-
2	480	34.8 kg	8.7 kg	-
3	720	34.8 kg	-	99.0 kg
4	960	34.8 kg	8.7 kg	-
5	1200	34.8 kg	-	-
6	1440	34.8 kg	8.7 kg	99.0 kg

IV.B. Development & Selection of Isotopic Ratios

With output data obtained from reactor core physics and fuel burnup simulations, analyses of various isotopes were necessary for determining if isotopic characteristics exist within the material, which are unique to the PFBR. The ultimate goal being the development of a suite of isotopic ratios capable of attributing the source reactor from which separated weapons-grade plutonium would have been extracted. As mentioned previously, the “three cycles” radial blanket group comes closest to the target fuel burnup of 1 MWd/kg, and is the material of reference for isotopic analysis. The MCNPX output prints mass and radioactivity data for all the isotopes present in the irradiated fuel, which has mass above a threshold limit. The default threshold limit for isotope mass is 1E-10 grams.[23] Table XII, attached in Appendix B, contains mass and activity information for all isotopes existing at the end of the last 60-day decay period, for the three cycles material.

It would be extremely time consuming to measure every isotope present within the material. Therefore, certain characteristics were evaluated in determining which isotopes would be selected for the fission product to plutonium ratio analysis. Selected isotopes are reported in Table VII, as the expected mass and activity of each isotope which would be present in 1 kg of PUREX separated plutonium. One benefit to reporting the selected isotopes as ratios per mass of plutonium is the ability to scale the data to the mass of the interdicted weapons-grade plutonium. Selection was based on (a) the amount of isotope production, at least a few pico-grams per kg of plutonium, (b) the probability of detection (high gamma energy > 100 keV, long half-life > 100 days, high radioactivity > 1 micro-curie), (c) reactor type dependency in isotope production, and (d) the PUREX plutonium reprocessing decontamination factor (DF) of the isotope. Specific decontamination factors on an elemental basis could not be found in open literature; hence, a DF of 10^6 was applied universally. Although, the same DF is applied to all isotopes, with the exception of plutonium, it is still an important characteristic. Given that the material is separated, fission products will be reduced to trace contaminants in the nearly pure plutonium. For fission products with a small amount of production, the inclusion of a DF from separation results in levels which are undetectable. In Table VII, the isotopes are classified into four groups namely, Prompt Gamma, Delayed Alpha, Other Gamma, and Mass Spectrometry based on the type of detection and how fast results can be obtained. Results can be acquired in a few hours with gamma spectroscopy, whereas it can require on the order of a days and weeks for alpha spectroscopy and mass spectrometry processes, respectively.

Table VII

Selected isotopes per kg of PUREX processed plutonium from PFBR radial blanket fuel.

Candidate Isotope	Expected mass (g) per 1 kg Pu with DF of 10^6	Expected activity (Ci) per 1 kg Pu with DF of 10^6
Prompt Gamma		
^{137}Cs	3.29E-06	2.87E-04
^{144}Ce	1.12E-06	3.57E-03
Delayed Alpha		
^{239}Pu	9.81E+02	6.08E+01
^{242}Pu	2.83E-03	1.12E-05
Other Gamma		
^{134}Cs	4.12E-08	5.33E-05
^{125}Sb	3.99E-08	4.19E-05
^{154}Eu	1.41E-08	3.80E-06
Mass Spectrometry		
^{85}Rb	1.97E-07	Stable Isotope
^{90}Sr	1.09E-06	1.54E-04
^{148}Nd	1.05E-06	Stable Isotope
^{147}Pm	9.56E-07	8.87E-04
^{150}Sm	6.17E-08	Stable Isotope

Table VII contains data on the expected mass and expected radioactivity of selected isotopes within a kilogram of separated weapons-grade plutonium produced in the radial blanket of the PFBR. The same data was collected from the fuel of an Indian PHWR discharged at 1 MWD/kg.[12] The ratio of isotope mass per unit plutonium from the PHWR divided by the isotope mass per unit plutonium from the PFBR depicts the isotope ratio's reactor dependency. These values are given in Table VIII. Several important observations can be drawn from Table VII and Table VIII and are discussed in the following paragraphs.

Table VIII

Reactor dependency of selected isotope ratios

Candidate Isotope	Ratio of expected mass PHWR/PFBR
Prompt Gamma	
^{137}Cs	12.86
^{144}Ce	28.80
Delayed Alpha	
^{239}Pu	0.98
^{242}Pu	19.77
Other Gamma	
^{134}Cs	3.16
^{125}Sb	5.93
^{154}Eu	3.72
Mass Spectrometry	
^{85}Rb	19.00
^{90}Sr	22.29
^{148}Nd	12.51
^{147}Pm	15.48
^{150}Sm	107.99

The radioactivity concentration of ^{137}Cs and ^{144}Ce isotopes are sufficiently high in 1 kg of plutonium and gamma spectroscopy measurements can be made quickly (prompt measurements) once such material has been interdicted. Both ^{137}Cs and ^{134}Ce undergo beta radiation decay followed by gamma emissions of 662 keV and 134 keV, respectively. The commonly used burnup monitor, ^{137}Cs, is an interesting isotope to note when being used to display a reactor dependency.

We found that selected fission product to plutonium ratios provide more information and result in larger differences between reactors, than just the isotope mass. The radio-isotope ^{137}Cs, for example, is an attractive isotope for selection. The individual fission yield is high at around 6%, it has a long half-life of over 30 years, and the gamma radiation is easily measurable. However, ^{137}Cs is a direct fission product with a fission yield that is constant regardless of fissile isotope or neutron energy. The amount of ^{137}Cs can provide information on the burnup of a material but no information regarding the source reactor. The ratio of ^{137}Cs to plutonium, though, is found in this study to result in a significant difference between the PFBR and PHWR. The ratios of fission products to plutonium have the ability to decipher between fast and thermal reactors. This is due, in large part, to the amount of plutonium the PFBR breeds. The PFBR has a larger percentage of ^{238}U in the depleted uranium fuel in addition to the effect of a fast neutron spectrum. Thus the PFBR radial blanket produces much more plutonium per initial loading of uranium (~1% of ^{238}U is converted to ^{239}Pu) than the PHWR.

The radioactivities of ^{239}Pu and ^{242}Pu isotopes are sufficiently high in 1 kg of plutonium and alpha spectroscopy measurements can be made. However, sample preparations are needed for performing alpha spectrometry, which makes this method slower than prompt gamma radiation measurements. Both ^{239}Pu and ^{242}Pu undergo alpha decay with energies of 5156 keV and 4901 keV, respectively. These alpha energies are distinct enough to be separately seen in the alpha spectra. A fast or thermal neutron spectrum irradiation of the fuel can likely be determined from an alpha or mass spectrometry measurement of ^{239}Pu and ^{242}Pu, alone. The PHWR to PFBR ratio of ^{239}Pu concentration is 0.98, while the ratio of ^{242}Pu concentration is 19.15. This indicates that much less ^{242}Pu is present in the plutonium produced in the fast spectrum. This is a result of the relative differences in neutron interaction cross-sections between absorption and fission at varying neutron energies. Lower concentrations of heavier plutonium isotopes, specifically ^{241}Pu and ^{242}Pu, are present in the PFBR blanket fuel due to fission being more likely than radiative capture at fast neutron energies.

The next set of isotopes ^{134}Cs, ^{125}Sb, and ^{154}Eu are again proposed to be measured via gamma spectroscopy. These three isotopes all decay via beta radiation and a subsequent gamma emission, with the gamma energies high enough to be detected easily. The radioactivity concentrations for these gamma emitting isotopes, however, are orders-of-magnitude less than the prompt gamma measurement isotopes, ^{137}Cs and ^{144}Ce. Mass spectrometry is anticipated as the measurement technique for ^{85}Rb, ^{90}Sr, ^{148}Nd, ^{147}Pm, and ^{150}Sm. The isotopes ^{85}Rb, ^{148}Nd, and ^{150}Sm are stable and are thus undetectable using radiation measurements. The isotopes ^{90}Sr and ^{147}Pm are pure beta radiation emitters without any gamma energy emissions. Additionally, isotopes having a range in values for both reactor dependency and isotope mass number were considered desirable during selection. Of the isotopes proposed to be measured using mass spectroscopy, ^{150}Sm is particularly significant. The PHWR to PFBR ratio of ^{150}Sm concentration is ~107, meaning plutonium produced in a thermal neutron spectrum will have two orders-of-magnitude more ^{150}Sm contamination than plutonium produced in a fast spectrum. The source of this large difference is a result of the radiative capture cross-section of the well-known fission product neutron poison, ^{149}Sm. The second most important neutron absorber in nuclear reactor physics, ^{149}Sm, has a very large cross-section for absorption of thermal neutrons. A plot obtained from reference 32of the ^{149}Sm radiative capture cross-section per incident neutron energy is shown in Figure 16.[32] The dominant neutron energy of the PFBR is 100 keV to 400 keV, whereas the dominant neutron energy of the PHWR is 0.01 eV to 0.1 eV. When applying these dominant neutron energies to the cross-section plot in Figure 16, it can be seen that the ^{149}Sm neutron absorption cross-section in the PFBR is less than 1 barn, while the ^{149}Sm neutron absorption cross-section in the PHWR is around 1E+5 barns (1 barn = 1E-24 cm^2).

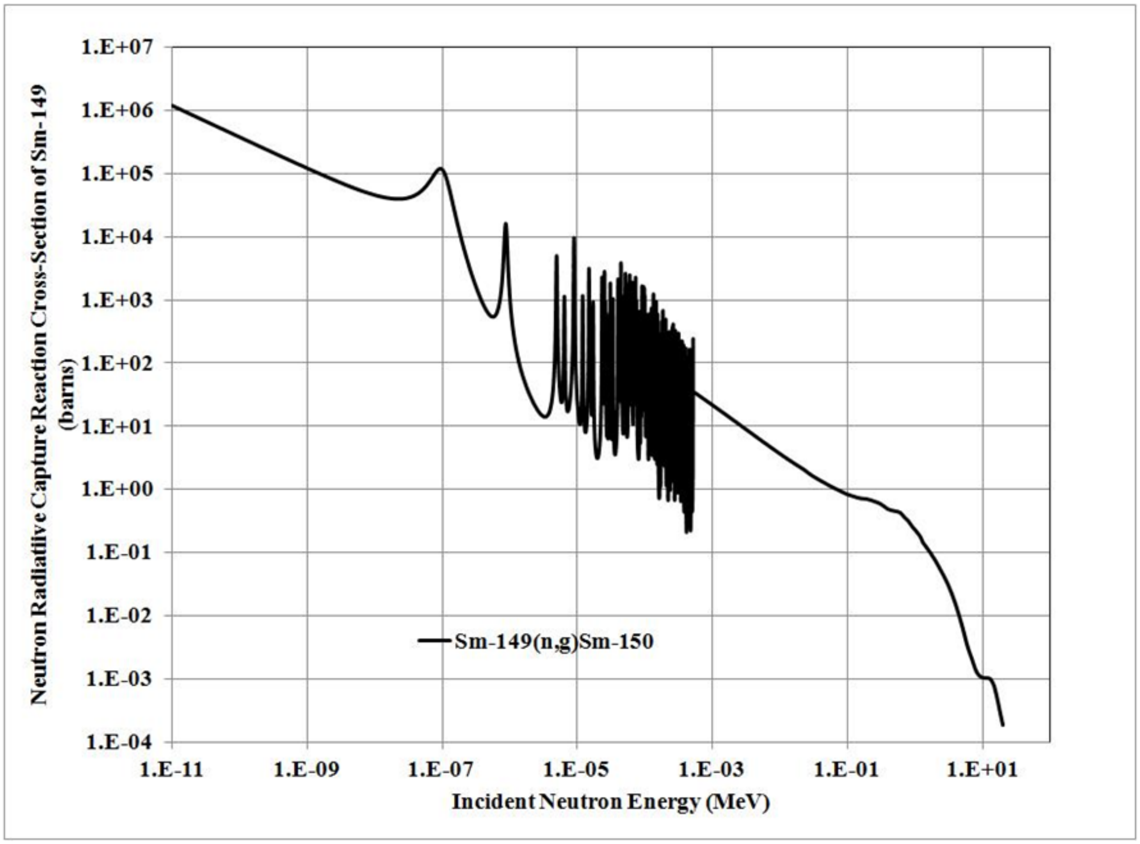

Figure 16. Plot of the neutron radiative capture cross-section for ^{149}Sm.

IV.C. Stochastic Uncertainty

The MCNPX code used to simulate core operation is based on the principles of stochastic methods for solving the Boltzmann radiation transport equation. Because of the stochastic nature of the solution method, the burnup simulations were repeated by altering the stochastic procedures to estimate the stochastic uncertainty associated with the predicted values of fission product and plutonium isotope concentrations. The cycle 1 simulation was repeated by changing the random number seed, changing the sampling procedures, and resulting in nine independent simulations. For every burnup time step in fuel cycle 1 (180-days), the average isotope concentration in radial blanket fuel (μ) and one sigma standard deviation (σ) values for each isotope were calculated from the results of the nine independent simulations. The issue came in propagating the random error calculated in cycle 1 to the final isotope concentrations at the end of cycle 3. However, it was found, by plotting the data for the selected isotope mass from the nine cycle-1 simulations (8 burnup time steps data points) that the variance (σ^2) increases roughly linearly with isotope mass. An example plot obtained for ^{137}Cs is shown in Figure 17. Similar plots for the other eleven selected isotopes showed the correlation between mass and variance. The regression line equation and fit for the twelve isotope plots are listed in Table IX. It was determined that, using the regression line equation, an estimate of the variance can be extrapolated out to the final isotope mass at the end of cycle 3. The variance was then adjusted for a larger sample size. The nine independent simulations were performed at an earlier time in the research with 9E+5 particle histories, while the final production simulations were run with 2E+7 histories. The larger number of particles increases the precision of the simulations; however, limits on computational time and power made running the nine independent simulations again with 2E+7 histories unviable. The relative random error (σ/μ) was thus obtained for the selected isotopes and is listed in Table X. From Table X it can be observed that the relative random error in predicted isotope concentrations are insignificant and are in the range of 0.019% to 0.054%. This small error indicates that the differences in isotopic compositions seen in the simulations are not due to the Monte Carlo method's random behavior.

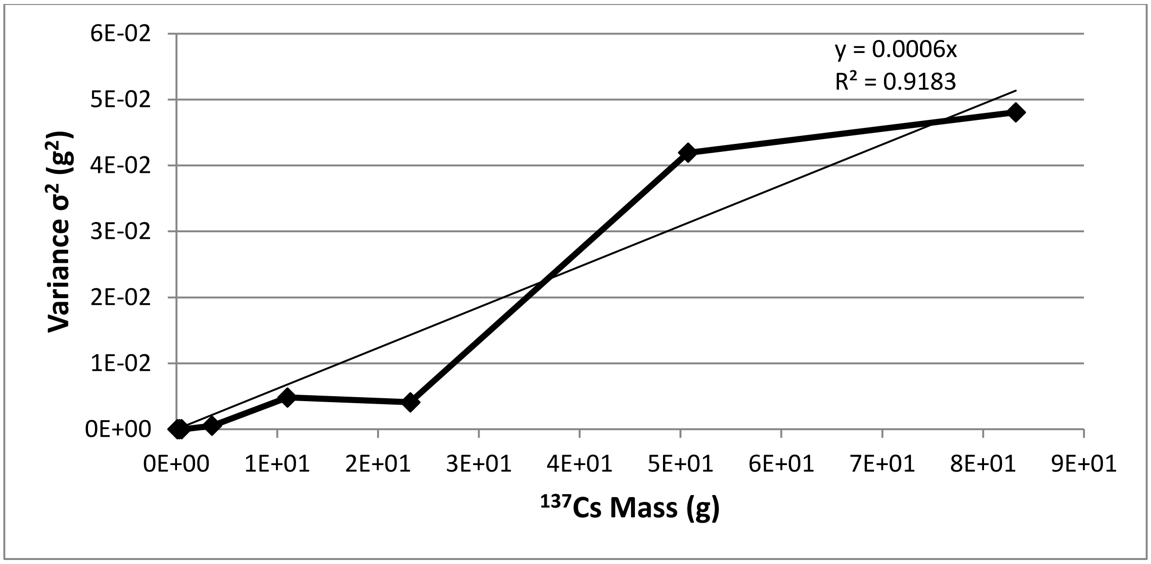

Figure 17. Plot of variance per average mass of ^{137}Cs from nine cycle-1 simulations.

Table IX

Linear regression equation and fit between variance and mass for the selected isotopes.

Isotope	Regression Line Equation*	Regression Line Fit (R^2)
^{137}Cs	y = 0.0006x	0.9183
^{144}Ce	y = 0.0004x	0.8896
^{239}Pu	y = 0.0819x	0.9243
^{242}Pu	y = (5.0E-6)x	1
^{134}Cs	y = (2.0E-5)x	0.9831
^{125}Sb	y = (5.0E-6)x	0.9468
^{154}Eu	y = (3.0E-6)x	0.9585
^{85}Rb	y = (3.0E-5)x	0.9178
^{90}Sr	y = (2.0E-4)x	0.8971
^{148}Nd	y = (3.0E-4)x	0.9450
^{147}Pm	y = (2.0E-4)x	0.9565
^{150}Sm	y = (4.0E-5)x	0.9920

*x being the respective mass of the isotope in grams

Table X

Stochastic uncertainty associated with MCNPX simulations.

Isotope	Relative Random Error (%)
^{137}Cs	0.029
^{144}Ce	0.040
^{239}Pu	0.019
^{242}Pu	0.090
^{134}Cs	0.047
^{125}Sb	0.024
^{154}Eu	0.031
^{85}Rb	0.026
^{90}Sr	0.029
^{148}Nd	0.036
^{147}Pm	0.031
^{150}Sm	0.054

The possibility exists for other sources of error in the model simulations that can affect the isotopic results. Monte Carlo methods have two types of uncertainties; random and systematic. Table X gives the random uncertainty associated with the Monte Carlo method for the twelve selected isotopes. The systematic uncertainty is associated with how close to reality the model is. We assume the systematic uncertainty is small. Uncertainty in the isotopes' neutron interaction cross-sections used in the simulation has the possibility to lead to larger error, however this analysis is beyond the scope of this thesis.

IV.D. Isotopic Ratios of the Same Element

Although the isotopes of an element behave very differently in nuclear reactions, they have very similar chemical properties. The fact that the isotopes of an element have similar chemical properties means they will behave similarly during PUREX chemical separation.[18] Therefore, select isotope ratios of the same element may infer details of the reactor system while being independent from the chemical separation process used. Table XI gives ratios of the mass of isotopes of the same element present in weapons-grade plutonium produced in a PFBR and PHWR. The values for the isotope ratios found in PHWR plutonium are then divided by the PFBR values to represent the reactor dependency of the isotope of the same element ratios.

Table XI

Mass ratios for isotopes of the same element.

Isotope Ratio	Ratio of Isotope Mass from PFBR	Ratio of Isotope Mass from PHWR	Reactor Comparison PHWR / PFBR
^{137}Cs / ^{134}Cs	8.00E+01	3.25E+02	4.07
^{144}Ce / ^{142}Ce	4.18E-01	8.04E-01	1.92
^{150}Sm / ^{154}Sm	5.04E-01	8.88E+00	17.6
^{242}Pu / ^{239}Pu	2.89E-06	5.83E-05	20.2

The ^{137}Cs / ^{134}Cs has an observable difference while the ratios of ^{150}Sm / ^{154}Sm and ^{242}Pu / ^{239}Pu both contain more than an order-of-magnitude difference between the

PFBR and PHWR. These three ratios could be measured by gamma spectroscopy, mass spectrometry, and alpha spectroscopy, respectively. It is therefore possible to deduce information of the producing reactor system from isotope ratios of the same element. The benefit of such ratios being, that there are no longer assumptions involved in determining which chemical separation process was used and applying the appropriate decontamination factors.

IV.E. Theoretical Procedures

In the event of an interdicted sample of weapons-grade plutonium multiple measurements of several sub-samples will be performed in order to obtain information on the material and its source as quickly as possible. Immediately gamma spectroscopy measurements will be started and within a few hours results can be drawn on the gamma emitting isotopes present in the material. Due to sample preparation times it is expected that results will be obtained from alpha spectroscopy and mass spectrometry on the order of a few days and a week, respectively. Measured isotopic results will be scaled based on the size of the sub-sample and compared with the expected mass of the selected isotopes in Table VII. As time progresses, results for more of the isotopes contained in Table VII will become available and the certainty in attributing the sample material to a fast or thermal neutron spectrum reactor type will increase.

V. CONCLUSIONS AND FUTURE WORK

V.A. Conclusions

The goal of this thesis was to develop a nuclear forensics capability for targeting plutonium produced in foreign fuel cycles. Monte Carlo computational radiation transport methods coupled with fuel burnup calculations were used to simulate the isotopic composition of plutonium produced in the radial blankets of the 500-MWe Indian Prototype Fast Breeder Reactor. Detailed investigation of fission product contaminants were analyzed to determine the feasibility of predicting intrinsic characteristics in separated weapons-grade plutonium produced by certain reactors, specifically a fast breeder reactor and thermal heavy water reactor. These two reactor types possess the capability to produce weapons-grade plutonium and will likely be operating in a non-safeguarded manner in some countries.

The radiation transport code, MCNPX-2.7, along with the burnup/depletion code, CINDER90, was used to computationally simulate the operation of the PFBR. The PFBR radial blanket fuel will be discharged with a low burnup of around 1 MWD/kg during normal operation; thus, resulting in the average production of around 100 kg of weapons-grade plutonium per year. The data output by MCNPX-2.7 for the fission product and actinide isotopics of the PFBR radial blankets were analyzed to develop isotopic ratios expected to be present in separated weapons-grade plutonium which was produced in an FBR.

Isotope selection was based on four criteria: the amount of isotope production, the probability of isotope detection, the magnitude of reactor type dependency in the isotope's production, and the PUREX decontamination factor. By using this selection criteria, down-selection of the possible isotopes resulted in a list of twelve isotopic ratios. The twelve selected isotopes include: ^{85}Rb, ^{90}Sr, ^{125}Sb, ^{134}Cs, ^{137}Cs, ^{144}Ce, ^{147}Pm, ^{148}Nd, ^{150}Sm, ^{154}Eu, ^{239}Pu, and ^{242}Pu. Table VII reports the expected mass and activity of the selected isotopes present in 1 kg of separated plutonium, which was produced in the PFBR radial blanket. In the event of an interdicted sample Table VII gives a scalable database for the amount of an isotope expected to be present in material produced in a fast reactor system to compare versus measurement data.

Evaluation of isotopic ratios between the PFBR and PHWR helped to select isotope ratios which contain information dependent upon the reactor system. Table VIII shows the magnitude of the reactor dependency for the selected isotopes. It is clearly indicated from Table VIII that the suite of selected isotopes can attribute the source of separated weapons-grade plutonium to a fast or thermal neutron reactor system. The significance of some isotopes stand out from Table VIII.

When normalizing to total plutonium the concentration of ^{137}Cs is an order-of-magnitude larger in the thermal neutron system. This is due to the efficiency of the FBR system at breeding plutonium out of uranium. The rate of ^{137}Cs production remains constant, while they fast breeder system produces ten times more plutonium per initial uranium loading than the thermal neutron system.

A fast or thermal neutron spectrum irradiation of the fuel can likely be determined from an alpha or mass spectrometry measurement of ^{239}Pu and ^{242}Pu, alone. The PHWR to PFBR ratio of ^{239}Pu concentration is 0.98, while the ratio of ^{242}Pu concentration is 19.15. Much less ^{242}Pu is present in the plutonium produced in the fast spectrum as a result of fission being more likely than radiative capture at fast neutron energies.

Of the isotopes proposed to be measured using mass spectroscopy, ^{150}Sm is the most significant. The PHWR to PFBR ratio of ^{150}Sm concentration is ~107, meaning plutonium produced in a thermal neutron spectrum will have two orders-of-magnitude more ^{150}Sm contamination than plutonium produced in a fast spectrum. The source of this drastic ^{150}Sm difference is the very large thermal neutron absorption cross-section of the fission product poison, ^{149}Sm.

Lastly, isotope ratios of the same element were explored. The ratios of ^{137}Cs / ^{134}Cs, ^{150}Sm / ^{154}Sm, and ^{242}Pu / ^{239}Pu show that such ratios may lead to attribution of a source reactor system, while being independent of the chemical separation process used for plutonium separation.

In conclusion, the computational results indicate a suite of selected isotopic ratios can attribute separated weapons-grade plutonium to a fast or thermal neutron source reactor system.

V.B. Future Work

Experimental data is vital to the verification of the computational results. To accomplish this, samples of depleted UO_2 were irradiated at the Oak Ridge National

Laboratory – High Flux Isotope Reactor (ORNL-HFIR) facility. An image of the HFIR core can be seen in Figure 18.[33] Depleted UO_2 fuel samples were irradiated in a simulated fast neutron spectrum to replicate the PFBR irradiation. The samples were burnt to achieve a burnup between 0.85 – 1.25 MWd/kg. To achieve the fast spectrum, a gadolinium sheath was placed around the fuel samples during irradiation. The high thermal neutron absorption of gadolinium was expected to create a fast neutron spectrum environment with a fast to thermal flux ratio of ≥ 100.

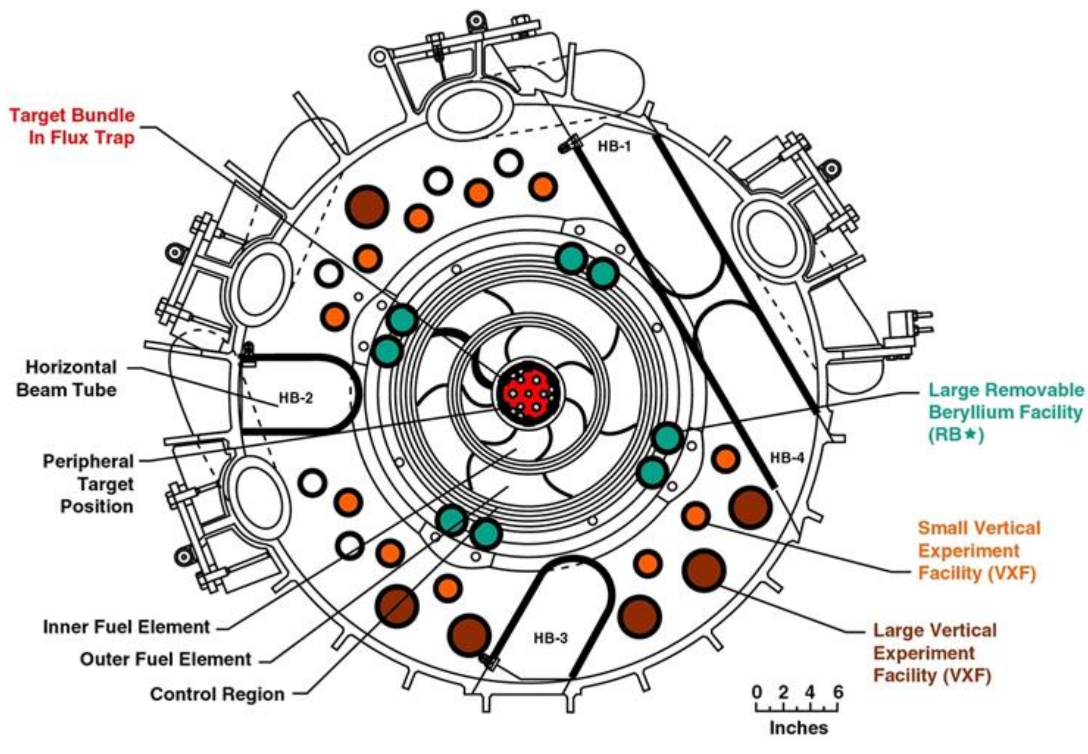

Figure 18. Image of the HFIR core.

The irradiated samples were received by Texas A&M University for chemical reprocessing. A lab scale PUREX process will be performed to separate the plutonium from fission products and uranium. The PUREX process was chosen for this research because it is the most commonly employed reprocessing technique currently in use at reprocessing facilities worldwide, including India. A challenge involved with using the PUREX process is attempting to accurately simulate this process in a laboratory setting. It is believed though, that reprocessing of weapons-grade plutonium will likely occur in a small batch process.

An MCNPX model of the ORNL-HFIR core will be completed with the fuel samples, sample holder, and gadolinium sheath in the irradiation location. Although the PFBR model is simulating the Indian PFBR, the fuel samples are being irradiated in a replicated fast neutron spectrum at HFIR. Thus, accuracy in the HFIR simulation when compared to the experimental samples will provide confidence in the MCNPX models, indirectly verifying the selected isotopes from the PFBR simulation.

Similar to the depleted UO_2 samples, samples of natural UO_2 will be irradiated at the ORNL-HFIR facility in the future. The natural UO_2 fuel samples will be irradiated in a thermal neutron spectrum to replicate the PHWR irradiation. Again, the burnup of the fuel will be to a level near 1 MWd/kg. The lab scale PUREX process will be repeated, as will an MCNPX model of the ORNL-HFIR core with the natural UO_2 fuel samples in place. The measured isotopic data will then be compared with the computational results in order to verify the PHWR model and simulations.

REFERENCES

1. H.R. 730 – 111th Congress, "Nuclear Forensics and Attribution Act," (2010). http://www.govtrack.us/congress/bills/111/hr730

2. K. J. MOODY, I. HUTCHEON, and P. M. GRANT, *Nuclear Forensics Analysis*, Taylor & Francis Group, Boca Raton, Fla (2005).

3. M. R. STERNAT, "Development of Technical Nuclear Forensics for Spent Research Reactor Fuel." Doctoral dissertation, Texas A&M University, College Station, TX (2012). http : / /hdl .handle .net /1969 .1 /148202.

4. Joint Working Group of American Physics Society and the American Association for the Advancement of Science, "Nuclear Forensics: Role, State of the Art, and Program Needs," (2013). http://www.aaas.org/sites/default/files/migrate/uploads/Nuclear_Forensics.pdf

5. Knolls Atomic Power Laboratory, "Nuclides and Isotopes, Chart of the Nuclides, 16th edition" Schenectady, NY (2002).

6. J. C. MARK, "Explosive Properties of Reactor-Grade Plutonium," *Science and Global Security*, **4**, 111-128 (1993).

7. WNA, "Fast Neutron Reactors," (2013). http://www.world-nuclear.org/info/Current-and-Future-Generation/Fast-Neutron-Reactors/#.UbYnaPk3t8E

8. S. C. CHETAL, V. BALASUBRAMANIYAN, P. CHELLAPANDI, P. MOHANAKRISHNAN, P. PUTHIYAVINAYAGAM, C.P. PILLAI, S. RAGHUPATHY, T. K. SHANMUGHAM, C. S. PILLAI, "The Design of the Prototype Fast Breeder Reactor," *Nuclear Engineering and Design*, **236**, 852-860 (2006).

9. A. GLASER, M. V. RAMANA, "Weapon-Grade Plutonium Production Potential in the Indian Prototype Fast Breeder Reactor," *Science and Global Security*, **15**, 85-105 (2007).

10. Council on Foreign Relations, "Implementation of the Indian-United States Joint Statement of July 18, 2005: Indian's Separation Plan," (2005). http://www.cfr.org/india/implementation-india-united-states-joint-statement-july-18-2005-indias-separation-plan/p16861

11. S. S. BAJAJ, A. R. GORE, “The Indian PHWR,” *Nuclear Engineering and Design,* **236**, 701-722 (2006).

12. T. M. COLES, “Computational Nuclear Forensics Analysis of Weapons-Grade Plutonium Separated From Fuel Irradiated in a Thermal Reactor,” Master’s thesis, Texas A&M University, College Station, TX (2014).

13. W. S. CHARLTON, B. L. FEAREY, C.W. NAKHLEH, T. A. PARISH, R. T. PERRY, J. POTHS, J. R. QUAGLIANO, W. D. STANBRO, W. B. WILSON, “Operator Declaration Verification Technique for Spent Fuel at Reprocessing Facilities,” *Nuclear Instruments and Methods in Physics Research,* **B 168**, 98-108 (2000).

14. M. R. SCOTT, “Nuclear Forensics: Attributing the Source of Spent Fuel Used in an RDD Event,” Master’s thesis, Texas A&M University, College Station, TX (2005).
http://hdl.handle.net/1969.1/2368.

15. M. WALLENIUS, P. PEERANI, L. KOCH, “Origin Determination of Plutonium Material in Nuclear Forensics,” *Journal of Radioanalytical and Nuclear Chemistry,* **246**, 317-321 (2000).

16. A. GLASER, “Isotopic Signatures of Weapon-Grade Plutonium from Dedicated Natural Uranium-Fueled Production Reactors and Their Relevance for Nuclear Forensics Analysis,” *Nuclear Science and Engineering,* **163**, 26-33 (2009).

17. P. D. WILSON, *The Nuclear Fuel Cycle: From Ore to Waste*, Oxford University Press, New York, (2001).

18. M. BENEDICT, T. H. PIGFORD, and H. W. LEVI, *Nuclear Chemical Engineering*, Second Edition, McGraw-Hill Series in Nuclear Engineering, New York, (1981).

19. Department of Energy, “DOE Fundamentals Handbook, Nuclear Physics and Reactor Theory,” Vol. 2, 34, DOE-HDBK-1019/1-93, (1993).
http://energy.gov/sites/prod/files/2013/06/f2/h1019v1.pdf

20. Nuclear Energy Agency, “JANIS 3.4, ENDF/B-VII.1,” (2013).
http://www.oecd-nea.org/janis/

21. P. RODRIGUEZ, S. B. BHOJE, “The FBR Program in India,” *Energy,* **23**, 629-636 (1998).

22. S. S. CHIRAYATH, G. HOLLENBECK, J. RAGUSA, P. NELSON, "Neutronic and Nonproliferation Characteristics of (PuO_2-UO_2) and (PuO_2-ThO_2) as Fast Reactor Fuels," *Nuclear Engineering and Design*, **239**, 1916-1924, (2009).

23. D. B. PELOWITZ, Editor, *MCNPX User's Manual*, Version 2.7.0, LA-CP-11-00438 Los Alamos National Laboratory, Los Alamos, NM (April 2011).

24. X-5 Monte Carlo Team, *MCNP – A General Monte Carlo N-Particle Transport Code*, Version 5, LANL Report No. LA-UR-03-1987 Los Alamos National Laboratory, Los Alamos, NM (2005).

25. L. L. CARTER, E. D. CASHWELL, *Particle-Transport Simulation with the Monte Carlo Method*, Los Alamos National Laboratory, Los Alamos, NM (1975).

26. M. FENSIN, "Development of the MCNPX Depletion Capability: A Monte Carlo Linked Depletion Method That Automates the Coupling Between MCNPX and CINDER90 for High Fidelity Burnup Calculations," Doctoral dissertation, University of Florida, Gainesville, FL (2008). http://ufdcimages.uflib.ufl.edu/UF/E0/02/19/46/00001/fensin_m.pdf

27. J. HENDRICKS, G. MCKINNEY, M. FENSIN, M. JAMES, R. JOHNS, J. DURKEE, J. FINCH, D. PELOWITZ, L. WATERS, M. JOHNSON, F. GALLMEIER, *MCNPX 2.6.0 Extensions*, LA-UR-08-2216 Los Alamos National Laboratory, Los Alamos, NM (April 2008).

28. A. G. CROFF, "ORIGEN2: A Versatile Computer Code for Calculating the Nuclide Compositions and Characteristics of Nuclear Materials," *Nuclear Technology*, **62**, 335-352 (1983).

29. D. REILLY, N. ENSSLIN, H. SMITH, *Passive Nondestructive Assay of Nuclear Materials*, US Department of Commerce, National Technical Information Service, Springfield, VA (1991).

30. Korean Atomic Energy Research Institute, "Table of Nuclides," (2013). http://atom.kaeri.re.kr

31. IAEA, "Safeguards Glossary 2001 Edition," *International Nuclear Verification Series No.3*, Vienna (2002). http://www-pub.iaea.org/MTCD/publications/PDF/nvs-3-cd/PDF/NVS3_prn.pdf

32. V. ZERKIN, “IAEA-Nuclear Data Section,” Multi-platform EXFOR-CIDNA-ENDF Project, *NDS, International Atomic Energy Agency*, Vienna (1999-2013).

33. Oak Ridge National Laboratory, “Neutron Sciences, Spallation Neutron Source-High Flux Isotope Reactor, Reactor Core Assembly,” (2014). http://neutrons.ornl.gov/facilities/HFIR/reactorassembly.shtml

APPENDIX A

```
FBR Core FIRST CRITICAL With Depleted UO2 Axial and Radial Blanket
c   Changing to a single burn/decay cycle and removing material concentrations manually *
BOC-3 * **** 2e7 particles ****
1    0     -1 17 -21 fill=1                     imp:n=1   $ Core inner
2    0     -101 102 -103 104 -105 106 lat=2 u=1   imp:n=1
      fill=-13:13 -13:13  0:0
      17 26R
      17 12R 17 17 6 6 6 6 6 6 6 6 6 17 17 17
      17 11R 17 6 6 6 6 6 6 6 6 6 6 6 6 17 17
      17 10R 6 6 6 6 900 900 900 900 900 900 900 6 6 6 6 17
      17 9R 6 6 6 900 900 900 901 901 901 901 900 900 900 6 6 6 17
      17 8R 6 6 900 900 902 901 901 803 802 801 802 901 902 900 900 6 6 17
      17 7R 6 6 900 900 901 803 801 802 803 802 801 802 803 901 900 900 6 6 17
      17 6R 6 6 900 901 803 801 801 803 804 23 804 803 801 802 901 901 900 6 &
       6 17
      17 5R 6 6 900 901 801 803 802 703 701 703 702 701 703 803 801 803 901 &
       900 6 6 17
      17 4R 6 6 900 901 802 801 804 703 702 702 701 703 702 701 804 803 801    &
       901 900 6 6 17
      17 3R 6 6 900 901 801 803 23 702 701 27 703 701 23 703 703 23 801 802    &
       901 900 6 6 17
      17 2R 6 6 900 900 901 801 804 703 702 702 701 702 701 702 702 701 804    &
       802 801 900 900 6 6 17
      17 1R 17 6 6 900 901 801 803 702 701 703 703 701 703 701 703 703 702 803 &
       803 901 900 6 6 17 17
      17 17 6 6 900 902 803 801 703 703 23 701 702 703 702 701 27 701 703 802  &
       801 902 900 6 6 17 17
      17 17 6 6 900 901 801 803 701 702 702 701 703 701 701 703 701 702 803    &
       801 901 900 6 6 17 17 1R
      17 6 6 900 900 802 803 804 703 701 702 701 702 703 702 702 703 804 803   &
       901 900 900 6 6 17 2R
      17 6 6 900 901 803 801 23 702 703 27 703 701 23 703 702 23 801 801 901   &
       900 6 6 17 3R
      17 6 6 900 901 801 802 804 703 702 701 702 703 702 701 804 803 802 901   &
       900 6 6 17 4R
      17 6 6 900 901 803 801 803 703 703 702 701 701 703 803 801 802 901 900 6 &
       6 17 5R
      17 6 6 900 901 901 802 801 803 804 23 804 803 801 802 802 901 900 6 6    &
       17 6R
      17 6 6 900 900 901 802 801 801 803 802 801 802 801 901 900 900 6 6 17 7R
      17 6 6 900 900 902 901 802 801 803 803 901 901 902 900 900 6 6 17 8R
      17 6 6 6 900 900 900 901 901 901 901 900 900 900 6 6 6 17 9R
      17 6 6 6 6 900 900 900 900 900 900 900 6 6 6 6 17 10R
      17 17 6 6 6 6 6 6 6 6 6 6 6 6 17 17 11R
```

```
     17 17 17 6 6 6 6 6 6 6 6 6 17 17 17 12R
     17 26R
C   Universe 701 is FUEL SA CORE INNER
3  0 -401 402 -403 404 -405 406 15 -16 fill=2 u=701 imp:n=1   $ SA hex can inner
4  0      -201 202 -203 204 -205 206 lat=2  u=2     imp:n=1
     fill=-9:9 -9:9 0:0
     12 18R
     12 8R           11 11 11 11 11 11 11 11 11                        12
     12 7R          11 11 11 11 11 11 11 11 11 11                       12
     12 6R         11 11 11 11 11 11 11 11 11 11 11                      12
     12 5R        11 11 11 11 11 11 11 11 11 11 11 11                     12
     12 4R       11 11 11 11 11 11 11 11 11 11 11 11 11                    12
     12 3R      11 11 11 11 11 11 11 11 11 11 11 11 11 11                   12
     12 2R     11 11 11 11 11 11 11 11 11 11 11 11 11 11 11                  12
     12 1R    11 11 11 11 11 11 11 11 11 11 11 11 11 11 11 11                 12
     12        11 11 11 11 11 11 11 11 11 11 11 11 11 11 11 11 11      12
     12         11 11 11 11 11 11 11 11 11 11 11 11 11 11 11 11        12 1R
     12          11 11 11 11 11 11 11 11 11 11 11 11 11 11 11          12 2R
     12           11 11 11 11 11 11 11 11 11 11 11 11 11 11            12 3R
     12            11 11 11 11 11 11 11 11 11 11 11 11 11              12 4R
     12             11 11 11 11 11 11 11 11 11 11 11 11                12 5R
     12              11 11 11 11 11 11 11 11 11 11 11                  12 6R
     12               11 11 11 11 11 11 11 11 11 11                    12 7R
     12                11 11 11 11 11 11 11 11 11                      12 8R
                                                 12 18R
5  2 -8.00 (-501 502 -503 504 -505 506)    &
     (401:-402:403:-404:405:-406) 15 -16   u=701   imp:n=1             $ SA hex can
6  3 -0.90304 (501:-502:503:-504:505:-506) &
      15 -16                          u=701   imp:n=1             $ SA hex can outer
7  11 0.05969518 -10 -15                  u=701   imp:n=1             $ SA bottom
8  12 0.03004312 -10  16 -18              u=701   imp:n=1             $ SA top homo plenum
9  15 0.05386495 -10  18 -19              u=701   imp:n=1             $ Core top SS
10 16 0.05761362 -10  19                  u=701   imp:n=1             $ Core top B4C
11 0              -4    -2                u=11    imp:n=1             $ plenum bot
12 0              -26 2 -8                u=11    imp:n=1             $ ax blank hole
13 501 -11.65154927  26 -4  2 -8          u=11    imp:n=1  vol=6.49425 $ ax blanket bot
14 0              -26 8 -9                u=11    imp:n=1             $ fuel hole
15 101 -10.64258118  26 -4  8 -9          u=11    imp:n=1  vol=21.6475 $ fuel 10.7737803
16 0               -26 9 -3               u=11    imp:n=1             $ ax blank hole
17 501 -11.65154927  26 -4  9 -3          u=11    imp:n=1  vol=6.49425 $ ax blanket top
18 0              -4  3                   u=11    imp:n=1             $ plenum top
19 0            4 -5                      u=11    imp:n=1             $ fuel clad gap
20 2 -8.00      5 -6                      u=11    imp:n=1             $ fuel clad
21 3 -0.90304   6 -7                      u=11    imp:n=1             $ Na out pin
22 3 -0.90304     -7                      u=12    imp:n=1             $ Na filling tube
C   Universe 702 is FUEL SA CORE INNER
23  0 -401 402 -403 404 -405 406 15 -16 fill=3 u=702 imp:n=1            $ SA hex can inner
24  0      -201 202 -203 204 -205 206 lat=2  u=3     imp:n=1
```

```
     fill=-9:9 -9:9 0:0
     39 18R
     39 8R          38 38 38 38 38 38 38 38 38                    39
     39 7R         38 38 38 38 38 38 38 38 38 38                   39
     39 6R        38 38 38 38 38 38 38 38 38 38 38                  39
     39 5R       38 38 38 38 38 38 38 38 38 38 38 38                 39
     39 4R      38 38 38 38 38 38 38 38 38 38 38 38 38                39
     39 3R     38 38 38 38 38 38 38 38 38 38 38 38 38 38               39
     39 2R    38 38 38 38 38 38 38 38 38 38 38 38 38 38 38              39
     39 1R   38 38 38 38 38 38 38 38 38 38 38 38 38 38 38 38             39
     39     38 38 38 38 38 38 38 38 38 38 38 38 38 38 38 38 38     39
     39      38 38 38 38 38 38 38 38 38 38 38 38 38 38 38 38      39 1R
     39       38 38 38 38 38 38 38 38 38 38 38 38 38 38 38       39 2R
     39        38 38 38 38 38 38 38 38 38 38 38 38 38 38        39 3R
     39         38 38 38 38 38 38 38 38 38 38 38 38 38         39 4R
     39          38 38 38 38 38 38 38 38 38 38 38 38          39 5R
     39           38 38 38 38 38 38 38 38 38 38 38           39 6R
     39            38 38 38 38 38 38 38 38 38 38            39 7R
     39             38 38 38 38 38 38 38 38 38             39 8R
                                              39 18R
25  2 -8.00 (-501 502 -503 504 -505 506)    &
     (401:-402:403:-404:405:-406) 15 -16   u=702   imp:n=1         $ SA hex can
26  3 -0.90304 (501:-502:503:-504:505:-506) &
      15 -16                    u=702   imp:n=1         $ SA hex can outer
27  11 0.05969518 -10 -15               u=702   imp:n=1         $ SA bottom
28  12 0.03004312 -10  16 -18           u=702   imp:n=1         $ SA top homo plenum
29  15 0.05386495 -10  18 -19           u=702   imp:n=1         $ Core top SS
30 16 0.05761362 -10  19                u=702   imp:n=1         $ Core top B4C
31 0            -4    -2               u=38    imp:n=1         $ plenum bot
32 0            -26 2 -8               u=38    imp:n=1         $ ax blank hole
33 502 -11.65154927  26 -4  2 -8         u=38    imp:n=1  vol=6.49425 $ ax blanket bot
34 0            -26 8 -9               u=38    imp:n=1         $ fuel hole
35 102 -10.64258118  26 -4  8 -9         u=38    imp:n=1  vol=21.6475 $ fuel 10.7737803
36 0             -26 9 -3              u=38    imp:n=1         $ ax blank hole
37 502 -11.65154927  26 -4  9 -3         u=38    imp:n=1  vol=6.49425 $ ax blanket top
38 0            -4  3                  u=38    imp:n=1         $ plenum top
39 0          4 -5                     u=38    imp:n=1         $ fuel clad gap
40 2 -8.00      5 -6                   u=38    imp:n=1         $ fuel clad
41 3 -0.90304   6 -7                   u=38    imp:n=1         $ Na out pin
42 3 -0.90304     -7                   u=39    imp:n=1         $ Na filling tube
C   Universe 703 is FUEL SA CORE INNER
43  0 -401 402 -403 404 -405 406 15 -16 fill=5 u=703 imp:n=1         $ SA hex can inner
44  0      -201 202 -203 204 -205 206 lat=2  u=5     imp:n=1
     fill=-9:9 -9:9 0:0
     41 18R
     41 8R          40 40 40 40 40 40 40 40 40                    41
     41 7R         40 40 40 40 40 40 40 40 40 40                   41
     41 6R        40 40 40 40 40 40 40 40 40 40 40                  41
```

```
     41 5R         40 40 40 40 40 40 40 40 40 40 40 40                   41
     41 4R        40 40 40 40 40 40 40 40 40 40 40 40 40                 41
     41 3R       40 40 40 40 40 40 40 40 40 40 40 40 40 40               41
     41 2R      40 40 40 40 40 40 40 40 40 40 40 40 40 40 40             41
     41 1R     40 40 40 40 40 40 40 40 40 40 40 40 40 40 40 40           41
     41       40 40 40 40 40 40 40 40 40 40 40 40 40 40 40 40 40         41
     41        40 40 40 40 40 40 40 40 40 40 40 40 40 40 40 40        41 1R
     41         40 40 40 40 40 40 40 40 40 40 40 40 40 40 40         41 2R
     41          40 40 40 40 40 40 40 40 40 40 40 40 40 40          41 3R
     41           40 40 40 40 40 40 40 40 40 40 40 40 40           41 4R
     41            40 40 40 40 40 40 40 40 40 40 40 40            41 5R
     41             40 40 40 40 40 40 40 40 40 40 40             41 6R
     41              40 40 40 40 40 40 40 40 40 40              41 7R
     41               40 40 40 40 40 40 40 40 40               41 8R
                                         41 18R
45  2 -8.00 (-501 502 -503 504 -505 506)    &
     (401:-402:403:-404:405:-406) 15 -16   u=703   imp:n=1             $ SA hex can
46  3 -0.90304 (501:-502:503:-504:505:-506) &
      15 -16                          u=703   imp:n=1             $ SA hex can outer
47  11 0.05969518 -10 -15                u=703   imp:n=1             $ SA bottom
48  12 0.03004312 -10  16 -18             u=703   imp:n=1             $ SA top homo plenum
49  15 0.05386495 -10  18 -19             u=703   imp:n=1             $ Core top SS
50 16 0.05761362 -10  19                 u=703   imp:n=1             $ Core top B4C
51 0              -4    -2               u=40    imp:n=1             $ plenum bot
52 0              -26 2 -8               u=40    imp:n=1             $ ax blank hole
53 503 -11.65154927  26 -4  2 -8          u=40    imp:n=1  vol=6.49425 $ ax blanket bot
54 0              -26 8 -9               u=40    imp:n=1             $ fuel hole
55 103 -10.64258118  26 -4  8 -9          u=40    imp:n=1  vol=21.6475 $ fuel 10.7737803
56 0               -26 9 -3              u=40    imp:n=1             $ ax blank hole
57 503 -11.65154927  26 -4  9 -3          u=40    imp:n=1  vol=6.49425 $ ax blanket top
58 0              -4  3                  u=40    imp:n=1             $ plenum top
59 0            4 -5                     u=40    imp:n=1             $ fuel clad gap
60 2 -8.00      5 -6                     u=40    imp:n=1             $ fuel clad
61 3 -0.90304   6 -7                     u=40    imp:n=1             $ Na out pin
62 3 -0.90304     -7                     u=41    imp:n=1             $ Na filling tube
C Universe 801 is Fuel SA CORE OUTER
63 0 -401 402 -403 404 -405 406 15 -16 fill=22 u=801 imp:n=1             $ SA hex can inner
64 0      -201 202 -203 204 -205 206 lat=2  u=22     imp:n=1
     fill=-9:9 -9:9 0:0
     14 18R
     14 8R           13 13 13 13 13 13 13 13 13                      14
     14 7R          13 13 13 13 13 13 13 13 13 13                    14
     14 6R         13 13 13 13 13 13 13 13 13 13 13                  14
     14 5R        13 13 13 13 13 13 13 13 13 13 13 13                14
     14 4R       13 13 13 13 13 13 13 13 13 13 13 13 13              14
     14 3R      13 13 13 13 13 13 13 13 13 13 13 13 13 13            14
     14 2R     13 13 13 13 13 13 13 13 13 13 13 13 13 13 13          14
     14 1R    13 13 13 13 13 13 13 13 13 13 13 13 13 13 13 13        14
```

```
     14       13 13 13 13 13 13 13 13 13 13 13 13 13 13 13 13 13       14
     14        13 13 13 13 13 13 13 13 13 13 13 13 13 13 13 13        14 1R
     14         13 13 13 13 13 13 13 13 13 13 13 13 13 13 13         14 2R
     14          13 13 13 13 13 13 13 13 13 13 13 13 13 13          14 3R
     14           13 13 13 13 13 13 13 13 13 13 13 13 13           14 4R
     14            13 13 13 13 13 13 13 13 13 13 13 13            14 5R
     14             13 13 13 13 13 13 13 13 13 13 13             14 6R
     14              13 13 13 13 13 13 13 13 13 13              14 7R
     14               13 13 13 13 13 13 13 13 13               14 8R
     14 18R
65 2 -8.00 (-501 502 -503 504 -505 506)    &
     (401:-402:403:-404:405:-406) 15 -16   u=801   imp:n=1             $ SA hex can
66 3 -0.90304 (501:-502:503:-504:505:-506) &
      15 -16                          u=801   imp:n=1            $ SA hex can outer
67 11 0.05969518 -10 -15                 u=801   imp:n=1            $ SA bottom
68 12 0.03004312 -10  16 -18              u=801   imp:n=1            $ SA top homo plenum
69 15 0.05386495 -10  18 -19              u=801   imp:n=1            $ Core top SS
70 16 0.05761362 -10  19                u=801   imp:n=1            $ Core top B4C
71 0             -4    -2                u=13    imp:n=1            $ plenum bot
72 0             -26 2 -8                u=13    imp:n=1            $ ax blank hole
73 511 -11.65154927  26 -4  2 -8          u=13    imp:n=1  vol=6.49425 $ ax blanket bot
74 0             -26 8 -9                u=13    imp:n=1            $ fuel hole
75 401 -10.67464722  26 -4  8 -9          u=13    imp:n=1  vol=21.6475 $ fuel 10.80996965
76 0              -26 9 -3               u=13    imp:n=1            $ ax blank hole
77 511 -11.65154927 26  -4  9 -3          u=13    imp:n=1  vol=6.49425 $ ax blanket top
78 0             -4  3                  u=13    imp:n=1            $ plenum top
79 0           4 -5                     u=13    imp:n=1            $ fuel clad gap
80 2 -8.00      5 -6                     u=13    imp:n=1            $ fuel clad
81 3 -0.90304   6 -7                      u=13    imp:n=1            $ Na out pin
82 3 -0.90304     -7                      u=14    imp:n=1            $ Na filling tube
C Universe 802 is Fuel SA CORE OUTER
83 0 -401 402 -403 404 -405 406 15 -16 fill=26 u=802 imp:n=1             $ SA hex can inner
84 0      -201 202 -203 204 -205 206 lat=2  u=26     imp:n=1
     fill=-9:9 -9:9 0:0
     43 18R
     43 8R           42 42 42 42 42 42 42 42 42                     43
     43 7R          42 42 42 42 42 42 42 42 42 42                    43
     43 6R         42 42 42 42 42 42 42 42 42 42 42                   43
     43 5R        42 42 42 42 42 42 42 42 42 42 42 42                  43
     43 4R       42 42 42 42 42 42 42 42 42 42 42 42 42                 43
     43 3R      42 42 42 42 42 42 42 42 42 42 42 42 42 42                43
     43 2R     42 42 42 42 42 42 42 42 42 42 42 42 42 42 42               43
     43 1R    42 42 42 42 42 42 42 42 42 42 42 42 42 42 42 42              43
     43       42 42 42 42 42 42 42 42 42 42 42 42 42 42 42 42 42       43
     43        42 42 42 42 42 42 42 42 42 42 42 42 42 42 42 42        43 1R
     43         42 42 42 42 42 42 42 42 42 42 42 42 42 42 42         43 2R
     43          42 42 42 42 42 42 42 42 42 42 42 42 42 42          43 3R
     43           42 42 42 42 42 42 42 42 42 42 42 42 42           43 4R
```

```
     43            42 42 42 42 42 42 42 42 42 42 42 42                43 5R
     43             42 42 42 42 42 42 42 42 42 42 42                 43 6R
     43              42 42 42 42 42 42 42 42 42 42                  43 7R
     43               42 42 42 42 42 42 42 42 42                   43 8R
     43 18R
85 2 -8.00 (-501 502 -503 504 -505 506)    &
     (401:-402:403:-404:405:-406) 15 -16   u=802   imp:n=1             $ SA hex can
86 3 -0.90304 (501:-502:503:-504:505:-506) &
      15 -16                          u=802   imp:n=1             $ SA hex can outer
87 11 0.05969518 -10 -15                    u=802   imp:n=1             $ SA bottom
88 12 0.03004312 -10  16 -18                u=802   imp:n=1             $ SA top homo plenum
89 15 0.05386495 -10  18 -19                u=802   imp:n=1             $ Core top SS
90 16 0.05761362 -10  19                    u=802   imp:n=1             $ Core top B4C
91 0              -4    -2                u=42    imp:n=1             $ plenum bot
92 0              -26 2 -8                u=42    imp:n=1             $ ax blank hole
93 512 -11.65154927  26 -4  2 -8           u=42    imp:n=1  vol=6.49425 $ ax blanket bot
94 0              -26 8 -9                u=42    imp:n=1             $ fuel hole
95 402 -10.67464722  26 -4  8 -9           u=42    imp:n=1  vol=21.6475 $ fuel 10.80996965
96 0               -26 9 -3               u=42    imp:n=1             $ ax blank hole
97 512 -11.65154927 26  -4  9 -3           u=42    imp:n=1  vol=6.49425 $ ax blanket top
98 0              -4  3                   u=42    imp:n=1             $ plenum top
99 0            4 -5                      u=42    imp:n=1             $ fuel clad gap
100 2 -8.00      5 -6                     u=42    imp:n=1             $ fuel clad
101 3 -0.90304   6 -7                      u=42    imp:n=1             $ Na out pin
102 3 -0.90304     -7                      u=43    imp:n=1             $ Na filling tube
C Universe 803 is Fuel SA CORE OUTER
103 0 -401 402 -403 404 -405 406 15 -16 fill=29 u=803 imp:n=1             $ SA hex can inner
104 0      -201 202 -203 204 -205 206 lat=2  u=29     imp:n=1
     fill=-9:9 -9:9 0:0
     45 18R
     45 8R           44 44 44 44 44 44 44 44 44                   45
     45 7R          44 44 44 44 44 44 44 44 44 44                  45
     45 6R         44 44 44 44 44 44 44 44 44 44 44                 45
     45 5R        44 44 44 44 44 44 44 44 44 44 44 44                45
     45 4R       44 44 44 44 44 44 44 44 44 44 44 44 44               45
     45 3R      44 44 44 44 44 44 44 44 44 44 44 44 44 44              45
     45 2R     44 44 44 44 44 44 44 44 44 44 44 44 44 44 44             45
     45 1R    44 44 44 44 44 44 44 44 44 44 44 44 44 44 44 44            45
     45      44 44 44 44 44 44 44 44 44 44 44 44 44 44 44 44 44           45
     45       44 44 44 44 44 44 44 44 44 44 44 44 44 44 44 44          45 1R
     45        44 44 44 44 44 44 44 44 44 44 44 44 44 44 44           45 2R
     45         44 44 44 44 44 44 44 44 44 44 44 44 44 44            45 3R
     45          44 44 44 44 44 44 44 44 44 44 44 44 44             45 4R
     45           44 44 44 44 44 44 44 44 44 44 44 44              45 5R
     45            44 44 44 44 44 44 44 44 44 44 44               45 6R
     45             44 44 44 44 44 44 44 44 44 44                45 7R
     45              44 44 44 44 44 44 44 44 44                 45 8R
     45 18R
```

```
105 2 -8.00 (-501 502 -503 504 -505 506)    &
     (401:-402:403:-404:405:-406) 15 -16    u=803   imp:n=1             $ SA hex can
106 3 -0.90304 (501:-502:503:-504:505:-506) &
      15 -16                            u=803   imp:n=1             $ SA hex can outer
107 11 0.05969518 -10 -15                  u=803   imp:n=1             $ SA bottom
108 12 0.03004312 -10  16 -18              u=803   imp:n=1             $ SA top homo plenum
109 15 0.05386495 -10  18 -19              u=803   imp:n=1             $ Core top SS
110 16 0.05761362 -10  19                  u=803   imp:n=1             $ Core top B4C
111 0              -4    -2                u=44    imp:n=1             $ plenum bot
112 0              -26 2 -8                u=44    imp:n=1             $ ax blank hole
113 513 -11.65154927  26 -4  2 -8          u=44    imp:n=1  vol=6.49425 $ ax blanket bot
114 0              -26 8 -9                u=44    imp:n=1             $ fuel hole
115 403 -10.67464722  26 -4  8 -9          u=44    imp:n=1  vol=21.6475 $ fuel 10.80996965
116 0               -26 9 -3               u=44    imp:n=1             $ ax blank hole
117 513 -11.65154927 26  -4  9 -3          u=44    imp:n=1  vol=6.49425 $ ax blanket top
118 0              -4  3                   u=44    imp:n=1             $ plenum top
119 0            4 -5                      u=44    imp:n=1             $ fuel clad gap
120 2 -8.00      5 -6                      u=44    imp:n=1             $ fuel clad
121 3 -0.90304   6 -7                      u=44    imp:n=1             $ Na out pin
122 3 -0.90304     -7                      u=45    imp:n=1             $ Na filling tube
C   Universe 804 is FUEL SA CORE OUTER/INNER  *Filled with Core I fuel for the first two
cylces and replaced with Core II fuel for the third cycle
123  0 -401 402 -403 404 -405 406 15 -16 fill=30 u=804 imp:n=1             $ SA hex can inner
124  0      -201 202 -203 204 -205 206 lat=2  u=30     imp:n=1
     fill=-9:9 -9:9 0:0
     47 18R
     47 8R           46 46 46 46 46 46 46 46 46                    47
     47 7R          46 46 46 46 46 46 46 46 46 46                   47
     47 6R         46 46 46 46 46 46 46 46 46 46 46                  47
     47 5R        46 46 46 46 46 46 46 46 46 46 46 46                 47
     47 4R       46 46 46 46 46 46 46 46 46 46 46 46 46                47
     47 3R      46 46 46 46 46 46 46 46 46 46 46 46 46 46               47
     47 2R     46 46 46 46 46 46 46 46 46 46 46 46 46 46 46              47
     47 1R    46 46 46 46 46 46 46 46 46 46 46 46 46 46 46 46             47
     47      46 46 46 46 46 46 46 46 46 46 46 46 46 46 46 46 46            47
     47       46 46 46 46 46 46 46 46 46 46 46 46 46 46 46 46          47 1R
     47        46 46 46 46 46 46 46 46 46 46 46 46 46 46 46          47 2R
     47         46 46 46 46 46 46 46 46 46 46 46 46 46 46          47 3R
     47          46 46 46 46 46 46 46 46 46 46 46 46 46          47 4R
     47           46 46 46 46 46 46 46 46 46 46 46 46          47 5R
     47            46 46 46 46 46 46 46 46 46 46 46          47 6R
     47             46 46 46 46 46 46 46 46 46 46          47 7R
     47              46 46 46 46 46 46 46 46 46          47 8R
                                              47 18R
125  2 -8.00 (-501 502 -503 504 -505 506)    &
     (401:-402:403:-404:405:-406) 15 -16     u=804   imp:n=1             $ SA hex can
126  3 -0.90304 (501:-502:503:-504:505:-506) &
      15 -16                            u=804   imp:n=1             $ SA hex can outer
```

```
127  11 0.05969518 -10 -15                  u=804   imp:n=1             $ SA bottom
128  12 0.03004312 -10  16 -18              u=804   imp:n=1             $ SA top homo plenum
129  15 0.05386495 -10  18 -19              u=804   imp:n=1             $ Core top SS
130 16 0.05761362 -10  19                   u=804   imp:n=1             $ Core top B4C
131 0              -4    -2                 u=46    imp:n=1             $ plenum bot
132 0              -26 2 -8                 u=46    imp:n=1             $ ax blank hole
133 514 -11.65154927  26 -4  2 -8           u=46    imp:n=1  vol=6.49425 $ ax blanket bot
134 0              -26 8 -9                 u=46    imp:n=1             $ fuel hole
135 404 -10.67464722  26 -4  8 -9           u=46    imp:n=1  vol=21.6475 $ fuel 10.7737803
136 0               -26 9 -3                u=46    imp:n=1             $ ax blank hole
137 514 -11.65154927  26 -4  9 -3           u=46    imp:n=1  vol=6.49425 $ ax blanket top
138 0              -4  3                    u=46    imp:n=1             $ plenum top
139 0            4 -5                       u=46    imp:n=1             $ fuel clad gap
140 2 -8.00      5 -6                       u=46    imp:n=1             $ fuel clad
141 3 -0.90304   6 -7                       u=46    imp:n=1             $ Na out pin
142 3 -0.90304     -7                       u=47    imp:n=1             $ Na filling tube
C Universe 4 is Na tube of FA size
143  3 -0.90304     -10                     u=4   imp:n=1   $ NA filling
C Universe 900 is Radial Blanket SA
144 0 -401 402 -403 404 -405 406 22 -20 fill=31 u=900 imp:n=1   $ SA hex can inner
145 0 -301 302 -303 304 -305 306 lat=2       u=31     imp:n=1
     fill=-5:5 -5:5 0:0
     16 10R
     16 4R                15 15 15 15 15               16
     16 3R              15 15 15 15 15 15             16
     16 2R            15 15 15 15 15 15 15           16
     16 1R          15 15 15 15 15 15 15 15         16
     16           15 15 15 15 15 15 15 15 15       16
     16             15 15 15 15 15 15 15 15         16 1R
     16               15 15 15 15 15 15 15           16 2R
     16                 15 15 15 15 15 15             16 3R
     16                   15 15 15 15 15               16 4R
     16 10R
146 2 -8.00 (-501 502 -503 504 -505 506)    &
    (401:-402:403:-404:405:-406) 22 -20    u=900   imp:n=1   $ SA hex can
147 3 -0.90304 (501:-502:503:-504:505:-506) &
     22 -20                          u=900   imp:n=1             $ SA hex can out
148 11 0.05969518 -10 -15                  u=900   imp:n=1             $ SA bottom
149 13 0.06846700 -10  15 -22              u=900   imp:n=1             $ RBPSS
150 14 0.02912191 -10  20 -18              u=900   imp:n=1             $ RBPT
151 15 0.05386495 -10  18 -19              u=900   imp:n=1             $ RBSS top
152 16 0.05761362 -10  19                  u=900   imp:n=1             $ RBB4C top
153 0              -11 -2                  u=15    imp:n=1             $ rad blank ple bot
154 600 -10.59230329 -11  2 -3             u=15    imp:n=1  vol=204.603 $ rad blanket
155 0              -11  3                  u=15    imp:n=1             $ rad blank ple top
156 0               11 -12                 u=15    imp:n=1             $ blank clad gap
157 2 -8.00         12 -13                 u=15    imp:n=1             $ blanket clad
158 3 -0.90304      13 -10                 u=15    imp:n=1             $ NA out blanket
```

```
159 3 -0.90304     -10                      u=16    imp:n=1            $ NA filling tube
C Universe 901 is Radial Blanket SA
160 0 -401 402 -403 404 -405 406 22 -20 fill=32 u=901 imp:n=1          $ SA hex can inner
161 0 -301 302 -303 304 -305 306 lat=2       u=32     imp:n=1
      fill=-5:5 -5:5 0:0
      49 10R
      49 4R               48 48 48 48 48              49
      49 3R              48 48 48 48 48 48             49
      49 2R             48 48 48 48 48 48 48            49
      49 1R            48 48 48 48 48 48 48 48           49
      49              48 48 48 48 48 48 48 48 48          49
      49               48 48 48 48 48 48 48 48         49 1R
      49                48 48 48 48 48 48 48          49 2R
      49                 48 48 48 48 48 48          49 3R
      49                  48 48 48 48 48          49 4R
                                       49 10R
162 2 -8.00 (-501 502 -503 504 -505 506)    &
     (401:-402:403:-404:405:-406) 22 -20    u=901   imp:n=1            $ SA hex can
163 3 -0.90304 (501:-502:503:-504:505:-506) &
      22 -20                            u=901   imp:n=1            $ SA hex can out
164 11 0.05969518 -10 -15                 u=901   imp:n=1            $ SA bottom
165 13 0.06846700 -10  15 -22             u=901   imp:n=1            $ RBPSS
166 14 0.02912191 -10  20 -18             u=901   imp:n=1            $ RBPT
167 15 0.05386495 -10  18 -19             u=901   imp:n=1            $ RBSS top
168 16 0.05761362 -10  19                 u=901   imp:n=1            $ RBB4C top
169 0              -11 -2                 u=48    imp:n=1            $ rad blank ple bot
170 601 -10.59230329 -11  2 -3            u=48    imp:n=1  vol=204.603 $ rad blanket
171 0              -11  3                 u=48    imp:n=1            $ rad blank ple top
172 0               11 -12                u=48    imp:n=1            $ blank clad gap
173 2 -8.00          12 -13               u=48    imp:n=1            $ blanket clad
174 3 -0.90304       13 -10               u=48    imp:n=1            $ NA out blanket
175 3 -0.90304     -10                    u=49    imp:n=1            $ NA filling tube
C Universe 902 is Radial Blanket SA
176 0 -401 402 -403 404 -405 406 22 -20 fill=33 u=902 imp:n=1           $ SA hex can inner
177 0 -301 302 -303 304 -305 306 lat=2       u=33     imp:n=1
      fill=-5:5 -5:5 0:0
      51 10R
      51 4R               50 50 50 50 50              51
      51 3R              50 50 50 50 50 50             51
      51 2R             50 50 50 50 50 50 50            51
      51 1R            50 50 50 50 50 50 50 50           51
      51              50 50 50 50 50 50 50 50 50          51
      51               50 50 50 50 50 50 50 50         51 1R
      51                50 50 50 50 50 50 50          51 2R
      51                 50 50 50 50 50 50          51 3R
      51                  50 50 50 50 50          51 4R
                                       51 10R
178 2 -8.00 (-501 502 -503 504 -505 506)    &
```

```
    (401:-402:403:-404:405:-406) 22 -20    u=902   imp:n=1              $ SA hex can
179 3 -0.90304 (501:-502:503:-504:505:-506) &
     22 -20                            u=902   imp:n=1             $ SA hex can out
180 11 0.05969518 -10 -15                  u=902   imp:n=1             $ SA bottom
181 13 0.06846700 -10  15 -22              u=902   imp:n=1             $ RBPSS
182 14 0.02912191 -10  20 -18              u=902   imp:n=1             $ RBPT
183 15 0.05386495 -10  18 -19              u=902   imp:n=1             $ RBSS top
184 16 0.05761362 -10  19                  u=902   imp:n=1             $ RBB4C top
185 0              -11 -2                u=50    imp:n=1             $ rad blank ple bot
186 602 -10.59230329 -11  2 -3             u=50    imp:n=1  vol=204.603 $ rad blanket
187 0              -11  3                u=50    imp:n=1             $ rad blank ple top
188 0               11 -12                u=50    imp:n=1             $ blank clad gap
189 2 -8.00         12 -13                 u=50    imp:n=1             $ blanket clad
190 3 -0.90304      13 -10                  u=50    imp:n=1             $ NA out blanket
191 3 -0.90304     -10                     u=51    imp:n=1             $ NA filling tube
C Universe 904 is Fuel SA CORE OUTER *All universe 904 will be replaced with 901 at
second refueling
192 0 -401 402 -403 404 -405 406 15 -16 fill=34 u=904 imp:n=1            $ SA hex can inner
193 0      -201 202 -203 204 -205 206 lat=2  u=34     imp:n=1
    fill=-9:9 -9:9 0:0
    53 18R
    53 8R           52 52 52 52 52 52 52 52 52                      53
    53 7R          52 52 52 52 52 52 52 52 52 52                    53
    53 6R         52 52 52 52 52 52 52 52 52 52 52                  53
    53 5R        52 52 52 52 52 52 52 52 52 52 52 52                53
    53 4R       52 52 52 52 52 52 52 52 52 52 52 52 52              53
    53 3R      52 52 52 52 52 52 52 52 52 52 52 52 52 52            53
    53 2R     52 52 52 52 52 52 52 52 52 52 52 52 52 52 52          53
    53 1R    52 52 52 52 52 52 52 52 52 52 52 52 52 52 52 52        53
    53      52 52 52 52 52 52 52 52 52 52 52 52 52 52 52 52 52      53
    53       52 52 52 52 52 52 52 52 52 52 52 52 52 52 52 52        53 1R
    53        52 52 52 52 52 52 52 52 52 52 52 52 52 52 52          53 2R
    53         52 52 52 52 52 52 52 52 52 52 52 52 52 52            53 3R
    53          52 52 52 52 52 52 52 52 52 52 52 52 52              53 4R
    53           52 52 52 52 52 52 52 52 52 52 52 52                53 5R
    53            52 52 52 52 52 52 52 52 52 52 52                  53 6R
    53             52 52 52 52 52 52 52 52 52 52                    53 7R
    53              52 52 52 52 52 52 52 52 52                      53 8R
    53 18R
194 2 -8.00 (-501 502 -503 504 -505 506)    &
    (401:-402:403:-404:405:-406) 15 -16    u=904   imp:n=1              $ SA hex can
195 3 -0.90304 (501:-502:503:-504:505:-506) &
     15 -16                            u=904   imp:n=1             $ SA hex can outer
196 11 0.05969518 -10 -15                  u=904   imp:n=1             $ SA bottom
197 12 0.03004312 -10  16 -18              u=904   imp:n=1             $ SA top homo plenum
198 15 0.05386495 -10  18 -19              u=904   imp:n=1             $ Core top SS
199 16 0.05761362 -10  19                  u=904   imp:n=1             $ Core top B4C
200 0              -4    -2               u=52    imp:n=1             $ plenum bot
```

```
201 0             -26 2 -8                 u=52    imp:n=1            $ ax blank hole
202 524 -11.65154927  26 -4  2 -8           u=52    imp:n=1  vol=6.49425 $ ax blanket bot
203 0             -26 8 -9                 u=52    imp:n=1            $ fuel hole
204 604 -10.67464722  26 -4  8 -9           u=52    imp:n=1  vol=21.6475 $ fuel 10.80996965
205 0              -26 9 -3                u=52    imp:n=1            $ ax blank hole
206 524 -11.65154927 26  -4  9 -3           u=52    imp:n=1  vol=6.49425 $ ax blanket top
207 0             -4  3                  u=52    imp:n=1            $ plenum top
208 0           4 -5                     u=52    imp:n=1            $ fuel clad gap
209 2 -8.00      5 -6                     u=52    imp:n=1            $ fuel clad
210 3 -0.90304   6 -7                      u=52    imp:n=1            $ Na out pin
211 3 -0.90304    -7                       u=53    imp:n=1            $ Na filling tube
C Universe 6 is SS reflector SA
212 11 0.05969518  -10 -15                u=6   imp:n=1   $ SS Refl Ass bot
213 7  0.09365394  -10  15 -8             u=6   imp:n=1   $ SS Reflector B4C
214 8  0.06154800  -10  8  -20            u=6   imp:n=1   $ SS Reflector
215 14 0.02912191  -10  20 -18             u=6   imp:n=1   $ SS reflector top
216 7  0.09365394  -10  18               u=6   imp:n=1   $ SS refle B4C top
C Universe 17 is B4C Shield SA
217 11 0.05969518  -10  -15               u=17  imp:n=1   $ B4C SHLD bottom
218 17 0.01835245  -10  15 -23             u=17  imp:n=1   $ SHLD Plenum bot
219 7  0.09365394   -10 23 -24            u=17  imp:n=1   $ B4C Shld I layer
220 17 0.01835245  -10  24 -25             u=17  imp:n=1   $ SHLD Plenum top
221 18 0.06221962  -10  25                u=17  imp:n=1   $ SHLD SS top
C Universe 18 is CSR/DSR
222 9  0.03393119   -10 -8               u=18  imp:n=1   $ CSR/DSR bottom
223 10 0.06340921   -10  8 -14            u=18  imp:n=1   $ CSR/DSR
224 9  0.03393119   -10  14              u=18  imp:n=1   $ CSR/DSR top
C   Universe 19 is Diluent SA *All universe 19 will be replaced with 703 at first refueling
225 11 0.05969518 -10 -15                u=19  imp:n=1            $ SA bottom
226 13 0.06846700 -10  15 -22             u=19  imp:n=1            $ RBPSS
227 20 0.02324489 -10  22 -2              u=19  imp:n=1            $ RB Plenum bot
228 19 0.05133189 -10  2  -3              u=19  imp:n=1  vol= 43740 $ Diluent with RBP
229 20 0.02324489 -10  3  -20             u=19  imp:n=1            $ RB Plenum top
230 14 0.02912191 -10  20 -18             u=19  imp:n=1            $ RBPT
231 15 0.05386495 -10  18 -19             u=19  imp:n=1            $ RBSS top
232 16 0.05761362 -10  19                u=19  imp:n=1            $ RBB4C top
C Universe 23 is pinwise CSR
233 0 -401 402 -403 404 -405 406 36 -37 fill=36 u=23 imp:n=1          $ SA hex can inner
234 0 -601 602 -603 604 -605 606 lat=2      u=36    imp:n=1
     fill=-3:3 -3:3 0:0
     21 6R
     21 2R               20 20 20              21
     21 1R             20 20 20 20              21
     21              20 20 20 20 20            21
     21               20 20 20 20             21 1R
     21                20 20 20              21 2R
     21 6R
235 2 -8.00 (-501 502 -503 504 -505 506)    &
```

```
    (401:-402:403:-404:405:-406) 36 -37    u=23  imp:n=1   $ SA hex can
236 3 -0.90304 (501:-502:503:-504:505:-506) &
     36 -37                          u=23  imp:n=1   $ SA hex can out
237 9 0.03393119 -10 -36                  u=23  imp:n=1   $ CSR Follower bot
238 9 0.03393119 -10  37                  u=23  imp:n=1   $ CSR Follower top
239 22 -2.4       -27 -40             u=20  imp:n=1   $ CSR pin bot
240 21 -2.4       -27  40 -41            u=20  imp:n=1   $ CSR pin mid
241 22 -2.4       -27  41             u=20  imp:n=1   $ CSR pin top
242 0             27 -28              u=20  imp:n=1   $ CSR clad gap
243 2 -8.00        28 -29             u=20  imp:n=1   $ CSR clad
244 3 -0.90304      29 -10             u=20  imp:n=1   $ NA out CSR
245 3 -0.90304     -10                u=21  imp:n=1   $ NA filling tube
C Universe 27 is pinwise DSR
246 0 -401 402 -403 404 -405 406 38 -39 fill=37 u=27 imp:n=1 $ SA hex can inner
247 0 -601 602 -603 604 -605 606 lat=2      u=37    imp:n=1
     fill=-3:3 -3:3 0:0
     25 6R
     25 2R              24 24 24              25
     25 1R              24 24 24 24              25
     25               24 24 24 24 24             25
     25                24 24 24 24              25 1R
     25                 24 24 24               25 2R
     25 6R
248 2 -8.00 (-501 502 -503 504 -505 506)    &
    (401:-402:403:-404:405:-406) 38 -39    u=27  imp:n=1   $ SA hex can
249 3 -0.90304 (501:-502:503:-504:505:-506) &
     38 -39                          u=27  imp:n=1   $ SA hex can out
250 9 0.03393119 -10 -38                  u=27  imp:n=1   $ DSR Follower bot
251 9 0.03393119 -10  39                  u=27  imp:n=1   $ DSR Follower top
252  21 -2.4       -33                u=24  imp:n=1   $ DSR pin mid
253  0             33 -34             u=24  imp:n=1   $ DSR clad gap
254  2 -8.00        34 -35             u=24  imp:n=1   $ DSR clad
255  3 -0.90304      35 -10             u=24  imp:n=1   $ NA out DSR
256  3 -0.90304     -10                u=25  imp:n=1   $ NA filling tube
C   Universe 28 is ALSO Diluent SA *Both universe 28 will be replaced with 702 at second
refueling
257 11 0.05969518 -10 -15              u=28  imp:n=1            $ SA bottom
258 13 0.06846700 -10  15 -22            u=28  imp:n=1            $ RBPSS
259 20 0.02324489 -10  22 -2            u=28  imp:n=1            $ RB Plenum bot
260 23 0.05133189 -10  2  -3            u=28  imp:n=1  vol= 43740  $ Diluent with RBP
261 20 0.02324489 -10  3  -20            u=28  imp:n=1            $ RB Plenum top
262 14 0.02912191 -10  20 -18            u=28  imp:n=1            $ RBPT
263 15 0.05386495 -10  18 -19            u=28  imp:n=1            $ RBSS top
264 16 0.05761362 -10  19              u=28  imp:n=1            $ RBB4C top
265 0 1:-17:21 imp:n=0

1    cz  155                              $ core vessel rad
2    pz  0                               $ blanket bottom
```

```
3    pz  160                                    $ blanket top
4    cz  0.2775                                   $ fuel pellet rad
5    cz  0.285                                   $ fuel clad ID
6    cz  0.33                                   $ fuel clad OD
7    cz  5.0                                   $ outer pin Na
8    pz  30                                    $ bot blank end
9    pz  130                                   $ top blank start
10   cz  20                                    $ dummy NA
11   cz  0.638                                   $ radi blank rad
12   cz  0.6565                                   $ blank clad ID
13   cz  0.7165                                   $ blank clad OD
14   pz  141                                   $ CRF top Start
15   pz  -75                                   $ plenum bottom
16   pz  183                                   $ plenum top
17   pz  -101                                   $ SA bottom
18   pz  191.5                                   $ remaining plenum
19   pz  257.0                                   $ SA SS top
20   pz  170                                   $ Rad blnk ple top
21   pz  267                                   $ Core B4C top
22   pz  -60                                   $ RB ple bot SS
23   pz  3.9                                   $ SHLD plenum bot
24   pz  238.2                                   $ B4C shld top
25   pz  248.4                                   $ SHPL top
26   cz  0.09                                   $ fuel annular rad
27   cz  0.87                                   $ CSRB4C pellet OR
28   cz  1.02                                   $ CSRB4C clad IR
29   cz  1.12                                   $ CSRB4C clad OR
C The following three cards are not required any more
C 30   pz  50                                   $ CSRnatB4C bot
C 31   pz  121                                   $ CSRnatB4C top
C 32   pz  131                                   $ DSRB4C top
33   cz  0.89                                   $ DSRB4C pellet OR
34   cz  1.00                                   $ DSRB4C clad IR
35   cz  1.07                                   $ DSRB4C clad OR
C ************************************************************************
C The following PZ's are for pin wise CSR and DSR inserion and withdrawal
C Change the comment card accordingly
C ************************************************************************
C 36   pz  29.0      $ CSR DOWN (bottom edge)
C 37   pz 140.0      $ CSR DOWN (top edge)
36   pz 137.5      $ CSR UP   (bottom edge)
37   pz 248.5      $ CSR UP   (top edge)
C 38   pz  29.5      $ DSR DOWN (bottom edge)
C 39   pz 130.5      $ DSR DOWN (top edge)
38   pz 131.5      $ DSR UP (bottom edge)
39   pz 232.5      $ DSR UP (top edge)
```

```
C
********************************************************************************
*
C following pairs are CSR down &  up >>>  how the pin axial profile change
C
********************************************************************************
*
C 40   pz  49.0      $ CSR DOWN (bottom nat B4C pin top)
C 41   pz 120.0      $ CSR DOWN (mid enrich B4C pin top)
40   pz 157.5      $ CSR UP   (bottom nat B4C pin top)
41   pz 228.5      $ CSR UP   (mid enrich B4C pin top)
C
********************************************************************************
*
101  px  6.75                              $ hexside FA
102  px -6.75                              $ hexside FA
103  p   1  1.7320508076 0  13.5           $ hexside FA
104  p   1  1.7320508076 0 -13.5           $ hexside FA
105  p  -1  1.7320508076 0  13.5           $ hexside FA
106  p  -1  1.7320508076 0 -13.5           $ hexside FA
201  py  0.4125                            $ hexside pin
202  py -0.4125                            $ hexside pin
203  p   1.7320508076  1 0  0.825          $ hexside pin
204  p   1.7320508076  1 0 -0.825          $ hexside pin
205  p   1.7320508076 -1 0  0.825          $ hexside pin
206  p   1.7320508076 -1 0 -0.825          $ hexside pin
301  py  0.8                               $ hexside pin
302  py -0.8                               $ hexside pin
303  p   1.7320508076  1 0  1.6            $ hexside pin
304  p   1.7320508076  1 0 -1.6            $ hexside pin
305  p   1.7320508076 -1 0  1.6            $ hexside pin
306  p   1.7320508076 -1 0 -1.6            $ hexside pin
401  px  6.26                              $ hexside FA
402  px -6.26                              $ hexside FA
403  p   1  1.7320508076 0  12.52          $ hexside FA
404  p   1  1.7320508076 0 -12.52          $ hexside FA
405  p  -1  1.7320508076 0  12.52          $ hexside FA
406  p  -1  1.7320508076 0 -12.52          $ hexside FA
501  px  6.58                              $ hexside FA
502  px -6.58                              $ hexside FA
503  p   1  1.7320508076 0  13.16          $ hexside FA
504  p   1  1.7320508076 0 -13.16          $ hexside FA
505  p  -1  1.7320508076 0  13.16          $ hexside FA
506  p  -1  1.7320508076 0 -13.16          $ hexside FA
601  py  1.2                               $ hexside pin
602  py -1.2                               $ hexside pin
603  p   1.7320508076  1 0  2.4            $ hexside pin
604  p   1.7320508076  1 0 -2.4            $ hexside pin
```

```
605  p   1.7320508076 -1 0  2.4                          $ hexside pin
606  p   1.7320508076 -1 0 -2.4

kcode 4000 1 100 5100
ksrc 0.15 0 80
burn   time= 0.3, 0.6, 0.6, 8.5, 20, 30, 60, 60, 60
       pfrac= 1, 1, 1, 1, 1, 1, 1, 1, 0
       power= 1250
       mat= 101, 102, 103, 401, &
             402, 403, 404, 501, 502, &
             503, 511, 512, 513, 514, &
             600, 601, 602
       matvol= 126832.919, 126832.919, 145622.981, 150320.496,
               103345.341, 140925.465, 56370.186, 76099.751, 76099.751,
               87373.788, 90192.298, 62007.205, 84555.279, 33822.112,
               898614.753, 524191.939, 74884.563
       bopt= 1.0 -24 1.0
c    Material 101 is from the output of BOC-2
m101    4009   -0.00003159
        6012   -0.8175
        6013   -24.96
        6014   -0.0006309
        7015   -0.04534
        8016   -159900
        8017   -0.004517
       30066   -0.0001049
       30067   -0.0004304
       30068   -0.0009347
       30070   -0.007126
       31069   -0.005577
       31071   -0.03342
       32072   -0.08508
       32073   -0.1241
       32074   -0.3187
       32076   -1.16
       33075   -0.482
       34076   -0.02092
       34077   -2.485
       34078   -4.935
       34079   -12.21
       34080   -19.9
       34082   -50.01
       35079   -0.0001455
       35081   -29.36
       36080   -0.0008921
       36082   -1.096
       36083   -73.37
       36084   -133.5
```

36085	-30.18
36086	-207.8
37085	-111.3
37086	-0.03891
37087	-275
38086	-2.642
38087	-0.01824
38088	-353
38089	-38.52
38090	-554.9
39088	-0.0001797
39089	-432.8
39090	-0.1442
39091	-72.38
40090	-10.56
40091	-613.5
40092	-833.4
40093	-1034
40094	-1168
40095	-153.9
40096	-1382
41094	-0.009213
41095	-122.6
42094	-0.01517
42095	-985.3
42096	-25.9
42097	-1430
42098	-1610
42100	-1888
43098	-0.0122
43099	-1623
44099	-0.0576
44100	-86.91
44101	-1822
44102	-2080
44103	-103.6
44104	-1945
44106	-820.4
45103	-1816
45106	-0.0007615
46102	-0.0004506
46104	-79.29
46105	-1477
46106	-626.1
46107	-922.9
46108	-709.2
46110	-212.7
47109	-334.7

47111	-0.01269
48108	-0.002961
48110	-17.26
48111	-111.2
48112	-64.66
48113	-39.43
48114	-30.94
48116	-20.59
49113	-0.02731
49115	-22.53
50114	-0.001446
50115	-1.208
50116	-1.534
50117	-22.41
50118	-20.71
50119	-19.02
50120	-20.15
50122	-24.46
50123	-1.835
50124	-40.21
50125	-0.01417
50126	-87.59
51121	-19.44
51123	-24.71
51124	-0.1165
51125	-44.91
51126	-0.005904
52122	-0.7428
52123	-0.009007
52124	-0.5654
52125	-8.103
52126	-3.692
52127	-0.02
52128	-292.6
52129	-0.003141
52130	-885
53127	-142
53129	-478.2
53131	-0.2622
54126	-0.0004783
54128	-7.092
54129	-0.09537
54130	-15.9
54131	-1400
54132	-2053
54133	-0.02409
54134	-2921
54136	-2752

55133	-2547
55134	-88.85
55135	-2841
55136	-0.3224
55137	-2569
56132	-0.0003224
56134	-17.02
56135	-0.1233
56136	-94.86
56137	-46.79
56138	-2482
56140	-4.156
57138	-0.04268
57139	-2310
57140	-0.6298
58139	-0.01831
58140	-2220
58141	-72.8
58142	-1979
58144	-868.2
59141	-2002
59143	-4.936
60142	-21.63
60143	-1750
60144	-788.2
60145	-1262
60146	-1160
60147	-0.8588
60148	-748.8
60150	-452.3
61146	-0.01936
61147	-645.4
61148	-0.02346
62146	-0.003767
62147	-126.1
62148	-72.93
62149	-483.4
62150	-98
62151	-271.4
62152	-347
62154	-120.3
63151	-1.3
63152	-0.1168
63153	-165.5
63154	-32.03
63155	-85.22
63156	-0.3436
64152	-0.07784

```
     64153   -0.002549
     64154   -1.436
     64155   -8.758
     64156   -76.57
     64157   -45.86
     64158   -35.09
     64160   -7.71
     65159   -15.49
     65160   -0.5375
     66160   -1.832
     66161   -3.999
     66162   -3.368
     66163   -1.4
     66164   -0.9046
     67165   -0.3717
     68166   -0.2748
     68167   -0.1152
     68168   -0.0503
     68170   -0.004627
     69169   -0.008066
     69171   -0.000838
     70172   -0.0005614
     92234   -0.6786
     92235.17c   -1481
     92236   -190.1
     92237   -0.01447
     92238.17c   -886100
     93236   -0.005099
     93237   -210.7
     94237   -0.002623
     94238   -81.26
     94239.17c   -149800
     94240   -65880
     94241   -11640
     94242   -3882
     94244   -0.02081
     95241   -644.8
     95242   -6.17
     95243   -250.3
     96242   -37.27
     96243   -1.001
     96244   -33.72
     96245   -1.376
     96246   -0.03487
     96247   -0.0006421
m102   92235.17c -0.0017256  $ -0.00173
     92238.17c -0.6973080  $ -0.69759
     94239.17c -0.1254001  $ -0.12521
```

```
       94240.60c -0.0450321  $ -0.04496
       94241.60c -0.0096691  $ -0.00965
       94242.60c -0.0024919  $ -0.00249
        8016.60c -0.1183732  $ -0.11837  changed wt as per Pu buildup table core I
c    Material 103 is from the output of BOC-2
m103    6012   -0.4705
        6013   -17.15
        6014   -0.0001622
        7015   -0.0261
        8016   -183400
        8017   -0.002514
       31069   -0.003248
       31071   -0.01946
       32072   -0.04913
       32073   -0.0726
       32074   -0.1835
       32076   -0.6714
       33075   -0.2841
       34076   -0.006115
       34077   -1.462
       34078   -2.843
       34079   -7.172
       34080   -11.42
       34082   -28.93
       35081   -17.42
       36080   -0.0004195
       36082   -0.3703
       36083   -42.96
       36084   -76.95
       36085   -17.91
       36086   -120.2
       37085   -64.74
       37086   -0.02051
       37087   -159.3
       38086   -0.7509
       38087   -0.003562
       38088   -204
       38089   -44.12
       38090   -323.9
       39089   -228.6
       39090   -0.08415
       39091   -81.19
       40090   -3.302
       40091   -317
       40092   -481.1
       40093   -599.8
       40094   -672
       40095   -169.5
```

40096	-799.3
41094	-0.003949
41095	-130.4
42094	-0.001929
42095	-438.7
42096	-5.093
42097	-840.1
42098	-922
42100	-1094
43099	-961.4
44099	-0.03272
44100	-20.97
44101	-1084
44102	-1172
44103	-119.3
44104	-1129
44106	-582.3
45103	-1015
46104	-15.35
46105	-880.9
46106	-220.1
46107	-551.8
46108	-386.4
46110	-123.1
47109	-194.8
47111	-0.01463
48108	-0.0008603
48110	-4.526
48111	-65.1
48112	-35.79
48113	-23.09
48114	-17.5
48116	-11.93
49113	-0.01128
49115	-13.48
50114	-0.00025
50115	-0.7017
50116	-0.3819
50117	-13
50118	-11.88
50119	-11.06
50120	-11.54
50122	-14.12
50123	-1.7
50124	-23.21
50125	-0.01682
50126	-50.49
51121	-11.41

51123	-13.8
51124	-0.05256
51125	-28.95
51126	-0.003924
52122	-0.2144
52123	-0.001395
52124	-0.1516
52125	-2.703
52126	-1.318
52128	-168.9
52130	-511
53127	-84.31
53129	-283.7
53131	-0.3105
54128	-1.867
54129	-0.01193
54130	-4.599
54131	-818.4
54132	-1177
54133	-0.02844
54134	-1687
54136	-1589
55133	-1505
55134	-26.23
55135	-1653
55136	-0.2242
55137	-1495
56134	-2.984
56135	-0.008789
56136	-37.38
56137	-15.33
56138	-1432
56140	-4.927
57138	-0.01712
57139	-1335
57140	-0.7465
58139	-0.005921
58140	-1277
58141	-85.85
58142	-1143
58144	-649.5
59141	-1123
59143	-5.844
60142	-4.642
60143	-1033
60144	-294.1
60145	-743.7
60146	-655.9

60147	-1.007
60148	-435
60150	-262.9
61147	-436.5
61148	-0.01241
62147	-44.06
62148	-19.29
62149	-302.7
62150	-28.84
62151	-176.8
62152	-181.4
62154	-70.16
63151	-0.5214
63152	-0.01735
63153	-104.1
63154	-10.3
63155	-50.88
63156	-0.3583
64152	-0.01049
64154	-0.2757
64155	-3.074
64156	-41.68
64157	-26.9
64158	-18.71
64160	-4.47
65159	-9.396
65160	-0.2386
66160	-0.4596
66161	-2.377
66162	-1.788
66163	-0.8033
66164	-0.4914
67165	-0.2218
68166	-0.1533
68167	-0.06641
68168	-0.02498
68170	-0.002684
92234	-0.311
92235.17c	-2146
92236	-120.5
92237	-0.01673
92238.17c	-1049000
93236	-0.001618
93237	-131.8
94237	-0.003003
94238	-25.98
94239.17c	-182500
94240	-72850

```
       94241   -14000
       94242   -4138
       94244   -0.01015
       95241   -422.8
       95242   -1.977
       95243   -146.1
       96242   -12.44
       96243   -0.1717
       96244   -9.73
       96245   -0.2011
       96246   -0.002377
m2     26000.55c -0.66598
        6000.66c -0.00052
       24000.50c -0.13800
       28000.50c -0.15200
       42000.66c -0.01460
       14000.60c -0.00920
       25055.60c -0.01740
       22000.62c -0.00230                    $ SS
m3     11023.62c 1.0                         $ Na
c    Material 401 is from the output of BOC-2
m401    4009   -0.00002569
        6012   -0.7768
        6013   -23.77
        6014   -0.000397
        7015   -0.04309
        8016   -190000
        8017   -0.003203
       30067   -0.0004042
       30068   -0.0008995
       30070   -0.007165
       31069   -0.005611
       31071   -0.03433
       32072   -0.08688
       32073   -0.1284
       32074   -0.3244
       32076   -1.182
       33075   -0.499
       34076   -0.01275
       34077   -2.564
       34078   -4.98
       34079   -12.55
       34080   -20.11
       34082   -50.36
       35079   -0.0001509
       35081   -30.44
       36080   -0.0008473
       36082   -0.7548
```

36083	-73.97
36084	-131.2
36085	-30.3
36086	-206.6
37085	-112.4
37086	-0.02327
37087	-274
38086	-1.605
38087	-0.008727
38088	-350
38089	-37.83
38090	-551.7
39089	-429.1
39090	-0.1434
39091	-71.7
40090	-10.41
40091	-613.7
40092	-831.1
40093	-1039
40094	-1162
40095	-153.8
40096	-1390
41094	-0.007922
41095	-122.7
42094	-0.01226
42095	-1004
42096	-16.09
42097	-1459
42098	-1616
42100	-1914
43098	-0.01003
43099	-1670
44099	-0.05891
44100	-53.45
44101	-1888
44102	-2067
44103	-103.7
44104	-1980
44106	-838.3
45103	-1876
45106	-0.0007781
46102	-0.0003736
46104	-49.16
46105	-1548
46106	-596.4
46107	-971.7
46108	-698.9
46110	-219.8

47109	-348.6
47111	-0.01282
48108	-0.002469
48110	-10.44
48111	-116
48112	-64.54
48113	-40.9
48114	-31.2
48116	-20.99
49113	-0.02333
49115	-23.63
50114	-0.000796
50115	-1.239
50116	-0.9763
50117	-22.9
50118	-20.96
50119	-19.34
50120	-20.41
50122	-24.93
50123	-1.882
50124	-40.97
50125	-0.01426
50126	-89.47
51121	-20.07
51123	-25.4
51124	-0.07513
51125	-46.66
51126	-0.004034
52122	-0.4713
52123	-0.003715
52124	-0.3797
52125	-8.476
52126	-2.705
52127	-0.02036
52128	-298.1
52129	-0.003121
52130	-890.3
53127	-147.9
53129	-490.9
53131	-0.2607
54126	-0.0003969
54128	-4.334
54129	-0.03612
54130	-10.14
54131	-1424
54132	-2050
54133	-0.02385
54134	-2933

54136	-2766
55133	-2606
55134	-53.8
55135	-2880
55136	-0.2228
55137	-2588
56132	-0.0002632
56134	-10.27
56135	-0.05015
56136	-72.16
56137	-47.22
56138	-2495
56140	-4.111
57138	-0.03814
57139	-2330
57140	-0.623
58139	-0.01458
58140	-2221
58141	-72.82
58142	-1989
58144	-872
59141	-2033
59143	-4.943
60142	-12.29
60143	-1795
60144	-774.8
60145	-1289
60146	-1141
60147	-0.8553
60148	-753.5
60150	-457.8
61146	-0.01658
61147	-689.2
61148	-0.01525
62146	-0.003195
62147	-136.8
62148	-45.3
62149	-516.7
62150	-59.6
62151	-301.8
62152	-323
62154	-122.7
63151	-1.565
63152	-0.08651
63153	-178.2
63154	-21.03
63155	-85.8
63156	-0.3152

```
     64152   -0.05399
     64153   -0.001033
     64154   -0.9366
     64155   -9.341
     64156   -74.86
     64157   -47.32
     64158   -33.65
     64160   -7.955
     65159   -16.38
     65160   -0.3432
     66160   -1.177
     66161   -4.191
     66162   -3.239
     66163   -1.42
     66164   -0.8815
     67165   -0.3921
     68166   -0.274
     68167   -0.1177
     68168   -0.04584
     68170   -0.004722
     69169   -0.007995
     69171   -0.0008108
     70172   -0.0005267
     92234   -0.6528
     92235.17c   -1913
     92236   -144
     92237   -0.01247
     92238.17c   -981600
     93236   -0.003954
     93237   -194
     94237   -0.003088
     94238   -74.82
     94239.17c   -234600
     94240   -100300
     94241   -18450
     94242   -5821
     94244   -0.01142
     95241   -1100
     95242   -7.212
     95243   -245.9
     96242   -37.83
     96243   -0.6003
     96244   -19.93
     96245   -0.506
     96246   -0.007651
m402   92235.17c -0.0015732  $ -0.00157
     92238.17c -0.6357256  $ -0.63568
     94239.17c -0.1678273  $ -0.16786
```

```
      94240.60c -0.0602681  $ -0.06028
      94241.60c -0.0129404  $ -0.01294
      94242.60c -0.0033350  $ -0.00334
       8016.60c -0.1183303  $ -0.11833  changed wt as per Pu buildup table  core II
c    Material 403 is from the output of BOC-2
m403    6012   -0.3893
       6013   -14.14
       6014   -0.00009539
       7015   -0.0216
       8016   -178000
       8017   -0.001603
      31069   -0.002885
      31071   -0.01769
      32072   -0.04461
      32073   -0.06625
      32074   -0.1662
      32076   -0.6066
      33075   -0.2586
      34076   -0.003682
      34077   -1.326
      34078   -2.547
      34079   -6.484
      34080   -10.26
      34082   -25.79
      35081   -15.81
      36080   -0.0003684
      36082   -0.2562
      36083   -38.11
      36084   -66.97
      36085   -15.91
      36086   -105.6
      37085   -57.56
      37086   -0.01209
      37087   -140.2
      38086   -0.449
      38087   -0.002313
      38088   -179
      38089   -38.65
      38090   -284.6
      39089   -200.3
      39090   -0.07395
      39091   -71.65
      40090   -2.883
      40091   -279.4
      40092   -424.8
      40093   -532.5
      40094   -593.2
      40095   -151.2
```

40096	-711
41094	-0.003199
41095	-116.4
42094	-0.001487
42095	-392.2
42096	-3.128
42097	-754.3
42098	-822.4
42100	-981
43099	-866.1
44099	-0.02943
44100	-12.41
44101	-981.8
44102	-1043
44103	-107.4
44104	-1017
44106	-528.5
45103	-918.7
46104	-9.111
46105	-811.4
46106	-189.4
46107	-507.4
46108	-346.1
46110	-112.7
47109	-179.3
47111	-0.01338
48108	-0.0006807
48110	-2.615
48111	-59.91
48112	-32.25
48113	-21.13
48114	-15.8
48116	-10.77
49113	-0.009386
49115	-12.35
50115	-0.6372
50116	-0.2333
50117	-11.77
50118	-10.69
50119	-9.956
50120	-10.4
50122	-12.77
50123	-1.553
50124	-21
50125	-0.01519
50126	-45.84
51121	-10.37
51123	-12.5

51124	-0.03393
51125	-26.41
51126	-0.002688
52122	-0.1324
52123	-0.0006923
52124	-0.102
52125	-2.467
52126	-0.9772
52128	-152.8
52130	-455.9
53127	-76.95
53129	-255.2
53131	-0.2765
54128	-1.101
54129	-0.004769
54130	-2.888
54131	-733.4
54132	-1045
54133	-0.02523
54134	-1501
54136	-1415
55133	-1350
55134	-15.2
55135	-1480
55136	-0.1605
55137	-1336
56134	-1.726
56135	-0.004795
56136	-28.79
56137	-13.69
56138	-1276
56140	-4.358
57138	-0.01452
57139	-1192
57140	-0.6604
58139	-0.004516
58140	-1133
58141	-76.78
58142	-1018
58144	-578.8
59141	-1005
59143	-5.234
60142	-2.576
60143	-926.8
60144	-257.2
60145	-665.8
60146	-576.9
60147	-0.8997

60148	-386.7
60150	-234.9
61147	-398.9
61148	-0.007476
62147	-40.38
62148	-11.32
62149	-276.1
62150	-16.69
62151	-165
62152	-155.9
62154	-63.16
63151	-0.4976
63152	-0.0111
63153	-95.68
63154	-6.171
63155	-46.17
63156	-0.3119
64152	-0.006463
64154	-0.1648
64155	-2.822
64156	-37.07
64157	-24.46
64158	-16.5
64160	-4.085
65159	-8.656
65160	-0.1454
66160	-0.2801
66161	-2.197
66162	-1.582
66163	-0.7273
66164	-0.4377
67165	-0.2049
68166	-0.1379
68167	-0.0603
68168	-0.02152
68170	-0.002418
92234	-0.2526
92235.17c	-2041
92236	-76.7
92237	-0.01288
92238.17c	-936900
93236	-0.001106
93237	-102.5
94237	-0.003352
94238	-22.26
94239.17c	-234200
94240	-92660
94241	-18230

```
      94242   -5240
      94244   -0.005569
      95241   -564.1
      95242   -1.86
      95243   -126.6
      96242   -10.97
      96243   -0.09684
      96244   -5.545
      96245   -0.0766
      96246   -0.0005938
m404   92235.17c -0.0015732  $ -0.00157
      92238.17c -0.6357256  $ -0.63568
      94239.17c -0.1678273  $ -0.16786
      94240.60c -0.0602681  $ -0.06028
      94241.60c -0.0129404  $ -0.01294
      94242.60c -0.0033350  $ -0.00334
       8016.60c -0.1183303  $ -0.11833  core II fuel
c    Material 501 is from the output of BOC-2
m501    6012   -0.05483
       6013   -1.764
       7015   -0.003023
       8016   -105100
       8017   -0.001511
      30070   -0.0002267
      31069   -0.000106
      31071   -0.000658
      32072   -0.001626
      32073   -0.00262
      32074   -0.006223
      32076   -0.03216
      33075   -0.01076
      34076   -0.0001749
      34077   -0.06928
      34078   -0.145
      34079   -0.3302
      34080   -0.5305
      34082   -1.54
      35081   -0.8165
      36082   -0.01566
      36083   -2.546
      36084   -5.218
      36085   -1.024
      36086   -7.979
      37085   -3.869
      37086   -0.0006188
      37087   -10.41
      38086   -0.03627
      38087   -0.0001231
```

38088	-13.71
38089	-1.914
38090	-21.54
39089	-16.55
39090	-0.005596
39091	-3.41
40090	-0.3549
40091	-22.35
40092	-29.2
40093	-34.3
40094	-35.41
40095	-6.114
40096	-42.4
41095	-4.729
42095	-28.01
42096	-0.3558
42097	-41.77
42098	-45.13
42100	-52.25
43099	-46.65
44099	-0.001612
44100	-0.9355
44101	-49.29
44102	-51.98
44103	-3.68
44104	-44.19
44106	-17.64
45103	-45.19
46104	-0.8033
46105	-34.33
46106	-9.223
46107	-17.45
46108	-10.37
46110	-3.085
47109	-4.886
47111	-0.0003279
48110	-0.09612
48111	-1.667
48112	-0.9956
48113	-0.6928
48114	-0.5739
48116	-0.445
49113	-0.0002025
49115	-0.4638
50115	-0.02431
50116	-0.01452
50117	-0.4741
50118	-0.4616

50119	-0.4452
50120	-0.4378
50122	-0.5247
50123	-0.04483
50124	-0.8403
50125	-0.0004897
50126	-1.657
51121	-0.4252
51123	-0.5385
51124	-0.00126
51125	-0.9753
52122	-0.00666
52124	-0.005407
52125	-0.1323
52126	-0.0368
52127	-0.0006337
52128	-6.143
52130	-23.2
53127	-3.102
53129	-12.41
53131	-0.0109
54128	-0.06582
54129	-0.0002805
54130	-0.1581
54131	-38
54132	-57.8
54133	-0.001039
54134	-84.37
54136	-76.06
55133	-73.48
55134	-1.364
55135	-78.27
55136	-0.006852
55137	-70.73
56134	-0.2376
56135	-0.0006542
56136	-1.481
56137	-1.068
56138	-69.74
56140	-0.1726
57138	-0.0002782
57139	-64.84
57140	-0.02615
58140	-63.09
58141	-2.957
58142	-56.4
58144	-28.72
59141	-57.29

59143	-0.2081
60142	-0.3297
60143	-51.57
60144	-21.07
60145	-38.99
60146	-35.76
60147	-0.03647
60148	-22.02
60150	-12.84
61147	-20.91
61148	-0.0004962
62147	-3.43
62148	-1.298
62149	-14.7
62150	-1.812
62151	-7.858
62152	-7.409
62154	-2.719
63151	-0.0342
63152	-0.001616
63153	-4.468
63154	-0.4465
63155	-1.74
63156	-0.009662
64152	-0.0008996
64154	-0.01781
64155	-0.1523
64156	-1.412
64157	-0.8458
64158	-0.5598
64160	-0.1117
65159	-0.2795
65160	-0.004323
66160	-0.01169
66161	-0.05567
66162	-0.04374
66163	-0.0196
66164	-0.01198
67165	-0.005454
68166	-0.004128
68167	-0.001853
68168	-0.000712
69169	-0.000174
92234	-0.0448
92235.17c	-1589
92236	-86.08
92237	-0.001586
92238.17c	-762600

```
       93237   -21.93
       94238   -1.569
       94239.17c   -14900
       94240   -460.6
       94241   -12.41
       94242   -0.1468
       95241   -0.2471
       95242   -0.0003901
       95243   -0.001527
       96242   -0.002198  $ axial blanket
m502   92235.17c -0.00218
       92238.17c -0.87932
        8016.60c -0.11850                     $ axial blanket
c    Material 503 is from the output of BOC-2
m503    6012   -0.03146
        6013   -1.203
        7015   -0.001738
        8016   -120600
        8017   -0.0008497
       31071   -0.0002149
       32072   -0.0005094
       32073   -0.0009352
       32074   -0.002091
       32076   -0.01362
       33075   -0.004096
       34077   -0.02926
       34078   -0.06328
       34079   -0.137
       34080   -0.2201
       34082   -0.6819
       35081   -0.3474
       36082   -0.00381
       36083   -1.179
       36084   -2.506
       36085   -0.4749
       36086   -3.819
       37085   -1.781
       37086   -0.0002544
       37087   -4.964
       38086   -0.008543
       38088   -6.561
       38089   -1.562
       38090   -10.4
       39089   -7.314
       39090   -0.002703
       39091   -2.685
       40090   -0.09952
       40091   -9.589
```

40092	-13.61
40093	-15.77
40094	-15.75
40095	-4.346
40096	-19.05
41095	-3.25
42095	-9.807
42096	-0.05691
42097	-18.37
42098	-19.55
42100	-22.56
43099	-20.37
44099	-0.0006873
44100	-0.1803
44101	-20.99
44102	-21.57
44103	-2.47
44104	-17.5
44106	-7.399
45103	-17.85
46104	-0.1201
46105	-13.85
46106	-2.317
46107	-6.221
46108	-3.271
46110	-0.9511
47109	-1.521
47111	-0.0001755
48110	-0.01372
48111	-0.508
48112	-0.323
48113	-0.2384
48114	-0.2028
48116	-0.1752
49115	-0.1723
50115	-0.008889
50116	-0.002444
50117	-0.18
50118	-0.1834
50119	-0.1812
50120	-0.1738
50122	-0.2034
50123	-0.01888
50124	-0.3103
50125	-0.0002929
50126	-0.5673
51121	-0.1672
51123	-0.2095

51124	-0.0004295
51125	-0.3636
52122	-0.001424
52124	-0.001205
52125	-0.02931
52126	-0.008259
52128	-2.235
52130	-9.651
53127	-1.143
53129	-5.108
53131	-0.00809
54128	-0.0108
54130	-0.03369
54131	-16.23
54132	-24.91
54133	-0.0007959
54134	-37.09
54136	-32.82
55133	-32.25
55134	-0.3188
55135	-33.7
55136	-0.003037
55137	-30.57
56134	-0.03503
56136	-0.3588
56137	-0.278
56138	-30.32
56140	-0.131
57139	-28.34
57140	-0.01985
58140	-27.61
58141	-2.194
58142	-24.64
58144	-15.7
59141	-24.35
59143	-0.1597
60142	-0.05801
60143	-23.21
60144	-6.557
60145	-17.73
60146	-16.13
60147	-0.02822
60148	-9.855
60150	-5.679
61147	-10.37
61148	-0.0001972
62147	-0.9791
62148	-0.2864

```
     62149   -6.845
     62150   -0.4442
     62151   -3.537
     62152   -2.858
     62154   -1.099
     63151   -0.009924
     63152   -0.0001782
     63153   -1.91
     63154   -0.1052
     63155   -0.6934
     63156   -0.005789
     64154   -0.002712
     64155   -0.03872
     64156   -0.4945
     64157   -0.3008
     64158   -0.1836
     64160   -0.03465
     65159   -0.09427
     65160   -0.001038
     66160   -0.001765
     66161   -0.01674
     66162   -0.01248
     66163   -0.005221
     66164   -0.00321
     67165   -0.001501
     68166   -0.001135
     68167   -0.000562
     68168   -0.0002193
     92234   -0.02438
     92235.17c   -2016
     92236   -51.32
     92237   -0.001617
     92238.17c   -885500
     93237   -12.33
     94238   -0.4195
     94239.17c   -8822
     94240   -138.7
     94241   -2.072
     94242   -0.01142      $ axial blanket
c    Material 511 is from the output of BOC-2
m511    6012   -0.04317
      6013   -1.413
      7015   -0.002378
      8016   -124500
      8017   -0.001112
     30070   -0.0001265
     31071   -0.0003623
     32072   -0.0008583
```

32073	-0.001531
32074	-0.003467
32076	-0.02021
33075	-0.006206
34077	-0.04346
34078	-0.09231
34079	-0.2064
34080	-0.3334
34082	-1.009
35081	-0.5231
36082	-0.00682
36083	-1.712
36084	-3.583
36085	-0.679
36086	-5.519
37085	-2.598
37086	-0.0002605
37087	-7.163
38086	-0.01581
38088	-9.385
38089	-1.237
38090	-14.84
39089	-11.4
39090	-0.003856
39091	-2.222
40090	-0.252
40091	-15.54
40092	-19.77
40093	-23.04
40094	-23.35
40095	-3.796
40096	-28.24
41095	-2.954
42095	-18.91
42096	-0.1592
42097	-27.46
42098	-29.46
42100	-34.07
43099	-30.42
44099	-0.001054
44100	-0.4009
44101	-31.85
44102	-33.11
44103	-2.18
44104	-27.32
44106	-10.28
45103	-29.08
46104	-0.3461

46105	-21.4
46106	-5.46
46107	-10.1
46108	-5.633
46110	-1.662
47109	-2.649
47111	-0.0001684
48110	-0.03394
48111	-0.8925
48112	-0.5488
48113	-0.3958
48114	-0.3324
48116	-0.2737
49115	-0.2772
50115	-0.01436
50116	-0.005709
50117	-0.2856
50118	-0.2866
50119	-0.2718
50120	-0.2713
50122	-0.319
50123	-0.0226
50124	-0.4861
50125	-0.0002471
50126	-0.8998
51121	-0.2615
51123	-0.3312
51124	-0.0005251
51125	-0.543
52122	-0.002731
52124	-0.002425
52125	-0.07698
52126	-0.01543
52127	-0.0003431
52128	-3.518
52130	-14.6
53127	-1.764
53129	-7.386
53131	-0.006332
54128	-0.02342
54130	-0.06321
54131	-24.03
54132	-36.66
54133	-0.000613
54134	-54.25
54136	-49.02
55133	-47.42
55134	-0.5847

55135	-49.88
55136	-0.002993
55137	-45.02
56134	-0.1041
56135	-0.0001982
56136	-0.6642
56137	-0.7033
56138	-44.57
56140	-0.105
57139	-42.04
57140	-0.0159
58140	-41.34
58141	-1.796
58142	-36.25
58144	-18.79
59141	-37.53
59143	-0.1275
60142	-0.1407
60143	-34.55
60144	-14.27
60145	-26.17
60146	-23.71
60147	-0.02253
60148	-14.55
60150	-8.487
61147	-14.23
61148	-0.0002246
62147	-2.472
62148	-0.5931
62149	-10.25
62150	-0.8325
62151	-5.227
62152	-4.485
62154	-1.699
63151	-0.02463
63152	-0.0007274
63153	-2.899
63154	-0.1953
63155	-1.053
63156	-0.005114
64152	-0.0004248
64154	-0.008001
64155	-0.09867
64156	-0.8022
64157	-0.4776
64158	-0.296
64160	-0.05989
65159	-0.1502

```
       65160   -0.001494
       66160   -0.004155
       66161   -0.029
       66162   -0.02113
       66163   -0.009649
       66164   -0.005828
       67165   -0.002783
       68166   -0.002047
       68167   -0.0009631
       68168   -0.0002622
       92234   -0.0353
       92235.17c   -2027
       92236   -66.29
       92237   -0.001143
       92238.17c   -911400
       93237   -17.08
       94238   -0.7946
       94239.17c   -11420
       94240   -220.9
       94241   -4.099
       94242   -0.0293
       95241   -0.08086
       96242   -0.0004389      $ axial blanket
m512   92235.17c -0.00218
       92238.17c -0.87932
        8016.60c -0.11850                          $ axial blanket
c    Material 513 is from the output of BOC-2
m513    6012   -0.02186
        6013   -0.8553
        7015   -0.001204
        8016   -116700
        8017   -0.0005618
       31071   -0.0001197
       32072   -0.0002706
       32073   -0.0005514
       32074   -0.00118
       32076   -0.008378
       33075   -0.00233
       34077   -0.01797
       34078   -0.03919
       34079   -0.08403
       34080   -0.1363
       34082   -0.4328
       35081   -0.2174
       36082   -0.001711
       36083   -0.7581
       36084   -1.629
       36085   -0.3031
```

36086	-2.501
37085	-1.144
37086	-0.000113
37087	-3.238
38086	-0.003832
38088	-4.255
38089	-0.9934
38090	-6.788
39089	-4.755
39090	-0.001764
39091	-1.729
40090	-0.06547
40091	-6.296
40092	-8.803
40093	-10.14
40094	-10.05
40095	-2.717
40096	-12.25
41095	-2.046
42095	-6.334
42096	-0.02588
42097	-11.73
42098	-12.45
42100	-14.35
43099	-12.89
44099	-0.0004353
44100	-0.07985
44101	-13.26
44102	-13.56
44103	-1.502
44104	-10.77
44106	-4.397
45103	-11.28
46104	-0.05486
46105	-8.5
46106	-1.372
46107	-3.62
46108	-1.82
46110	-0.5206
47109	-0.8384
48110	-0.004928
48111	-0.2757
48112	-0.182
48113	-0.138
48114	-0.1191
48116	-0.107
49115	-0.1031
50115	-0.005289

50116	-0.001061
50117	-0.1087
50118	-0.1133
50119	-0.1108
50120	-0.1072
50122	-0.1235
50123	-0.009475
50124	-0.18
50125	-0.0001455
50126	-0.3092
51121	-0.1023
51123	-0.1283
51124	-0.0001991
51125	-0.2034
52122	-0.0006203
52124	-0.0005866
52125	-0.01689
52126	-0.003641
52128	-1.285
52130	-5.996
53127	-0.6479
53129	-2.957
53131	-0.004705
54128	-0.004641
54130	-0.01428
54131	-10.03
54132	-15.43
54133	-0.0004686
54134	-23.16
54136	-20.64
55133	-20.14
55134	-0.1411
55135	-20.95
55136	-0.001362
55137	-19.01
56134	-0.01561
56136	-0.1639
56137	-0.1747
56138	-18.88
56140	-0.07999
57139	-17.88
57140	-0.01212
58140	-17.59
58141	-1.344
58142	-15.4
58144	-10.08
59141	-15.46
59143	-0.09767

60142 -0.02586
60143 -14.83
60144 -4.226
60145 -11.43
60146 -10.33
60147 -0.01746
60148 -6.289
60150 -3.639
61147 -6.758
62147 -0.6499
62148 -0.1324
62149 -4.564
62150 -0.2084
62151 -2.257
62152 -1.742
62154 -0.6694
63151 -0.006515
63153 -1.208
63154 -0.04745
63155 -0.4218
63156 -0.003146
64154 -0.001232
64155 -0.02419
64156 -0.2853
64157 -0.1703
64158 -0.09889
64160 -0.01882
65159 -0.0504
65160 -0.0003943
66160 -0.0006834
66161 -0.008707
66162 -0.005998
66163 -0.002554
66164 -0.001563
67165 -0.0007649
68166 -0.0005635
68167 -0.0002928
92234 -0.01744
92235.17c -2011
92236 -34.54
92237 -0.001109
92238.17c -859900
93237 -8.731
94238 -0.2061
94239.17c -5924
94240 -63.95
94241 -0.7165
94242 -0.002649 $ axial blanket

```
m514   92235.17c -0.00218
       92238.17c -0.87932
        8016.60c -0.11850                           $ axial blanket
m524   92235.17c -0.00218
       92238.17c -0.87932
        8016.60c -0.11850                           $ axial blanket
c    Material 600 is from the output of BOC-2
m600    6012   -0.1795
        6013   -5.883
        7015   -0.009862
        8016   -1128000
        8017   -0.00706
       31071   -0.001016
       32072   -0.003617
       32073   -0.006839
       32074   -0.01542
       32076   -0.1051
       33075   -0.03016
       34077   -0.2186
       34078   -0.452
       34079   -0.9642
       34080   -1.597
       34082   -4.602
       35081   -2.454
       36082   -0.02443
       36083   -7.842
       36084   -16.27
       36085   -3.168
       36086   -25.57
       37085   -12.18
       37087   -33.24
       38086   -0.05052
       38088   -43.79
       38089   -5.617
       38090   -69.22
       39089   -52.99
       39090   -0.01798
       39091   -10.06
       40090   -1.187
       40091   -71.96
       40092   -90.26
       40093   -104.4
       40094   -105.6
       40095   -16.74
       40096   -125.9
       41095   -13.05
       42095   -85.8
       42096   -0.538
```

42097	-122.8
42098	-130.2
42100	-150.1
43099	-135.3
44099	-0.00469
44100	-1.247
44101	-139.4
44102	-142.3
44103	-9.143
44104	-114.7
44106	-42.1
45103	-124.4
46104	-1.062
46105	-90.07
46106	-22.04
46107	-41.42
46108	-22.57
46110	-6.759
47109	-10.74
48110	-0.1014
48111	-3.645
48112	-2.262
48113	-1.657
48114	-1.401
48116	-1.179
49115	-1.187
50115	-0.06122
50116	-0.01947
50117	-1.231
50118	-1.232
50119	-1.162
50120	-1.175
50122	-1.378
50123	-0.09213
50124	-2.093
50126	-3.805
51121	-1.134
51123	-1.436
51124	-0.001674
51125	-2.304
52122	-0.00853
52124	-0.008023
52125	-0.334
52126	-0.05403
52127	-0.00145
52128	-15.26
52130	-62.69
53127	-7.717

53129	-32.77
53131	-0.02695
54128	-0.0767
54130	-0.1989
54131	-105.2
54132	-158.8
54133	-0.002596
54134	-238.9
54136	-214.6
55133	-210.2
55134	-1.852
55135	-218.6
55136	-0.01031
55137	-197.9
56134	-0.3328
56136	-2.355
56137	-3.125
56138	-197.6
56140	-0.4558
57139	-186.9
57140	-0.06907
58140	-183.4
58141	-7.812
58142	-161.3
58144	-83.94
59141	-167.4
59143	-0.559
60142	-0.4383
60143	-155.7
60144	-64.24
60145	-116.9
60146	-104.2
60147	-0.09751
60148	-63.7
60150	-36.55
61147	-63.47
62147	-11.19
62148	-1.933
62149	-45.22
62150	-2.72
62151	-22.79
62152	-18.55
62154	-7.037
63151	-0.1104
63152	-0.00233
63153	-12.45
63154	-0.605
63155	-4.37

```
      63156   -0.02028
      64154   -0.02499
      64155   -0.4171
      64156   -3.253
      64157   -1.951
      64158   -1.182
      64160   -0.2422
      65159   -0.6105
      65160   -0.004164
      66160   -0.0111
      66161   -0.1167
      66162   -0.08222
      66163   -0.03804
      66164   -0.0228
      67165   -0.01102
      68166   -0.008048
      68167   -0.002752
      92234   -0.1497
      92235.17c   -19110
      92236   -426
      92237   -0.005009
      92238.17c   -8296000
      93237   -73.39
      94238   -2.342
      94239.17c   -68130
      94240   -933.8
      94241   -14.46
      94242   -0.07244
      95241   -0.3203    $ radial blanket
m601   92235.17c -0.00218
      92238.17c -0.87932
       8016.60c -0.11850                    $ radial blanket
m602   92235.17c -0.00218
      92238.17c -0.87932
       8016.60c -0.11850                    $ radial blanket
m604   92235.17c -0.0015732  $ -0.00157
      92238.17c -0.6357256  $ -0.63568
      94239.17c -0.1678273  $ -0.16786
      94240.60c -0.0602681  $ -0.06028
      94241.60c -0.0129404  $ -0.01294
      94242.60c -0.0033350  $ -0.00334
       8016.60c -0.1183303  $ -0.11833  core II fuel
m7     26054.62c 0.49285e-03
      26056.62c 0.77367e-02
      26057.62c 0.17867e-03
      26058.62c 0.23778e-04
      24050.62c 0.83368e-04
      24052.62c 0.16077e-02
```

```
       24053.62c 0.18230e-03
       24054.62c 0.45377e-04
       28058.62c 0.12397e-02
       28060.62c 0.47752e-03
       28061.62c 0.20759e-04
       28062.62c 0.66175e-04
       28064.62c 0.16862e-04
       42000.66c 0.16722e-03
        6012.50c 0.15150e-01
       11023.62c 0.55700e-02
        1001.62c 0.95384e-20
       14000.60c 0.15859e-03
       25055.62c 0.25943e-03
        5010.66c 0.11915e-01
        5011.66c 0.48262e-01                $ B4C Shld & SS bot
m8     26054.62c 0.25312e-02
       26056.62c 0.39734e-01
       26057.62c 0.91763e-03
       26058.62c 0.12212e-03
       24050.62c 0.54017e-04
       24052.62c 0.10417e-02
       24053.62c 0.11812e-03
       24054.62c 0.29402e-04
       28058.62c 0.52485e-02
       28060.62c 0.20217e-02
       28061.62c 0.87891e-04
       28062.62c 0.28017e-03
       28064.62c 0.71392e-04
       42000.66c 0.96251e-03
        6012.50c 0.83109e-04
       11023.62c 0.64104e-02
        1001.62c 0.95384e-20
       14000.60c 0.65748e-03
       25055.62c 0.11766e-02                $ SS Reflector
m9     26054.62c 0.54798e-03
       26056.62c 0.86021e-02
       26057.62c 0.19866e-03
       26058.62c 0.26438e-04
       24050.62c 0.92692e-04
       24052.62c 0.17875e-02
       24053.62c 0.20268e-03
       24054.62c 0.50453e-04
       28058.62c 0.13783e-02
       28060.62c 0.53091e-03
       28061.62c 0.23080e-04
       28062.62c 0.73574e-04
       28064.62c 0.18748e-04
       42000.66c 0.18592e-03
```

```
       6012.50c 0.28365e-04
       11023.62c 0.19719e-01
       1001.62c 0.95384e-20
       14000.60c 0.17636e-03
       25055.62c 0.28844e-03                    $ CSR/DSR follower
m10    26054.62c 0.62343e-03
       26056.62c 0.97865e-02
       26057.62c 0.22601e-03
       26058.62c 0.30078e-04
       24050.62c 0.10546e-03
       24052.62c 0.20336e-02
       24053.62c 0.23060e-03
       24054.62c 0.57401e-04
       28058.62c 0.15682e-02
       28060.62c 0.60405e-03
       28061.62c 0.26260e-04
       28062.62c 0.83709e-04
       28064.62c 0.21330e-04
       42000.66c 0.21153e-03
       5010.66c 0.15779e-01
       5011.66c 0.12131e-01
       6012.50c 0.69823e-02
       11023.62c 0.12380e-01
       1001.62c 0.95384e-20
       14000.60c 0.20061e-03
       25055.62c 0.32817e-03                    $ CSR/DSR homo
m11    26054.62c 0.19242e-02
       26056.62c 0.30205e-01
       26057.62c 0.69757e-03
       26058.62c 0.92834e-04
       24050.62c 0.32548e-03
       24052.62c 0.62765e-02
       24053.62c 0.71170e-03
       24054.62c 0.17716e-03
       28058.62c 0.48398e-02
       28060.62c 0.18643e-02
       28061.62c 0.81046e-04
       28062.62c 0.25835e-03
       28064.62c 0.65832e-04
       42000.66c 0.65284e-03
       6012.50c 0.99601e-04
       11023.62c 0.97907e-02
       1001.62c 0.95384e-20
       14000.60c 0.61914e-03
       25055.62c 0.10128e-02                    $ SA bottom
m12    26054.62c 0.78387e-03
       26056.62c 0.12305e-01
       26057.62c 0.28418e-03
```

```
       26058.62c 0.37819e-04
       24050.62c 0.13260e-03
       24052.62c 0.25571e-02
       24053.62c 0.28995e-03
       24054.62c 0.72175e-04
       28058.62c 0.19717e-02
       28060.62c 0.75950e-03
       28061.62c 0.33018e-04
       28062.62c 0.10525e-03
       28064.62c 0.26820e-04
       42000.66c 0.26597e-03
        6012.50c 0.40578e-04
       11023.62c 0.97126e-02
        1001.62c 0.99184e-20
       14000.60c 0.25224e-03
       25055.62c 0.41263e-03                    $ Core Plenum homog
m13    26054.62c 0.23927e-02
       26056.62c 0.37560e-01
       26057.62c 0.86743e-03
       26058.62c 0.11544e-03
       24050.62c 0.40474e-03
       24052.62c 0.78049e-02
       24053.62c 0.88502e-03
       24054.62c 0.22030e-03
       28058.62c 0.60183e-02
       28060.62c 0.23182e-02
       28061.62c 0.10078e-03
       28062.62c 0.32126e-03
       28064.62c 0.81863e-04
       42000.66c 0.81182e-03
        6012.50c 0.12386e-03
       11023.62c 0.64104e-02
        1001.62c 0.95384e-20
       14000.60c 0.76992e-03
       25055.62c 0.12595e-02                    $ RBPBSS
m14    26054.62c 0.29254e-03
       26056.62c 0.45923e-02
       26057.62c 0.10606e-03
       26058.62c 0.14114e-04
       24050.62c 0.49438e-04
       24052.62c 0.95424e-03
       24053.62c 0.10820e-03
       24054.62c 0.26934e-04
       28058.62c 0.73597e-03
       28060.62c 0.28349e-03
       28061.62c 0.12324e-04
       28062.62c 0.39286e-04
       28064.62c 0.10011e-04
```

```
        42000.66c 0.91980e-04
         6012.50c 0.10890e-04
        11023.62c 0.21539e-01
        14000.60c 0.94113e-04
        25055.62c 0.15398e-03                $ RBPT/RFTSS1
m15      6012.50c 0.83867e-04
        14000.60c 0.52075e-03
        25055.62c 0.85201e-03
        26054.62c 0.16187e-02
        26056.62c 0.25410e-01
        26057.62c 0.58684e-03
        26058.62c 0.78097e-04
        24050.62c 0.27381e-03
        24052.62c 0.52802e-02
        24053.62c 0.59873e-03
        24054.62c 0.14904e-03
        28058.62c 0.40722e-02
        28060.62c 0.15686e-02
        28061.62c 0.68192e-04
        28062.62c 0.21738e-03
        28064.62c 0.55391e-04
        42000.66c 0.54889e-03
        11023.62c 0.11882e-01                $ Core-SS
m16      5010.66c 0.47121e-02
         5011.66c 0.19329e-01
         6012.50c 0.60415e-02
        14000.60c 0.19450e-03
        25055.62c 0.31822e-03
        42000.66c 0.20501e-03
        11023.62c 0.11882e-01
        26054.62c 0.60458e-03
        26056.62c 0.94907e-02
        26057.62c 0.21918e-03
        26058.62c 0.29169e-04
        24050.62c 0.10227e-03
        24052.62c 0.19721e-02
        24053.62c 0.22362e-03
        24054.62c 0.55664e-04
        28058.62c 0.15209e-02
        28060.62c 0.58586e-03
        28061.62c 0.25469e-04
        28062.62c 0.81189e-04
        28064.62c 0.20688e-04                $ Core B4C
m17     26054.62c 0.49285e-03
        26056.62c 0.77367e-02
        26057.62c 0.17867e-03
        26058.62c 0.23778e-04
        24050.62c 0.83368e-04
```

```
      24052.62c 0.16077e-02
      24053.62c 0.18230e-03
      24054.62c 0.45377e-04
      28058.62c 0.12397e-02
      28060.62c 0.47752e-03
      28061.62c 0.20759e-04
      28062.62c 0.66175e-04
      28064.62c 0.16862e-04
      42000.66c 0.16722e-03
      6012.50c 0.25512e-04
      11023.62c 0.55700e-02
      1001.62c 0.95384e-20
      14000.60c 0.15859e-03
      25055.62c 0.25943e-03                $ SHPLenum
m18    26054.62c 0.20590e-02
      26056.62c 0.32322e-01
      26057.62c 0.74646e-03
      26058.62c 0.99340e-04
      24050.62c 0.34829e-03
      24052.62c 0.67164e-02
      24053.62c 0.76158e-03
      24054.62c 0.18957e-03
      28058.62c 0.51790e-02
      28060.62c 0.19949e-02
      28061.62c 0.86726e-04
      28062.62c 0.27646e-03
      28064.62c 0.70445e-04
      42000.66c 0.69860e-03
      6012.50c 0.10658e-03
      11023.62c 0.88178e-02
      1001.62c 0.95384e-20
      14000.60c 0.66254e-03
      25055.62c 0.10838e-02                $ SHLD SS top
m19    92235.17c 0.187309e-04
      92238.17c 0.747364e-02
      26000.55c 0.132470e-01
      24000.50c 0.301425e-02
      28000.50c 0.286071e-02
      8016.60c 0.149847e-01
      6012.50c 0.400788e-04
      11023.62c 0.903609e-02
      14000.60c 0.249138e-03
      25055.62c 0.407556e-03                $ diluent homog
m20    26054.62c 0.63886e-03
      26056.62c 0.10029e-01
      26057.62c 0.23161e-03
      26058.62c 0.30823e-04
      24050.62c 0.10807e-03
```

```
        24052.62c 0.20840e-02
        24053.62c 0.23631e-03
        24054.62c 0.58822e-04
        28058.62c 0.16070e-02
        28060.62c 0.61899e-03
        28061.62c 0.26910e-04
        28062.62c 0.85781e-04
        28064.62c 0.21858e-04
        42000.66c 0.21676e-03
         6012.50c 0.33070e-04
        11023.62c 0.66755e-02
         1001.62c 0.95384e-20
        14000.60c 0.20557e-03
        25055.62c 0.33629e-03                  $ Blanket plenum
m21     5010.66c 0.52
        5011.66c 0.28
        6012.50c 0.20                          $ pinwise CSRmid/DSR
m22     5010.66c 0.1592
        5011.66c 0.6408
        6012.50c 0.2000                        $ pinwise CSRtop/bot
m23    92235.17c 0.187309e-04
       92238.17c 0.747364e-02
       26000.55c 0.132470e-01
       24000.50c 0.301425e-02
       28000.50c 0.286071e-02
        8016.60c 0.149847e-01
        6012.50c 0.400788e-04
       11023.62c 0.903609e-02
       14000.60c 0.249138e-03
       25055.62c 0.407556e-03                 $ diluent homog
```

APPENDIX B

Table XII

Mass and activity values for every isotope printed in MCNPX output for “three cycles” radial blanket material at End-of-Life.

Isotope	ZAID	Mass (g)	Activity (Ci)
C-12	6012	2.677E-01	0.00E+00
C-13	6013	8.193E+00	0.00E+00
N-15	7015	1.471E-02	0.00E+00
O-16	8016	1.128E+06	0.00E+00
O-17	8017	1.018E-02	0.00E+00
Ga-71	31071	2.362E-03	0.00E+00
Ge-72	32072	6.952E-03	0.00E+00
Ge-73	32073	1.224E-02	0.00E+00
Ge-74	32074	2.832E-02	0.00E+00
Ge-76	32076	1.711E-01	0.00E+00
As-75	33075	5.204E-02	0.00E+00
Se-77	34077	3.582E-01	0.00E+00
Se-78	34078	7.336E-01	0.00E+00
Se-79	34079	1.611E+00	2.21E-01
Se-80	34080	2.653E+00	0.00E+00
Se-82	34082	7.495E+00	2.35E-16
Br-81	35081	4.051E+00	0.00E+00
Kr-82	36082	5.439E-02	0.00E+00
Kr-83	36083	1.253E+01	0.00E+00
Kr-84	36084	2.560E+01	0.00E+00
Kr-85	36085	4.984E+00	1.96E+03
Kr-86	36086	4.020E+01	0.00E+00
Rb-85	37085	1.951E+01	0.00E+00
Rb-86	37086	1.250E-03	1.02E+02
Rb-87	37087	5.234E+01	4.49E-06
Sr-86	38086	1.154E-01	0.00E+00
Sr-88	38088	6.880E+01	0.00E+00
Sr-89	38089	5.857E+00	1.70E+05
Sr-90	38090	1.078E+02	1.52E+04

Y-89	39089	8.610E+01	0.00E+00
Y-90	39090	2.802E-02	1.52E+04
Y-91	39091	1.062E+01	2.61E+05
Zr-90	40090	2.693E+00	0.00E+00
Zr-91	40091	1.186E+02	0.00E+00
Zr-92	40092	1.438E+02	0.00E+00
Zr-93	40093	1.676E+02	4.22E-01
Zr-94	40094	1.718E+02	0.00E+00
Zr-95	40095	1.858E+01	3.99E+05
Zr-96	40096	2.044E+02	0.00E+00
Nb-95	41095	1.461E+01	5.75E+05
Mo-95	42095	1.545E+02	0.00E+00
Mo-96	42096	1.403E+00	0.00E+00
Mo-97	42097	2.012E+02	0.00E+00
Mo-98	42098	2.150E+02	0.00E+00
Mo-100	42100	2.484E+02	0.00E+00
Tc-99	43099	2.228E+02	3.82E+00
Ru-99	44099	7.932E-03	0.00E+00
Ru-100	44100	3.072E+00	0.00E+00
Ru-101	44101	2.325E+02	0.00E+00
Ru-102	44102	2.403E+02	0.00E+00
Ru-103	44103	1.056E+01	3.41E+05
Ru-104	44104	1.987E+02	0.00E+00
Ru-106	44106	6.540E+01	2.17E+05
Rh-103	45103	2.154E+02	0.00E+00
Pd-104	46104	2.846E+00	0.00E+00
Pd-105	46105	1.547E+02	0.00E+00
Pd-106	46106	5.074E+01	0.00E+00
Pd-107	46107	7.576E+01	3.90E-02
Pd-108	46108	4.352E+01	0.00E+00
Pd-110	46110	1.315E+01	0.00E+00
Ag-109	47109	2.083E+01	0.00E+00
Cd-110	48110	2.974E-01	0.00E+00
Cd-111	48111	7.119E+00	0.00E+00
Cd-112	48112	4.285E+00	0.00E+00
Cd-113	48113	3.057E+00	1.04E-12
Cd-114	48114	2.547E+00	0.00E+00
Cd-116	48116	2.039E+00	0.00E+00
In-115	49115	2.109E+00	1.49E-11
Sn-115	50115	1.095E-01	0.00E+00

Sn-116	50116	5.039E-02	0.00E+00
Sn-117	50117	2.162E+00	0.00E+00
Sn-118	50118	2.122E+00	0.00E+00
Sn-119	50119	1.990E+00	0.00E+00
Sn-120	50120	2.021E+00	0.00E+00
Sn-122	50122	2.398E+00	0.00E+00
Sn-123	50123	1.351E-01	1.11E+03
Sn-124	50124	3.728E+00	0.00E+00
Sn-126	50126	7.052E+00	2.00E-01
Sb-121	51121	1.961E+00	0.00E+00
Sb-123	51123	2.516E+00	0.00E+00
Sb-124	51124	2.798E-03	4.90E+01
Sb-125	51125	3.957E+00	4.15E+03
Te-122	52122	2.044E-02	0.00E+00
Te-124	52124	1.910E-02	0.00E+00
Te-125	52125	8.395E-01	0.00E+00
Te-126	52126	1.227E-01	0.00E+00
Te-127	52127	1.795E-03	4.74E+03
Te-128	52128	2.732E+01	0.00E+00
Te-130	52130	1.058E+02	0.00E+00
I-127	53127	1.376E+01	0.00E+00
I-129	53129	5.575E+01	9.85E-03
I-131	53131	3.006E-02	3.73E+03
Xe-128	54128	1.996E-01	0.00E+00
Xe-130	54130	4.756E-01	0.00E+00
Xe-131	54131	1.752E+02	0.00E+00
Xe-132	54132	2.643E+02	0.00E+00
Xe-133	54133	2.857E-03	5.35E+02
Xe-134	54134	3.925E+02	0.00E+00
Xe-136	54136	3.556E+02	0.00E+00
Cs-133	55133	3.461E+02	0.00E+00
Cs-134	55134	4.081E+00	5.28E+03
Cs-135	55135	3.628E+02	4.18E-01
Cs-136	55136	1.493E-02	1.09E+03
Cs-137	55137	3.262E+02	2.84E+04
Ba-134	56134	1.058E+00	0.00E+00
Ba-135	56135	1.703E-03	0.00E+00
Ba-136	56136	5.194E+00	0.00E+00
Ba-137	56137	7.382E+00	0.00E+00
Ba-138	56138	3.258E+02	0.00E+00

Ba-140	56140	4.995E-01	3.66E+04
La-139	57139	3.072E+02	0.00E+00
La-140	57140	7.569E-02	4.21E+04
Ce-140	58140	3.013E+02	0.00E+00
Ce-141	58141	8.612E+00	2.46E+05
Ce-142	58142	2.652E+02	1.34E-11
Ce-144	58144	1.109E+02	3.53E+05
Pr-141	59141	2.785E+02	0.00E+00
Pr-143	59143	6.100E-01	4.11E+04
Nd-142	60142	1.112E+00	0.00E+00
Nd-143	60143	2.538E+02	0.00E+00
Nd-144	60144	1.298E+02	1.54E-10
Nd-145	60145	1.889E+02	7.77E-12
Nd-146	60146	1.690E+02	0.00E+00
Nd-147	60147	1.059E-01	8.57E+03
Nd-148	60148	1.039E+02	0.00E+00
Nd-150	60150	6.006E+01	0.00E+00
Pm-147	61147	9.474E+01	8.79E+04
Sm-147	62147	2.487E+01	5.71E-07
Sm-148	62148	4.560E+00	1.39E-12
Sm-149	62149	7.240E+01	8.69E-11
Sm-150	62150	6.114E+00	0.00E+00
Sm-151	62151	3.723E+01	9.80E+02
Sm-152	62152	3.245E+01	0.00E+00
Sm-154	62154	1.213E+01	0.00E+00
Eu-151	63151	2.528E-01	0.00E+00
Eu-152	63152	8.457E-03	1.49E+00
Eu-153	63153	2.085E+01	0.00E+00
Eu-154	63154	1.393E+00	3.77E+02
Eu-155	63155	7.393E+00	3.65E+03
Eu-156	63156	2.506E-02	1.38E+03
Gd-152	64152	3.707E-03	8.08E-14
Gd-154	64154	8.140E-02	0.00E+00
Gd-155	64155	1.002E+00	0.00E+00
Gd-156	64156	5.989E+00	0.00E+00
Gd-157	64157	3.581E+00	0.00E+00
Gd-158	64158	2.253E+00	0.00E+00
Gd-160	64160	4.714E-01	0.00E+00
Tb-159	65159	1.154E+00	0.00E+00
Tb-160	65160	8.485E-03	9.58E+01

Dy-160	66160	3.405E-02	0.00E+00
Dy-161	66161	2.311E-01	0.00E+00
Dy-162	66162	1.687E-01	0.00E+00
Dy-163	66163	7.950E-02	0.00E+00
Dy-164	66164	4.767E-02	0.00E+00
Ho-165	67165	2.264E-02	0.00E+00
Er-166	68166	1.663E-02	0.00E+00
Er-167	68167	6.552E-03	0.00E+00
U-234	92234	2.326E-01	1.45E-03
U-235	92235	1.842E+04	3.98E-02
U-236	92236	6.022E+02	3.90E-02
U-237	92237	4.863E-03	3.97E+02
U-238	92238	8.263E+06	2.78E+00
Np-237	93237	1.096E+02	7.73E-02
Pu-238	94238	5.128E+00	8.78E+01
Pu-239	94239	9.713E+04	6.03E+03
Pu-240	94240	1.889E+03	4.29E+02
Pu-241	94241	3.788E+01	3.91E+03
Pu-242	94242	2.804E-01	1.11E-03
Am-241	95241	1.199E+00	4.11E+00
Cm-242	96242	8.033E-03	2.66E+01